A PHYSICO-CHEMICAL INVESTIGATION ON THE SELECTIVE REDUCTION OF IRON OXIDES IN CHROMITE

A Thesis Submitted
In Partial Fulfilment of the Requirements
for the Degree of
DOCTOR OF PHILOSOPHY

BY
SAMARNATH BASU

to the

DEPARTMENT OF METALLURGICAL ENGINEERING
INDIAN INSTITUTE OF TECHNOLOGY KANPUR
AUGUST 1972

CERTIFICATE

Certified that this work on "A Physico-Chemical Investigation On The Selective Reduction Of Iron Oxides In Chromite" has been carried out under my supervision and that it has not been submitted elsewhere for a degree.

(A Ghosh)
Associate Professor
Department of Metallurgical Engineering
Indian Institute of Technology,
Kanpur-16

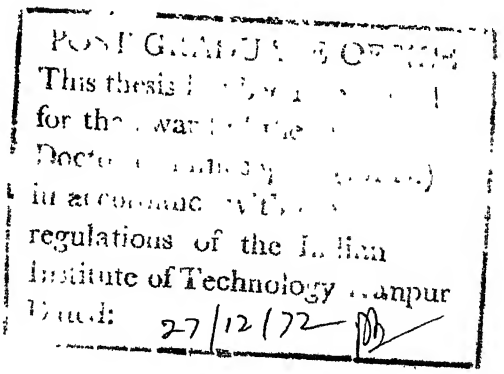

ACKNOWLEDGEMENTS

The author is indebted to Professor A. Ghosh for suggesting the problem, inspiring guidance throughout the work and the illuminating discussions he had with him.

He is grateful to Professor A. Paul, on leave from the Department of Glass Technology, Sheffield University, England, for the interest he had taken in the thermodynamic investigations and for the series of stimulating discussions he had with him.

The author is thankful to Professor K.P. Singh and Dr. H.S. Ray for helping with some experimental equipments and materials.

It is a pleasure to acknowledge the sincere efforts of Mr. V.N. Sharma in conducting the entire chemical analysis work and for his constant help in conducting the experiments. The author is also thankful to Mr. K.P. Mukherjee and Mr. B. Sharma for their help from time to time.

The author would like to thank the technical staff of the Department of Metallurgical Engineering of The Ohio State University, Ohio, U.S.A. for conducting the electron-probe microanalysis.

The cooperation of his friends like Dr. K.P. Jagannathan, and Messers Parimal Roychowdhury, Sibnath Mazumdar, Anwar Ali, Susanta Basu, Chandan Roy and Krishen

Luthra contributed positively in bringing the work to the present shape.

Finally he would like to thank Mr. R.N. Srivastava for his excellent typing.

CONTENTS

LIST OF TABLES

LIST OF FIGURES

FIGURE PAGE

LIST OF SYMBOLS

A = Surface area of a pellet, cm^2.

$\bar{a}$ = Coefficient as expressed by equation (VII-6).

$a_{Fe_{1.5}O_2}$ = Activity of half a molecule of magnetite in $FeFe_{2-x}Cr_xO_4$ solid solution.

$\bar{b}$ = Coefficient as expressed by equation (VII-7).

C_O = Concentration of reducible oxygen, moles of atomic O/cm^3.

C_{H_2}, C_{H_2O} = Concentrations of hydrogen and water vapour, gms/cm^3.

$D_{H_2}^{(eff)}$, $D_{H_2O}^{(eff)}$ = Effective diffusivities of hydrogen and water vapour through the product layer, cm^2/sec.

$D_{H_2-H_2O}$ = Binary diffusivity in the hydrogen-water vapour mixture, cm^2/sec.

F = Fractional reduction of a pellet.

ΔG° = Free energy change, calories.

K = Equilibrium constant.

K_m = Mass transfer coefficient, cm/sec.

$K_{m(H_2)}$, $K_{m(H_2O)}$ = Mass transfer coefficient for hydrogen and water vapour, cm/sec.

K_r = Specific rate constant for surface reaction, cm/sec.

M = Molecular weight.

Nu = Nusselt number
$= \frac{\text{mass transfer coefficient.(2.pellet radius)}}{\text{diffusivity}}$.

$N_{Fe_{1.5}O_2}$ = Mole fraction of magnetite in solution.

n_2 = Number of molecules in a unit cell.

$\frac{dn}{dt}$ = Rate of production of water vapour due to pellet reduction, gm/sec.

pO_2 = Partial pressure of oxygen.

pO_2° = Equilibrium oxygen partial pressure of Fe_3O_4/Fe mixture.

pH_2, pH_2O = Partial pressures of hydrogen and water vapour.

R = Universal gas constant, cals/°K/mole or cm^3-atm/°K/mole.

Re = Reynolds number
$= \frac{\text{velocity.density.(2.pellet radius)}}{\text{viscosity}}$.

Sc = Schmidt number $= \frac{\text{viscosity}}{\text{density.diffusivity}}$.

T = Absolute temperature, °K.

t = Time, sec.

t_c = Time required for complete reduction of a pellet, sec.

V = Volume of a unit cell, A^3.

X_o = Radius of a pellet, cm.

X_i = Distance of the reaction front from the centre of a pellet, cm.

ϵ = Porosity of a pellet.

ρ_a, ρ_T = Actual and theoretical density of a pellet, gms/cm^3.

μ_{O_2} = Oxygen potential, calories.

$\gamma_{Fe_{1.5}O_2}$ = Activity coefficient of half a molecule of magnetite in solution.

τ = Tortuosity.

δ = Concentration boundary layer thickness, cm.

Superscripts:

s = At the surface of pellet.

b = In the bulk gas phase.

SYNOPSIS

A PHYSICO-CHEMICAL INVESTIGATION ON THE SELECTIVE REDUCTION OF IRON OXIDES IN CHROMITE

A Thesis Submitted
In Partial Fulfilment of the Requirements
For the Ph.D. Degree
by
Samarnath Basu
to the
Department of Metallurgical Engineering
Indian Institute of Technology, Kanpur
August 1972

Thermodynamic and kinetic investigations were carried out on iron chromite system for a fundamental appraisal of the thermal beneficiation of low grade chromite ores, which involve selective reduction of iron oxides in the ore by some suitable reducing agent and the subsequent separation of metallic iron by leaching or magnetic separation. The natural chromite mineral is a solid solution between $FeO.Cr_2O_3$ and other spinels like $FeO.Fe_2O_3$, $MgO.Cr_2O_3$, $MgO.Al_2O_3$ etc., amongst which $FeO.Fe_2O_3$ is of special significance in determining the quality of the ore.

The thermodynamic investigation consisted of the determination of equilibrium oxygen potentials over mixtures of metallic iron and synthetically prepared solid solutions of $FeO.Cr_2O_3$ and $FeO.Fe_2O_3$ of different compositions near the $FeO.Cr_2O_3$ end in the temperature range of 850°C to 1050°C. Gas equilibration technique and a thermogravimetric apparatus were employed for this purpose. The required oxygen potentials were established by controlled hydrogen-water

vapour mixtures. The equilibrium oxygen potential data obtained on terminal $FeO.Cr_2O_3$ were in excellent agreement with the existing literature values. From the equilibrium oxygen potential data on spinels of different compositions, the activity-composition relationship in $FeO.Cr_2O_3$-$FeO.Fe_2O_3$ system was determined. The activity of $Fe_{1.5}O_2$ exhibited a strong negative departure from the Raoult's Law line.

In the kinetic investigation, rates of reduction of dense and porous spherical single pellets of $FeO.Cr_2O_3$ were studied thermogravimetrically at 1050°C in a stream of purified hydrogen.

In porous pellets, the reduction of Cr_2O_3 was not observed even upto the stage of complete reduction of FeO, a phenomenon supported by thermodynamic calculations. The interface between the product layer and the unreduced core was diffused over a finite zone instead of being sharp. The reduction data were quantitatively analyzed with the help of generalized rate equation for reduction of hematite by Spitzer, Manning and Philbrook, and it was found that the chemical reaction step was much slower compared to the other steps, viz., transport across the gas film and diffusion through porous product layer. This is consistent with other observations.

In the case of dense pellets the rates of reduction were an order of magnitude lower compared to those of porous pellets. Simultaneous reduction of Cr_2O_3 alongwith FeO

complicated the reduction process. The different phases appearing during reduction in the product layer were identified as unreduced $FeO.Cr_2O_3$, an alloy of Fe and Cr, and Cr_2O_3 by a combination of microstructural, electron-microprobe and chemical analysis. Three distinct zones could be detected in the product layer. The outermost zone consisted of an alloy of Fe-Cr, followed by the second one having Cr_2O_3 and Fe-Cr alloy as the predominant phases with some $FeO.Cr_2O_3$. The third zone, which is adjacent to the unreduced core was characterized by grains of $FeO.Cr_2O_3$ with Cr_2O_3 and metallic iron appearing along the grain boundaries. Quantitative analysis was not possible. Qualitative considerations and approximate calculations point out that in this case also gas-solid chemical reaction step is the likely rate-controlling one. The lower rate of dense pellet reduction as compared to the porous pellet case may be attributed to the much less gas-solid contact area available in the former case.

CHAPTER I

INTRODUCTION

For the production of ferro-alloys like ferro-chromium, ferro-titanium etc. the principal raw materials are iron bearing oxide minerals such as chromite, ilmenite etc. which consist of chemical compounds and solid solutions of iron oxides and oxides of other metals. In a ferro-alloy furnace, these minerals are reduced with a suitable reducing agent at high temperature in the presence of a slag-forming flux. The equilibrium oxygen potential over the mixture of a metal and its oxide is the most important parameter which determines the feasibility of reduction of any oxide at a particular temperature by a reducing agent for the production of the metal. Extensive thermodynamic investigations have been carried out for the determination of the free energy of formation of pure oxides as a function of temperature, as a result of which exhaustive information is available[1,2] about the common oxides of metallurgical interest. On the other hand such data are meagre on double oxides.

Again some of these minerals are of low grade and contain a very high proportion of iron oxides. Thermal beneficiation has been found to be an effective method of upgrading. However, not much fundamental investigations are available regarding rate and mechanism of selective reduction

of iron oxide in these minerals. India possesses a large reserve of low grade chromite ore which is a potential source of standard grade ferro-chrome provided its iron content can be lowered by the thermal beneficiation of the ore.

With the above in mind, a physico-chemical investigation of selective reduction of iron chromite was considered worthwhile because it could meet the following two-fold objective, viz.,

(1) Better general understanding of physico-chemical aspects of selective elimination of iron in double oxides by thermal beneficiation process, and

(2) Better understanding of selective reduction of low grade chromite minerals.

I-1 A SURVEY OF THE CHROMITE DEPOSITS:

The pure mineral iron chromite has the chemical formula $FeO.Cr_2O_3$ belonging to the group of oxides having spinel structure. Spinels can be represented by the general chemical formula, XY_2O_4, where X and Y represent two types of cations. The spinel structure is cubic with a large unit cell containing 32 oxygen ions and 8 and 16 cations of the X and Y type, respectively. The 32 oxygen ions are close-packed in cubic symmetry. This close packing contains 64 interstices each surrounded by 4 oxygen ions, i.e., tetrahedral sites with coordination number 4 and 32 interstices surrounded by 6 oxygen ions i.e. octahedral sites

with coordination number 6. In a spinel structure, 8 of these tetrahedral sites and 16 of the octahedral sites are occupied. Fig. 1 shows the unit cell of an ideal distortion-free spinel. In simple spinels, the combination of the valencies of the cations may be either 2 for X and 3 for Y or 4 for X and 2 for Y.

Depending upon the relative distribution of the cations X and Y within the octahedral or tetrahedral sites, spinels can be subdivided into two classes. In 'normal' spinels X ions occupy the tetrahedral sites and Y ions occupy octahedral sites, whereas, in 'inversed' spinels, half of the Y ions occupy the tetrahedral sites and the other half of the Y ions occupy octahedral sites alongwith the X ions.

In the pure mineral iron chromite ($FeO.Cr_2O_3$), X is the divalent cation Fe^{2+} and Y is the trivalent cation Cr^{3+}. The cation arrangement in $FeO.Cr_2O_3$ was determined in 1947 by Verwey and Heilman[3] and it was found to be a normal spinel.

A natural chromite deposit often contains, apart from pure iron chromite $FeO.Cr_2O_3$, variable amounts of other spinels like $FeO.Fe_2O_3$, $MgO.Cr_2O_3$, $MgO.Al_2O_3$, $FeO.Al_2O_3$, $MgO.Fe_2O_3$ etc. in solid solution with $FeO.Cr_2O_3$[4]. Amongst these, $FeO.Fe_2O_3$ (magnetite) is more commonly encountered in solid solution with $FeO.Cr_2O_3$. Chemical analysis of natural chromite spinels was carried out by a large number

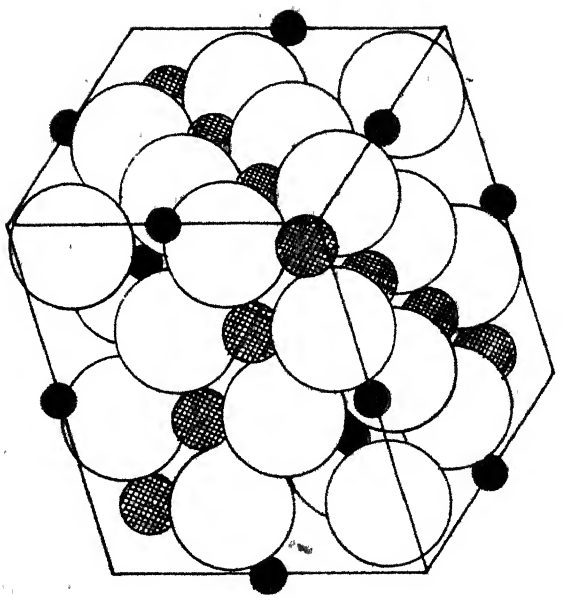

FIG.1: ARRANGEMENT AND PACKING OF ATOMS IN UNIT CELL OF IDEAL SPINEL STRUCTURE, LARGE SPHERES REPRESENT OXYGEN, SMALL BLACK SPHERES REPRESENT FOURFOLD COORDINATION, HATCHED SPHERES REPRESENT SIXFOLD COORDINATION.[3]

of research workers. Heiligman and Mikami[5] have presented an excellent compilation of composition of chromite ores of economic importance around the world. Table I shows their compilation excluding the Indian deposits. The data of Table I reveals the wide range of solid solution in chromite spinels as well as the large variation in Cr_2O_3 content.

India[6] possesses good resources of chromite including some belonging to the high grade. The inferred reserves of chromite ores of all grades are placed at 7.94 million tons by The Geological Survey of India. Important deposits of chromite are located in Orissa, Bihar and Mysore while some deposits of lesser importance are located in Andhra Pradesh, Maharastra and Tamil Nadu. Orissa is the most important chromite producing state in India both from the point of view of quality as well as quantity. Table II gives the details[6,7,8] of the location and grade of different deposits in India. It is clear from Table II that though the reserve of chromite ore in India is appreciable, only a small fraction of it is of high grade. From the point of manufacture of ferrochrome, Cr:Fe ratio of the starting material is extremely important and the minimum acceptable value of the ratio is 3:1 for the production of ferrochrome of a satisfactory grade containing about 68% Cr in the alloy[9]. Chromite ore conforming to this criterion is commonly known as metallurgical grade ore. Unfortunately a

TABLE I

Analysis of Chromite Ores of Economic Importance Around the World(5)

	Cuba		Philippine		Transwaal		Turkey		U.S.S.R.			South Rhodesia	
	Camaguey	Moa Bay	Masinloc Coto-Mine	Swart-Kop	Steel-poort	Groot-boom	Eskisehir district		Kempirsajsk	Saranovsk	Selukwe	Dyke	
Cr_2O_3	35.21	40.43	36.24	51.09	47.65	46.82	60.49	53.76	36.71	61.44	46.22	57.30	58.55	53.85
Al_2O_3	32.21	28.55	31.86	13.38	13.85	16.85	10.31	15.36	31.82	11.41	17.32	13.50	12.65	12.55
TiO_2	0.31	0.10	0.38	0.72	0.55	1.60	0.33	0.45	0.30	0.17	0.62	0.56	0.02	0.03
Fe_2O_3	2.83	2.22	2.97	8.54	9.75	5.11	3.25	5.67	5.09	nil	9.95	2.63	12.54	4.79
FeO	12.11	11.50	11.32	15.45	16.35	22.10	9.98	11.57	9.69	12.53	12.30	9.77	3.09	15.52
MgO	16.89	16.95	17.10	10.98	12.2	7.90	15.96	13.54	16.62	13.66	13.14	15.92	13.12	12.32
MnO	0.13	0.05	0.11	0.17	nil	0.05	0.12	0.06	0.23	0.16	0.24	0.08	0.09	0.18
CaO	0.28	Tr	nil	nil	nil	0.02	nil	nil	nil	nil	nil	nil	0.22	0.03
SiO_2	0.31	nil	nil	nil	nil	nil	nil	nil	nil	0.17	0.16	0.17	nil	nil

TABLE II

Chromite Ore Deposits of India[6,7,8]

State	District	Location	Grade		Reserve
Orissa	Keonjhar	Baula	High grade	Cr:Fe $\geq$ 3:1	(a) Total reserve of high grade ore with Cr:Fe $\geq$ 3:1 is approximately 2.5 million tons.
		Nausahi	-do-	Cr:Fe $\sim$ 3:1	
	Cuttuck	Saruabil	-do-	Cr:Fe $\geq$ 3:1	
		Kaliapani	Low grade	Cr:Fe $<$ 3:1	
	Dhenkanal	Kandiagandia, Kantalsuau	-do-	Cr:Fe $<$ 3:1	
Bihar	Singhbhum	Roroburu, Chitungburu	High grade	Cr:Fe $\sim$ 3:1	
		Jojohatu, Kittaburu, Kimsiburu	Low grade	Cr:Fe $<$ 3:1	
Mysore	Hasan	Byrapur, Bhaktaralhi, Jambur, Togadur, Arsikere, Chilkkenhali, Pansamudra	-do-	Cr:Fe $<$ 3:1	(b) Total reserve of low grade ore with Cr:Fe $<$ 3:1 is approximately 5.5 million tons.
	Mysore	Mysore, Nanjangud, Sinduvalli, Dodkanya, Dodkattur	-do-	Cr;Fe $<$ 3:1	
Andhra Pradesh	Warangal	Kondapalle	-do-	Cr:Fe $<$ 3:1	
	Krishna	--			
Tamil Nadu	Salem	Sithampundi, Molasi, Karungalpatti	-do-	Cr:Fe $<$ 3:1	
Maharastra	Bhandara	Panni, Belgatta	-do-	Cr:Fe $<$ 3:1	
	Ratnagiri	Vagda, Kankauli			

major fraction of the total Indian chromite deposit is not upto this mark and cannot be regarded as a metallurgical grade ore.

I-2 BENEFICIATION OF LOW GRADE CHROMITE ORE:

Quite a large number of investigations have been carried out on the upgrading of low grade chromite deposits in India[10-20] as well as in other countries[21-26] for their utilization in metallurgical industries for the manufacture of ferrochrome. The past investigations in this field can be broadly divided into two groups, viz., the mechanical methods and the chemical methods. In the Ore Dressing and Mineral Beneficiation Division of The National Metallurgical Laboratory, Jamshedpur, investigations[10-16] were carried out on low grade Indian Chromite ores from Bihar, Mysore and Orissa using ore dressing techniques like jigging, tabling, Humphrey's spiral, magnetic separation, flotation etc. i.e., the mechanical methods of separation. But these investigations met with little success in improving the Cr:Fe ratio of the ores. As pointed out already in the previous section, the impurity spinels like $FeO.Fe_2O_3$ usually occur in solid solution with $FeO.Cr_2O_3$ and as a result mechanical methods of separation of these spinels are not expected to be successful.

In the other class of beneficiation studies on chromite ores using chemical methods, selective reduction

of iron oxides in the ore by coal, coke, charcoal, carbon monoxide, methane, hydrogen or coke oven gas and separation of the metallic iron by acid leaching[17] or magnetic separation[9] were tried. Chatterjee and Sen[17] selectively reduced iron oxides in the low grade Indian chromites from Orissa and Mysore by coke, coal, charcoal and coke oven gas at a temperature range of 950°C to 1250°C and then leached out metallic iron with 1:2 dilute sulphuric acid at 105°C. The Cr:Fe ratio could be elevated to 8:1 from 2.9:1 with 80% recovery, and to 4:1 from 1.8:1 with 90% recovery in the case of Orissa and Mysore ores respectively.

Chlorination of the ore by treatment with chlorine at elevated temperature to convert the respective metallic oxides into their chlorides in vapour phase was also tried, but was found to be inconvenient. The difficulties like slow rates of diffusion of heavy chlorides from the interior of the ore, corrosive action of chlorine and the metallic chlorides, formation of liquid $CrCl_2$ and $MgCl_2$ etc. did not allow any further effective research for beneficiation in that direction. As a modified version of the total chlorination processes, selective chlorination of iron oxides was tried by some workers using a mixture of reducing agents like carbon[27], hydrocarbon[28] or hydrogen[29] alongwith chlorine or hydrochloric acid vapour. Athawale and Altekar[30] studied selective chlorination of iron oxides

in low grade chromite using hydrogen and chlorine in a fluidized bed unit and the results were encouraging. However, industrial scale practice of selective chlorination in India has to overcome main hurdles of chlorine resistant materials of construction and the associated high capital and operational cost alongwith the minor problems of health hazard and air pollution accompanying the use of chlorine gas. Hence, chemical beneficiation involving selective reduction of iron oxides in chromite and their subsequent removal of iron by magnetic separation and acid leaching appears to offer some advantages in a commercial scale.

Since this method of upgrading is promising, it is desirable that some studies should be directed towards the understanding of the physico-chemical aspects of the process before it is taken up in the pilot plant or commercial scale.

I-3 THE IRON-CHROMIUM-OXYGEN SYSTEM:

Investigations on the different phases involved in the Fe-Cr-O system at different temperatures started in the late forties. Chen and Chipman[31] investigated the Cr-O equilibrium in liquid iron at 1595°C using a controlled gas mixture of hydrogen and water vapour to determine the stability range of the chromite phase. Hilty et al[32] studied the different oxide phases appearing in equilibrium

with liquid Fe-Cr alloys at 1550°C, 1600°C and 1650°C and established the existence of two previously unknown oxide phases, one, a distorted spinel with composition intermediate between $FeO.Cr_2O_3$ and Cr_3O_4 and the other, Cr_3O_4. The isothermal section at 1600°C of the inferred phase diagram of Cr-Fe-O system was drawn by them and showed the liquidus surface. The spinel phase observed by Hilty et al was confirmed by the work of Koch et al[33]. Richard and White[34] and Woodhouse and White[35] investigated the equilibrium between spinel and sesquioxide solid solution in air at 1420°C-1650°C. Muan and Somiya[36] determined the approximate phase relationship in this system in air from 1400°C to 1650°C.

All the abovementioned studies were conducted either with no variation or with a very restricted variation of oxygen partial pressure. As a result, although the different oxide phases that are likely to be encountered in the Cr-Fe-O system were identified, their relative stabilities as a function of oxygen partial pressure were not clear from these investigations. Katsura and Muan[37] studied the equilibria of the different oxide phases at 1300°C as a function of oxygen partial pressure ranging from 0.21 atm (air) to 2.8×10^{-14} atm. Fig. 2 shows the isothermal section of the ternary phase diagram of the Cr_2O_3-Fe_2O_3-FeO system at 1300°C as determined by Katsura and Muan.

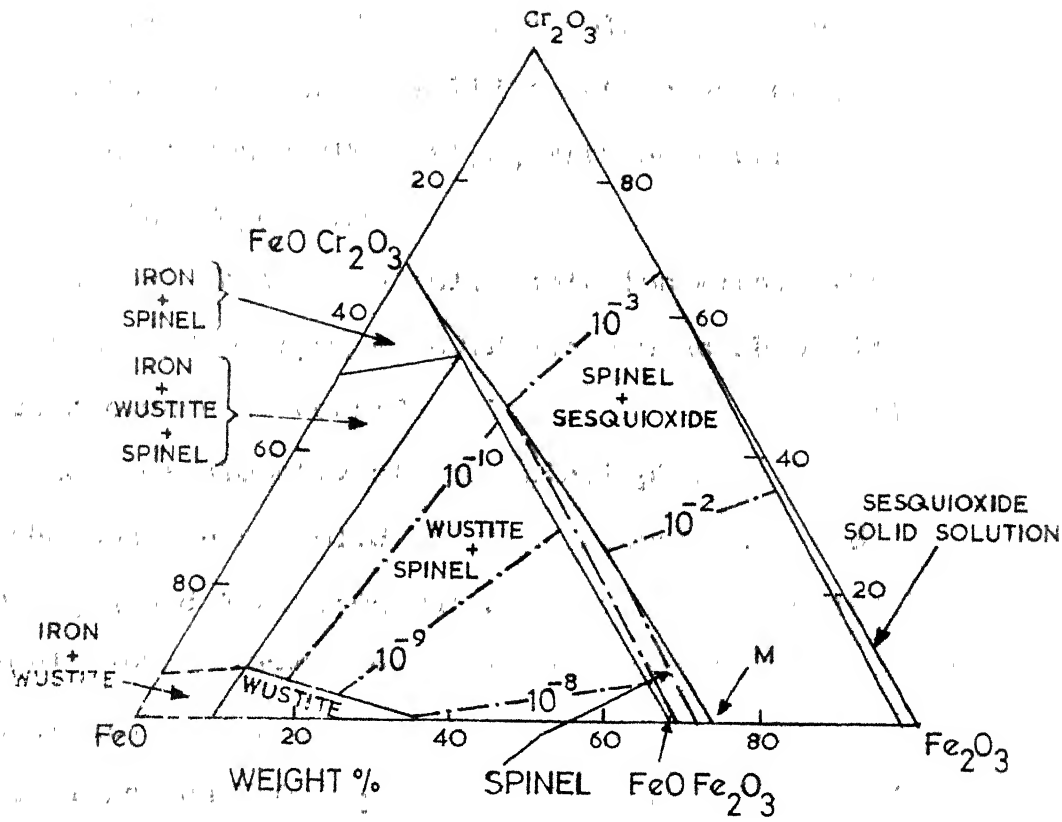

FIG. 2: ISOTHERMAL SECTION THROUGH THE SYSTEM $FeO-Cr_2O_3-Fe_2O_3$ AT 1300 °C[37]. LIGHT DASH-DOT LINES ARE OXYGEN ISOBARS.

Three oxide phases were found to be stable under the experimental conditions: sesquioxide solid solution, spinel solid solution and wustite solid solution. The compositions of the sesquioxide solid solution are well represented by the formula $(Fe, Cr)_2O_3$ with some non-stoichiometry at the Fe_2O_3 end.

The spinel phase is a solid solution within the composition area of $FeO.Cr_2O_3$ - $FeO.Fe_2O_3$ - M as shown in Fig. 2. Excess oxygen is considerable in the magnetite rich end. If the nonstoichiometry of the spinel phase is neglected, the continuous solid solution between the end members $FeO.Fe_2O_3$ and $FeO.Cr_2O_3$ can be represented by the general formula $FeFe_{2-x}Cr_xO_4$, where x is a variable parameter between the limits of 0 and 2 which correspond to the two terminal spinel phases $FeO.Fe_2O_3$ and $FeO.Cr_2O_3$ respectively. X-ray diffraction studies were carried out by Yearian et al[38] on $FeFe_{2-x}Cr_xO_4$ over the entire range of composition. It was found that the lattice parameter of the solid solution between the normal spinel $FeO.Cr_2O_3$ and inversed spinel $FeO.Fe_2O_3$ do not follow a linear relationship as predicted by Vegard's Law. The normal structure of the terminal chromite spinel $FeO.Cr_2O_3$ is maintained upto a value of $x = 1.28$ when the spinel is metal rich and then gradually undergoes inversion which is complete at a value of $x = 0.3$ for the metal rich spinel.

The wustite phase is characterized by an appreciable variation in anion to cation ratio as well as the presence of some Cr^{3+} ions in the structure. The other condensed phase appearing in the phase diagram is metallic iron containing about 0.1% Cr in solid solution.

Ribeud and Muan[39] determined the phase diagram of Cr_2O_3-iron oxide system in an atmosphere consisting of hydrogen and carbon monoxide in equal parts. Therefore this represents study at one oxygen isobar at any fixed temperature. The results are shown in Fig. 3(a) in terms of components FeO and Cr_2O_3 in a simplified manner although the system is not exactly binary because of the presence of Fe^{3+} ions in the condensed phase. Here FeO means total iron of the system represented as ferrous oxide. The extension of spinel solid solution phase area from $FeO.Cr_2O_3$ towards FeO side in Fig. 3(a) does not imply the existence of spinels with an anion to cation ratio lower than 4:3. The apparent excess FeO is due to the simplified pseudo binary representation of the phases. A similar binary phase diagram for Cr_2O_3 - FeO system was reported by Hoffmann[40] as shown in Fig. 3(b). The apparent discripancies between the diagrams 3(a) and 3(b) may be attributed to the method of equilibration adopted by Hoffmann in his experiments. In crucibles made of Cr_2O_3 and iron oxide, $FeO.Cr_2O_3$ was equilibrated with metallic iron at different temperatures

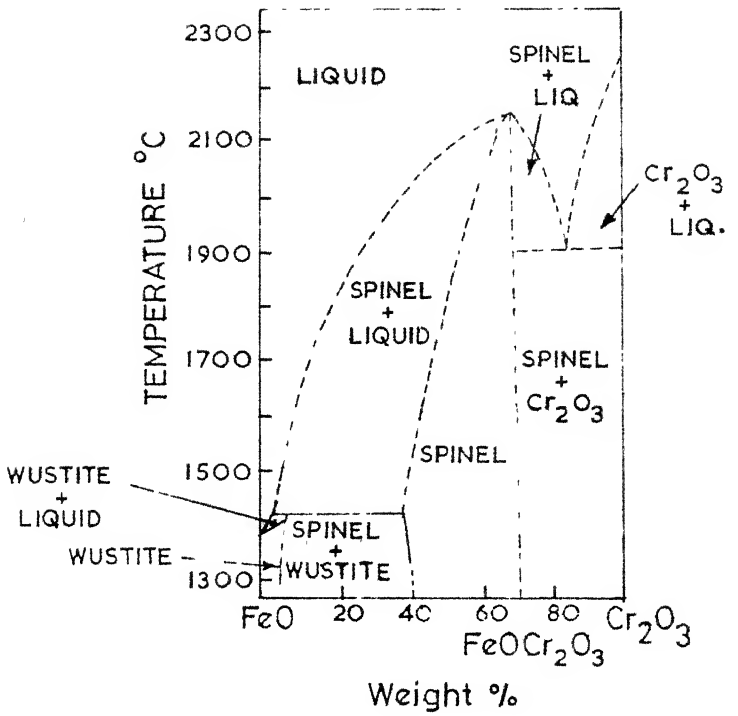

FIG. 3(a): PHASE DIAGRAM OF $FeO-Cr_2O_3$ SYSTEM IN AN ATMOSPHERE OF $CO:H_2 = 1:1$ [39]

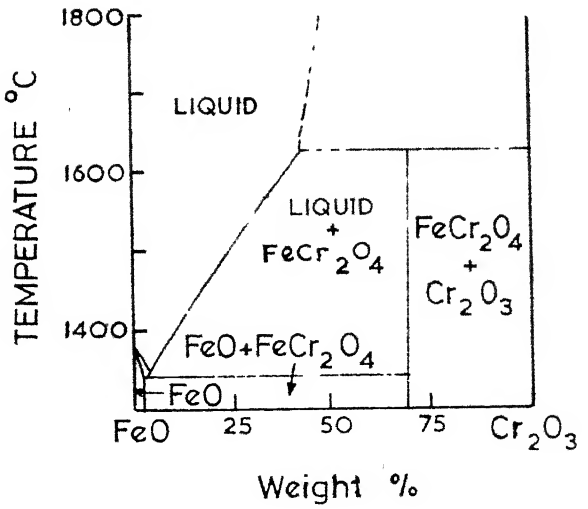

FIG. 3(b): PHASE DIAGRAM OF $FeO-Cr_2O_3$ SYSTEM [40]

in argon flushed and evacuated condition. This essentially indicates that oxygen in the gas phase which is an important component was uncertain. Also because of continuous flushing of gas the attainment of total equilibrium in Hoffmann's experiment is open to doubt.

As mentioned in the previous section, amongst other spinels appearing in solid solution with $FeO.Cr_2O_3$ in a natural ore, magnetite ($FeO.Fe_2O_3$) is of special significance. The effect of magnetite in lowering the Cr:Fe ratio of the ore is much more pronounced as compared to equal amounts of other impurity spinels. Hence, amongst all the phases shown in Fig. 2, the spinel solid solution $FeFe_{2-x}Cr_xO_4$ should be the centre of attention for chemical beneficiation of low grade ores by selective reduction of iron oxides in it for subsequent removal by leaching.

I-4 EXISTING THERMODYNAMIC DATA ON IRON CHROMITE:

The importance of oxygen potential data for a metal-metal oxide mixture for its reduction by a suitable reducing agent is well known. For the study of the preferrential reduction of iron oxides in the spinel $FeFe_{2-x}Cr_xO_4$, a precise knowledge about the oxygen potential over the mixture of iron and $FeFe_{2-x}Cr_xO_4$ is essential. However, the available literature is very scanty except for a few investigation on the terminal iron chromite,

$FeO.Cr_2O_3$.

Gas equilibration method was employed by most of the workers and either hydrogen-water vapour mixture or carbon dioxide-carbon monoxide mixture was used to set up oxygen potential in the equilibrating gas.

Boericke and Bangert[41] in 1946 determined the equilibrium hydrogen-water vapour ratio over mixture of $FeO.Cr_2O_3$, Cr_2O_3 and metallic iron between 1270°C to 1470°C and from that calculated the free energy of formation of iron chromite, $FeO.Cr_2O_3$. In 1963 Morozov and Novokharskii[42] passed pure and dry hydrogen through a 200 m.m. thick layer of iron chromite at constant temperature and measured the moisture content of the exit gas by its dew point, from which free energy of formation of iron chromite was calculated over a temperature of 800°C to 1400°C. Abendroth[43] also determined the equilibrium hydrogen-water vapour ratio over iron chromite by thermogravimetry. Katsura and Muan[37] while investigating the phase relationship in $FeO-Cr_2O_3-Fe_2O_3$ system at 1300°C determined the equilibrium oxygen partial pressure over a mixture of $FeO.Cr_2O_3$, Cr_2O_3 and metallic iron as 2.8×10^{-14} atm. by thermogravimetry. Kunnmann et al[44] determined equilibrium carbon monoxide-carbon dioxide ratio over iron chromite to compute its free energy of formation.

Compared to the abovementioned investigations using gas equilibration method only one investigation using a calcia stabilized zirconia solid electrolyte galvanic cell

with Fe-Fe_xO reference electrode was conducted by Tretyakov and Schmalzried[45] to determine the free energy of formation of $FeO.Cr_2O_3$.

Table III shows the results of all the experimental investigations on the free energy change of the reaction:

$$Fe(s) + \frac{1}{2}O_2(g) + Cr_2O_3(s) = FeO.Cr_2O_3(s) \quad \ldots (I\text{-}1)$$

In Table III the free energy change at 1300°K has also been included for comparison of results of different investigators. It is clear that considerable discripancy exists about the free energy of formation of terminal iron chromite spinel ($FeO.Cr_2O_3$). Moreover, no investigation has been carried out on the oxygen potential variation in spinel solid solution, $FeFe_{2-x}Cr_xO_4$. This is an essential parameter for the fundamental appraisal of the preferrential reduction of iron oxides in chromite spinels. Roychowdhury[46] attempted to set up a galvanic cell of the type used by Tretyakov and Schmalzried[45], to determine the oxygen potential over chromite spinels of different composition using a Ni-NiO reference electrode. Due to experimental difficulties the measurements could not be done. Hence it was decided to determine the oxygen potential of the solid solution $FeFe_{2-x}Cr_xO_4$ at various values of x in equilibrium with metallic iron by the other technique, viz., gas equilibration. As pointed out already gas equilibration has

Table III

Free Energy Change for the Reaction: $Fe(s) + \frac{1}{2}O_2(g) + Cr_2O_3(s) = FeO.Cr_2O_3(s)$

Method	Description	Investigator	Temp. range, °K	ΔG° cal/mole	ΔG° 1300°K cal/mole	Year
Gas Equilibration	Hydrogen-water vapour ratio determined over a mixture of $FeO.Cr_2O_3$, Cr_2O_3 and Fe	Boericke & Bengert[41]	1543 to 1683	-66150 +12.7T	-49640 extrapolated	1946
	H_2 passed through $FeO.Cr_2O_3$ bed at constant temperature at low flow rate and H_2O content of exit gas measured by its dew point	Morozor & Novokharskii[42]	1073 to 1673	-73000 +4.48TlogT +1.04T	-53325	1963
	Equilibrium $CO-CO_2$ mixture over $FeO.Cr_2O_3$ determined	Kunnmann, Rogers and Wold[44]	1073 to 1380	-68750 +16.6T	-47170	1963
	Equilibrium oxygen potential pressure over a mixture of $FeO.Cr_2O_3$, Cr_2O_3 and Fe determined thermogravimetrically	Katsura & Muan[37]	only at 1573	-48760 at 1573°K	--	1964
	Equilibrium hydrogen-water vapour ratio over $FeO.Cr_2O_3$ determined by thermogravimetry	Abendroth[43]	1173 to 1473	-74190 +16.5T	-52740	1966
Solid Electrolyte	The cell: $Fe, Cr_2O_3, FeO.Cr_2O_3/ZrO_2-CaO/Fe, Fe_xO$	Tretyakov & Schmalzried[45]	1023 to 1473	-76980 +21.22T	-49390	1963

been employed by several investigators[41-43,37] successfully on this system and as such is an excellent method which can be regarded as the only alternative to solid electrolyte method of determination of oxygen potential of solid oxides.

I-5 INVESTIGATIONS ON KINETICS OF SELECTIVE REDUCTION OF IRON OXIDES IN IRON CHROMITES AND OTHER DOUBLE OXIDES:

Feasibility of any process in an industrial scale is strongly dependent upon the rate at which it can be carried out. Selective reduction of iron oxides in chromite by a suitable reducing agent may be a feasible commercial proposition only if the rate of reduction is sufficiently high so that within a reasonable period of time reduction goes to completion or near completion. Hence information on the mechanism and the rates of selective reduction of iron oxides in chromite and the influence of physical and chemical variables such as porosity, gas composition, temperature etc. would be very desirable. One approach to this is to conduct a large number of reduction experiments on natural chromite ores and to obtain statistical information regarding the influence of these variables. But this approach would not allow us a good understanding of the mechanism because natural ore samples suffer from physical and chemical inhomogeneities. A more scientific approach will be to investigate pure synthetic iron chromite in order to obtain

a clear idea about kinetics of selective reduction and the influence of physical and chemical variables on these. Contemporary research activities[47,48] in connection with iron ore reduction in blast furnace or by other methods of iron production justify this approach.

The literature on reduction kinetics of double iron bearing oxides is scanty in comparison to the studies on simple oxides. Amongst the iron bearing double oxides, investigations on ilmenite are encountered more frequently than other oxides. Selective reduction of iron oxides in natural ilmenite ores with various reducing agents such as electrode graphite[49], charcoal[49,50], solid carbon[51], hydrogen[52-55], carbon monoxide[55] etc. were tried. Comprehensive account of work done on natural ilmenite upto late fifties have been compiled by Walsh et al[55]. Pure synthetically prepared ilmenite was also investigated by Kamal Hussain[53].

On the chromite system, Lisnyak and Eseev[56] studied the rates of reduction of natural iron chromite ore by solid carbon within a temperature range of 350°C to 1350°C by measuring the rate of generation of carbon monoxide. They found a gradual reduction of Fe^{3+} to Fe^{2+}, separation of metallic iron, part of which got converted into iron carbides by reaction with the carbon used for reduction and finally a late reduction of Cr_2O_3 to metallic chromium.

Synthetic and natural chromite reduction was further studied by Lisnyak et al[57] and the analysis of the product was conducted by X-rays. The observations of this study duplicated those reported earlier[56].

It is clear from the review of the existing literature that mechanism and kinetics of reduction of iron oxides in iron chromite has not been studied so far from a fundamental standpoint directed towards the understanding of the selective reduction phenomenon. Hence, it was decided to conduct experimental investigations on synthetically prepared $FeO.Cr_2O_3$ to study the rates and mechanism of reduction.

I-6 METHODS OF MEASUREMENT:

The present investigation has two fold objective:

(i) The determination of equilibrium oxygen potential over a mixture of metallic iron and synthetically prepared pure chromite spinel ($FeFe_{2-x}Cr_xO_4$) of various compositions including terminal iron chromite, $FeO.Cr_2O_3$.

(ii) The study of the rates and mechanism of preferrential reduction of iron oxides in iron chromite ($FeO.Cr_2O_3$).

(i) Measurement of Oxygen Potential:

It has been pointed out in section I-4 that an earlier attempts[46] to determine the oxygen potential of $FeFe_{2-x}Cr_xO_4$ by galvanic cell with solid electrolyte was not

successful due to experimental difficulties. Hence it was decided to employ the alternative method, viz., gas equilibration technique for this purpose. In the gas equilibration method all the chemical species involved in a chemical reaction are brought into close contact with each other and the equilibrium is established between the gas phase and the condensed phases. The composition of the gas phase is either known or is determined to evaluate the equilibrium constant. The design of the gas equilibration experiments may differ widely according to the investigators planning them, but the one using a thermogravimetric apparatus appears to be extremely convenient due to the ease of experimentation, quick equilibration and efficient control of the experiment. So it was decided to use a thermogravimetric apparatus for these experiments.

A mixture of hydrogen and water vapour develops a wide range of oxygen potential depending upon its composition. The oxygen partial pressure, pO_2, can be obtained from the following reaction:

$$H_2 + \tfrac{1}{2}O_2 = H_2O \qquad \ldots (I\text{-}2)$$

and

$$pO_2 = \left[\frac{1}{K_2}\left(\frac{pH_2O}{pH_2}\right)\right]^2 \qquad \ldots (I\text{-}3)$$

Where K_2 is the equilibrium constant for the reaction (I-2). The free energy change accompanying the reaction (I-2), ΔG_2°, is given by[2]

$$\Delta G_2^\circ = -56940 + 2.91.T.\ln T - 0.64 \times 10^{-3}.T^2 - 0.08 \times 10^5.T^{-1} - 8.11.T \quad \ldots(I\text{-}4)$$

and K_2 can be calculated as

$$-RT\ln K_2 = \Delta G_2^\circ \quad \ldots (I\text{-}5)$$

Once pO_2 is known, oxygen potential of the gas mixture, μO_2, may be obtained, as:

$$\mu O_2 = RT\ln pO_2 \quad \ldots (I\text{-}6)$$

The ready commercial availability of hydrogen adds to the advantages of using hydrogen-water vapour mixture apart from its ease of generation. Hence, in the present thermodynamic investigation it was decided to use a hydrogen-water vapour mixture for gas equilibration in a thermogravimetric apparatus.

A pellet containing $FeFe_{2-x}Cr_xO_4$ and iron (alongwith Cr_2O_3 in case of terminal composition $FeO.Cr_2O_3$) if suspended from the arm of a thermobalance into a furnace and allowed to come in contact with a hydrogen-water vapour mixture, may lose weight due to reduction or gain weight due to oxidation if the oxygen potential of the gas mixture is respectively lower or higher than that of the iron-$FeFe_{2-x}Cr_xO_4$ mixture at the furnace temperature. But if the oxygen potential of the gas mixture equals that of the iron-$FeFe_{2-x}Cr_xO_4$ mixture at that

temperature no change in weight of the pellet will be observed, representing the desired quantity for the gas equilibration experiments. Keeping the gas composition constant, the furnace temperature may be changed to obtain the temperature where there is no change in weight.

(ii) Kinetic Investigation:

In fundamental investigation on kinetics and mechanism of gas-solid reactions, the use of single pellet is widespread because of the ease of mathematical and physical tractability offered by an isolated single pellet compared to a fixed or moving bed of particles. The geometry of the single pellet, when spherical, simplifies the situation still further because a single dimension represents it adequately. So for kinetic studies it was decided to use spherical single pellets of synthetically prepared terminal iron chromite ($FeO.Cr_2O_3$).

The use of a dense pellet for kinetic investigation in a gas-solid system has an advantage over a porous pellet because of its ability to keep the reaction front at a sharp interface without allowing reaction to take place throughout the pellet and this in turn keeps the reaction more amenable to mathematical treatment. So for fundamental analysis of any gas-solid reaction dense pellets are more frequently chosen in comparison to porous pellets. Study of dense pellets normally yield other valuable informations as well.

But as porosity is a common physical variable in natural ores, it is desirable to investigate porous pellets also for any investigation to satisfy its practical utility. Hence, it was decided to use dense as well as porous spherical pellets of terminal iron chromite $FeO.Cr_2O_3$ for the reduction experiments.

Hydrogen would be used in the reduction experiments because of its easy availability, the fact that it is non-poisonous unlike carbon monoxide and its use is widespread as a reducing gas.

The use of thermogravimetric apparatus in kinetic investigations in gas-solid reactions is well established[47] because it allows measurement of weight changes either continuously or intermittently on reacting solid without interrupting the experiment. It is also capable of yielding data of good accuracy. Hence its choice for reduction experiments was only natural because of the previous decision to use thermogravimetry for the gas equilibration experiments also.

From earlier investigations[17] on thermal beneficiation of chromite ores it is evident that the rate of reduction is appreciable at a temperature around 1000°C. So it was decided to conduct the reduction experiments at 1050°C and a single temperature was chosen instead of a temperature range because before obtaining a clear and complete analysis of a gas-solid reaction at a fixed temperature, temperature dependence of rate does not add

much to the fundamental understanding of the process.

It is well known that measurement of rates of reduction in a thermogravimetric apparatus is not enough to give an insight into the reduction phenomenon. For a fundamental analysis it should be coupled with other investigations like microstructural investigation, X-ray diffraction analysis, etc. and these would be pursued in the present investigation also.

i-7 PLAN OF THE WORK:

It was planned (1) to prepare synthetic chromite, $FeFe_{2-x}Cr_xO_4$, of different compositions including terminal iron chromite $FeO.Cr_2O_3$ starting from pure Cr_2O_3, Fe_2O_3 and metallic iron powders.

(2) to design a gas train for generating a mixture of hydrogen and water vapour over a range of composition.

(3) to determine the oxygen potential of a mixture of metallic iron and $FeFe_{2-x}Cr_xO_4$ of different compositions by gas equilibration in a thermogravimetric apparatus over a temperature range of 850°C to 1050°C and calculate the thermodynamic parameters of the system permitted by these data.

(4) to study the rates of reduction of dense as well as porous spherical pellets of $FeO.Cr_2O_3$

at 1050°C in pure and dry hydrogen by thermogravimetry.

(5) to interpret the rate and mechanism of reduction of spherical pellets from the above thermogravimetric as well as auxilliary investigations such as microstructural examination, X-ray diffraction analysis, etc.

CHAPTER II

APPARATUS

The sketch of the apparatus is shown schematically in Fig. 1. The details of the apparatus can be discussed under two broad headings, viz., the gas train and the thermogravimetric set up.

II-1 GAS TRAIN:

The gas train consisted of arrangements for the removal of oxygen and moisture from commercial hydrogen and nitrogen gases, their flow measurement as well as generation of controlled hydrogen-water vapour mixtures for gas equilibration experiments.

(i) Purification and Metering of Hydrogen and Nitrogen:

This part of the gas train consisted of two separate channels, one for nitrogen and the other for hydrogen. The nitrogen gas was passed through a bubbler and a capillary flowmeter where the volumetric flowrate of the gas was registered. The outlet of the flowmeter was connected to a nichrome wound copper gauze furnace kept at 500°C, where the bulk of the oxygen present in the gas could be absorbed by copper turnings. The gas subsequently

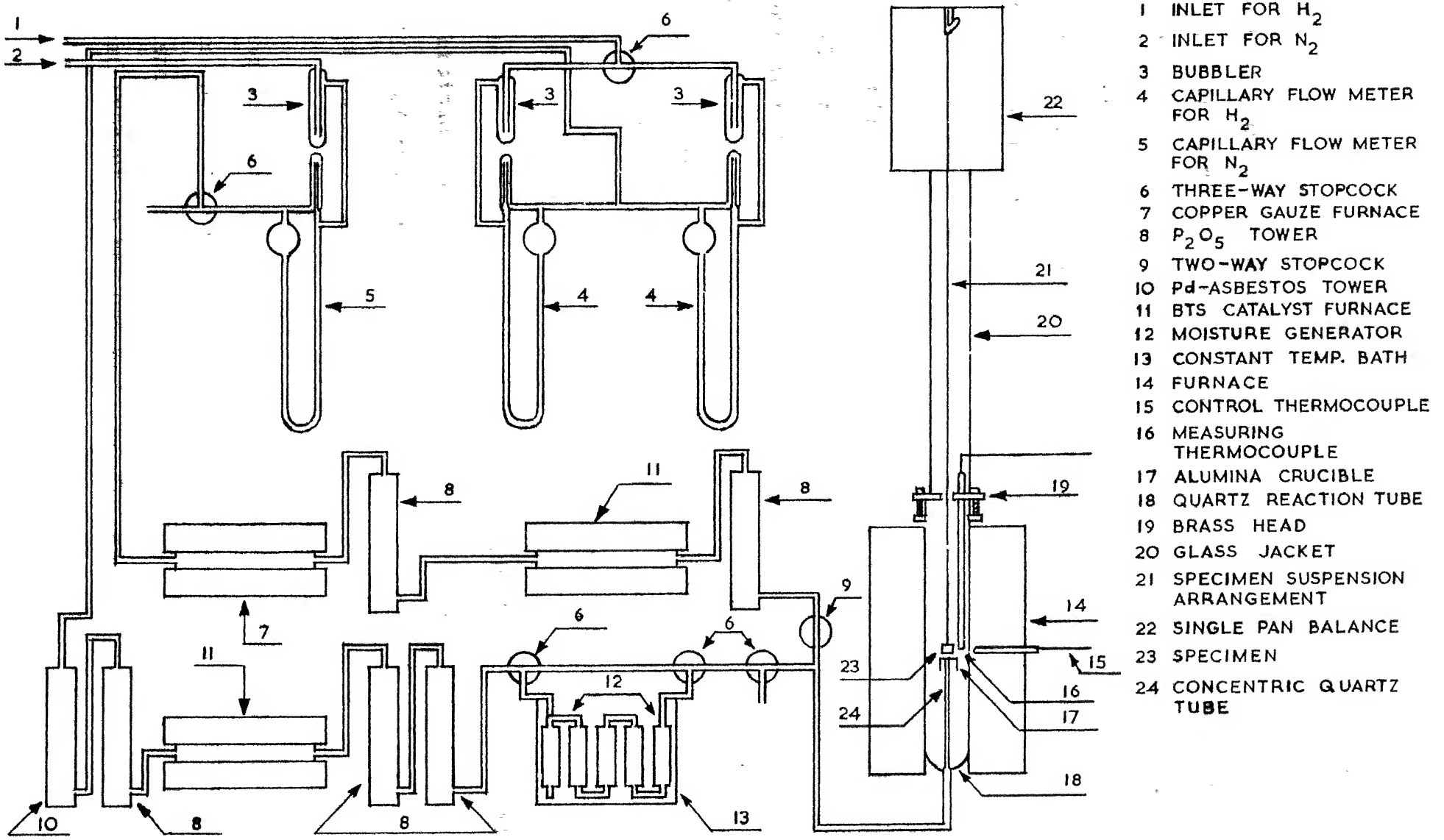

FIG. 4: SKETCH OF THE APPARATUS.

entered a tower filled with phosphorous pentoxide for removal of moisture from nitrogen. Any trace of oxygen that could escape the copper gauge furnace was absorbed when the gas was subsequently passed through a furnace at 200°C containing BTS catalyst. This catalyst contains finely divided copper on a suitable porous base. Because of the high specific surface area it can efficiently absorb oxygen at a much lower temperature range, viz., 150°C to 200°C. Its capability to bring down oxygen partial pressure in the gas flowing across it is much better as compared to a conventional copper gauze furnace. After the entrapment of the remaining oxygen in the BTS catalyst furnace, the nitrogen gas entered another tower filled with phosphorous pentoxide for absorption of any moisture that might have escaped the previous tower. The outlet of the gas tower was connected to the bottom of the reaction tube through a T-joint alongwith the hydrogen line. The moisture and oxygen free nitrogen gas so obtained was used to flush the reaction tube during the heating of the furnace to experimental temperature after introduction of specimen.

The inlet of hydrogen line consisted of two subchannels each containing a bubbler and a capillary flow-meter one meant for measurement of low volumetric flowrates and another for high volumetric flowrates. The bulk of the oxygen present in the gas was made to react with hydrogen by passing through palladized asbestos catalyst. Next the

gas entered a tower filled with phosphorous pentoxide for absorption of moisture. Traces of oxygen remaining in the hydrogen stream were subsequently converted into moisture by BTS catalyst kept inside a furnace at 200°C and the moisture so produced was removed by two phosphorous pentoxide towers kept next in the gas line. The oxygen and moisture-free hydrogen so obtained was introduced into the reaction chamber for the reduction experiments. Gas equilibration experiments required controlled hydrogen-water vapour mixtures. Therefore, in the latter case the hydrogen was passed through the H_2O vapour generator (described in the next subsection). A 36-gauge nichrome wire was wound round the glass tube connecting the outlet of the moisture generator and the bottom of the reaction tube. The nichrome wiring was used to heat up the tube to avoid condensation of moisture on the walls of the glass tube, whenever a high percentage of moisture was used in the gas mixture. Three-way stopcocks were employed to provide for by-passing of gases. To minimize heat loss the nichrome winding was covered up with an insulating winding of $\frac{1}{4}$ inch dia. asbestos rope.

(ii) Generation of Controlled Hydrogen-Water Vapour Mixture:

A mixture of hydrated and anhydrous oxalic acid crystals was chosen for this purpose. The hydrated acid decomposes according to equation (II-1):

$$(COOH)_2, 2H_2O = (COOH)_2 + 2H_2O \quad \ldots (II\text{-}1)$$

The equilibrium partial pressure of water vapour (pH_2O), which the ambient gas in contact with the mixture could develop, was determined first in 1920 by Baxter and Lansing[58] as a function of temperature as:

$$\log pH_2O \text{ (m.m.)} = 18.053 - \frac{9661}{T+250}, \quad 273.2 \leqslant T \leqslant 323.2°K \quad \ldots (II\text{-}2)$$

Fig. 5 shows the variation of equilibrium pH_2O as a function of temperature as expressed by equation (II-2). In their experiments, they took a powdered mixture of oxalic acid dihydrate with 10% anhydrous oxalic acid and passed a known volume of dry air through the mixture at a constant temperature inside a thermostat. pH_2O was determined by absorbing the moisture in dessicating towers.

Bookey and Tombs[59] in 1952 redetermined the pH_2O for the same range of temperature over this mixture and their experimental observation agreed accurately with the original equation (II-2) determined by Baxter and Lansing. Bookey and Tombs also studied the effect of variation of volumetric flow rate of ambient gas (hydrogen) on the equilibrium relationship. They observed that the relationship expressed by equation (II-2) remained valid even for a hydrogen flow rate of 20 litres/hour. This was the highest flowrate used in their experiments and might not necessarily

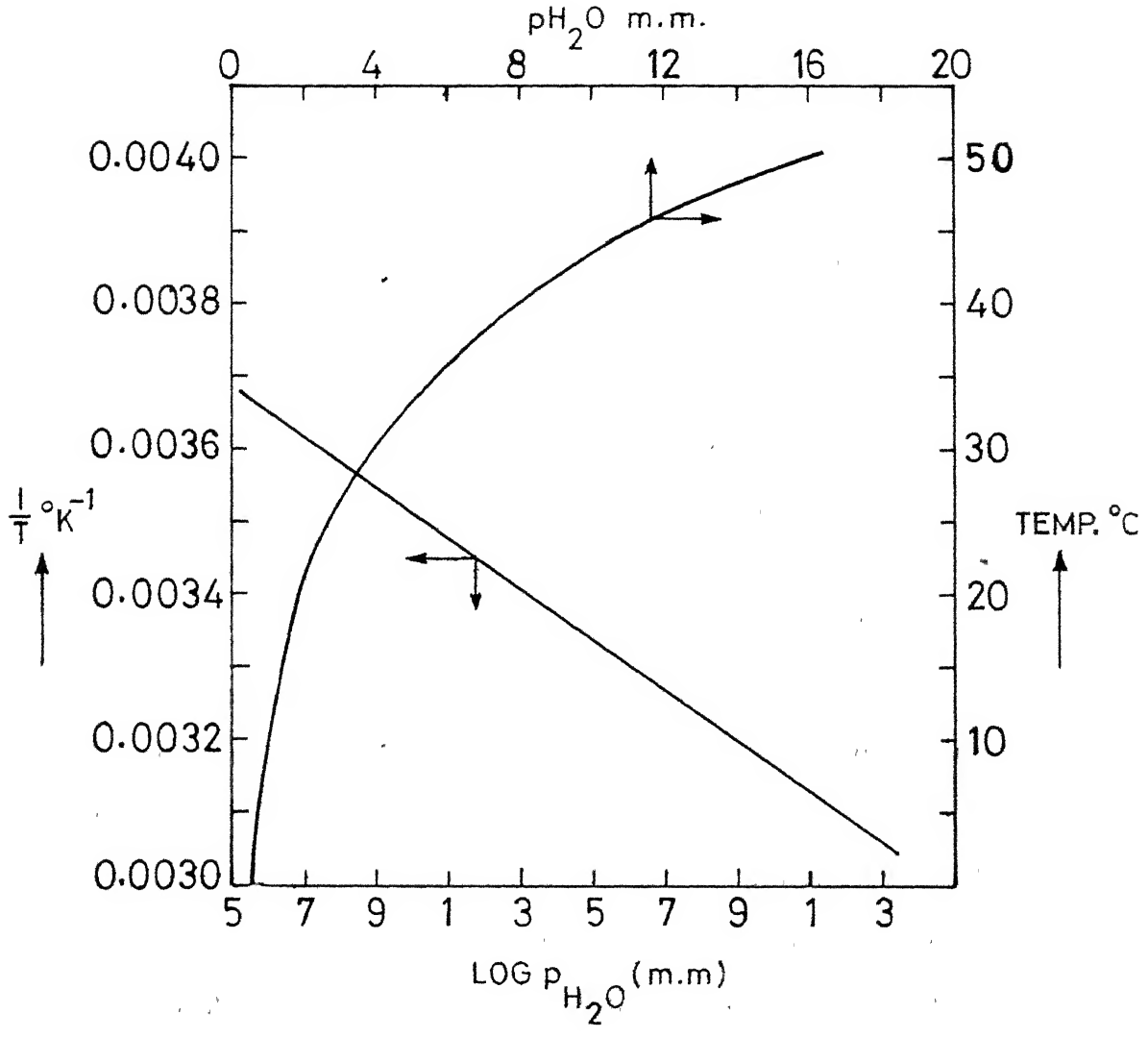

FIG. 5: VARIATION OF p_{H_2O} WITH TEMPERATURE IN $(COOH)_2 \cdot 2H_2O/(COOH)_2$ MIXTURE[58]

mean the limiting flowrate for the validity of equation (II-2).

From the existing data on the free energy of formation of terminal chromite, the equilibrium ratios of partial pressure of water vapour to hydrogen, pH_2O/pH_2, and then pH_2O values were calculated as a function of temperature in the range of 850°C-1050°C. It was observed that the pH_2O range established by the experiments of Baxter and Lansing[58], obtainable from the oxalic acid dihydrate covered most of the pH_2O values obtained by calculation from free energy data.

Hence it appeared that the oxalic acid dihydrate was an excellent source of low vapour pressure of moisture suitable for gas equilibration of chromite spinels and it was decided to use this.

A.R. grade oxalic acid dihydrate was taken and mixed in a porcelain morter and pestle with 10% anhydrous oxalic acid crystals. Anhydrous oxalic acid was prepared by heating the hydrated crystals in an air oven at 100°C for 10 to 15 minutes. The mixture was then ground to a fine powder and filled inside a series of glass U-tubes compactly blown together into one assembly. This assembly was subsequently placed inside a Fisher constant temperature water bath and it was glassblown into the hydrogen gas line. The inlet of the U-tube assembly was connected to oxygen and moisture free hydrogen gas source and the outlet was connected to

the reaction chamber via a three way stopcock with one arm open to the atmosphere. Depending upon the temperature of the water bath, the hydrogen gas flowing through the moisture generator should develop a definite water vapour partial pressure. The temperature of the water bath could be controlled to $\pm 0.1°C$ using a mercury expansion relay. Inside the water bath, no temperature difference could be detected from place to place because of good insulation and magnetic stirring. The bath temperature was measured by a mercury thermometer with 0.1°C calibration, kept near the outlet side.

II-2 THERMOGRAVIMETRIC SETUP:

This part of the apparatus consisted of (i) a furnace and a reaction tube with arrangements for its temperature measurement and control, (ii) a single pan balance kept vertically above the furnace, and an arrangement for suspending the specimen from the balance, and (iii) an arrangement for the control of gas flow in the reaction tube.

(i) The Furnace and Reaction Tube, Temperature Measurement and Control:

The assembly consisted of a kanthal-wound vertical furnace of 20 inch length. A fused quartz tube of $1\frac{3}{4}$ inch I.D. served as the reaction chamber. The temperature

of the furnace was controlled by a Leeds & Northrup model 6260 Electromax solid state controller actuated by a Pt/Pt - 10% Rh thermocouple. The accuracy of temperature control was $\pm$1°C. A constant temperature zone of about 2 inch length could be obtained at the centre of the furnace. At the top of the quartz reaction tube a brass head with two holes provided an airtight cover during the experiments. A chromel-alumel thermocouple with a sheath was placed at the centre of the reaction tube through one hole in the brass head. This thermocouple was placed to within $\frac{1}{4}$ inch of the specimen, and was used to record the temperature of the specimen during experiments with the help of a model 8686 Leeds & Northrup potentiometer. The other hole on the brass head was located centrally and was of 1 m.m. dia. It was used for suspending the specimen from the single pan balance into the reaction tube.

(ii) Specimen Suspension Arrangements:

Vertically above the reaction tube a single pan Mettler balance of type H15 was kept on a platform. From the hook of this balance a chromite pellet could be suspended at the centre of the reaction chamber with the help of a suspension system running through the central hole (of 1 m.m. dia.) on the brass head. The suspension system for thermodynamic experiments was made of three parts. The lower part in contact with the specimen was made of $\frac{1}{16}$ inch

dia. and 8 inch long transparent quartz rod with a small bead of $\frac{1}{8}$ inch dia. made by fusion at the lower end. The quartz rod passed through an $\frac{1}{16}$ inch dia hole drilled in the pellet which rested on the bead. Fig. 6 shows the specimen suspension arrangement for gas equilibration experiments. The middle part of the suspension system was a 36-gauge nichrome wire which passed through the central hole in the brass head, connecting the quartz rod with the upper part of suspension system. The upper part of the suspension system was made of $\frac{1}{16}$ inch dia inconel rod hung from the hook of the single pan balance upto a distance of 5 inch from the top of the brass head on the reaction tube. Such a suspension arrangement was chosen in order to prevent vibration of the optical scale of the balance, reaction between the pellet and nichrome wire, oxidation of nichrome wire and also to keep the hole on brass head as small as possible.

In the reduction experiments, since there was no moisture in the hydrogen gas, the oxidation of chromium in nichrome wire was not a problem, and hence the use of quartz rod could be avoided. A spherical pellet of chromite was kept on a nichrome basket which was suspended by the nichrome wire.

A glass tube of 1 inch dia. was used as a jacket around the suspension system from the bottom of the balance upto the brass head to prevent the convection current of air

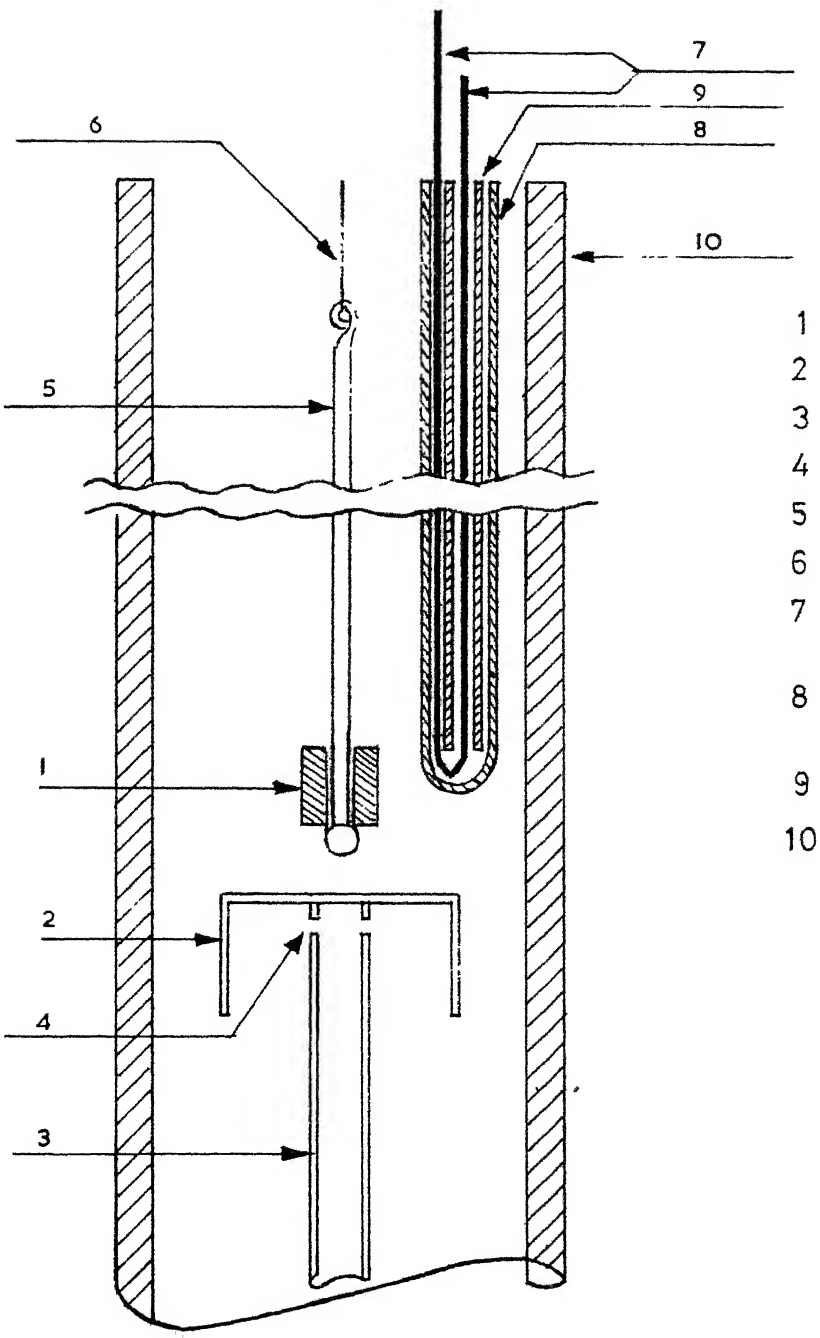

1 CYLINDRICAL PELLET
2 INVERTED ALUMINA CRUCIBLE
3 QUARTZ TUBE
4 HOLES IN QUARTZ TUBE
5 QUARTZ ROD
6 36 GAUGE NICHROME WIRE
7 CROMEL-ALUMEL THERMOCOUPLE
8 QUARTZ THERMOCOUPLE PROTECTION TUBE
9 PORCELAIN SHEATH
10 QUARTZ REACTION TUBE

FIG. 6: ARRANGEMENT INSIDE THE REACTION TUBE FOR GAS EQUILIBRATION EXPERIMENTS.

rising along the shell of the furnace from striking the suspension system. If uncontrolled, this would cause vibration of the optical scale of the balance. Such a vibration of the optical scale was found to reduce the sensitivity of the balance and made detection of small weight changes almost impossible. Preliminary trial on gas equilibration experiments without a jacket around the suspension system met with little success because of the difficulties in detection of the equilibrium point corresponding to no gain or loss in weight by the sample due to excessive vibration of the optical scale of the balance.

(iii) Control of Gas Flow Inside the Reaction Tube:

A flow rate of 200-250 c.c./min. of hydrogen-water vapour mixture for the gas equilibration experiments was decided already. As the diameter of the reaction tube was $1\frac{3}{4}$ inch the average velocity of the gas mixture came within the range of 0.21 cm/sec. to 0.27 cm/sec. The low velocity of the mixture, the large difference in molecular weight of the components of the gas mixture coupled with a high temperature gradient along the length of the reaction tube leads to the possibility of thermal diffusion. As a result of this, the ratio of pH_2O/pH_2 in contact with the chromite-iron pellet during the experiments might be different from the values set by the constant temperature bath.

This implied that the reaction tube required arrangements to minimize thermal diffusion. Fig. 6 shows the arrangement to achieve this.

By fusing a quartz tube of 5 m.m. I.D. concentric to the reaction tube at the bottom, the gas mixture could be taken up to the constant temperature zone of the reaction tube at the centre, at a high velocity (17-21 cms/sec) which should reduce thermal diffusion of the gas components to a negligibly small value. After reaching the constant temperature zone of the reaction tube through the thin tube, the gas mixture required some space to develop smooth flow pattern. Proper attainment of the temperature of experiment by the gas mixture should also be ensured. An inverted alumina crucible of 28 m.m. dia. and 10 m.m. length was put on the open end of the 5 m.m. dia. quartz tube. The gas could come out of the tube through a number of small holes drilled along the periphery of the quartz tube at its end. In and around the inverted alumina crucible the gas could develop smooth flow and a low velocity while traversing the constant temperature zone. Heat transfer calculations were carried out as per Martinelli's Equation[60] which is applicable to this type of situation, to check whether the gas mixture could be heated upto the experimental temperature during the time it was in contact with the constant temperature zone before coming into contact with the specimen. It was found that the heat transfer rate was more than enough and there was

no possibility of a significant temperature difference between the specimen and incoming gas.

For the reduction experiments, since no water vapour was present in the hydrogen gas, the problem of thermal diffusion did not arise. A volumetric flow rate of 500 c.c./min. was decided upon from preliminary experiments on dense and porous chromite pellets.

CHAPTER III

MATERIAL PREPARATION

III-1 THE BASIC RAW MATERIALS AND THEIR SPECIFICATIONS:

The basic raw materials used in the experiments and for preparation of materials are listed below alongwith their grades and sources.

Chromium Sesquioxide (Cr_2O_3): Fisher certified reagent grade, Fisher Scientific Co., U.S.A.

Ferric Oxide (Fe_2O_3): -do-

Iron Powder (Fe); -do-

Oxalic Acid Dihydrate ($(COOH)_2, 2H_2O$): Analytical reagent grade, British Drug House, Bombay, India.

III-2 PREPARATION OF SYNTHETIC CHROMITE FOR GAS EQUILIBRATION EXPERIMENTS:

Synthetic chromite was first prepared by Chatterjee and Sidhu[61] from pure FeO and Cr_2O_3 by fusion in an arc furnace. An equimolar mixture of FeO and Cr_2O_3 was taken in a graphite crucible and a 250 V., D.C. indirect arc was struck inside the crucible by an electrode placed eccentrically inside the graphite crucible. The crucible was rotated during arcing for uniform melting of the charge.

The first attempt to prepare chromite in this study was exactly in that line using a mixture of Fe_2O_3, Cr_2O_3 and metallic iron powder inside a graphite crucible and the arc was struck by a graphite electrode placed vertically above the charge in an argon atmosphere. But little success was achieved in that attempt due to the nonuniform melting of charge, localized over heating in the arc damaging the electrode because of the poor control of current through electrode during arcing.

Next attempt for chromite preparation was according to the method used by Roychowdhury[46]. According to that method stoichiometric amounts of Cr_2O_3, Fe_2O_3 and Fe were taken corresponding to each composition of chromite and mixed thoroughly under acetone in an agate morter and pestle. Cylindrical pellets of $\frac{3}{8}$ inch dia. were pressed out of that mixture in a die. The pellets were vacuum sealed inside quartz capsule and heated at 1000°C for seven days in a globar furnace. The sintered pellets were ground to fine powder and the same process of pelletizing, vacuum sealing and sintering was repeated to ensure complete conversion of the reactant to chromite. X-ray powder pattern of the chromite so produced after first and second sintering was taken in a Debye-Scherrer camera using chromium radiation. These patterns when compared with those of pure iron, Cr_2O_3 and Fe_2O_3 separately obtained under same condition indicated no

evidence of the presence of unreacted reactants in the final product. The 'd' values and the intensities of the different lines of chromite of terminal composition were compared with those of published data[61] and the agreement was good.

Chemical analysis of the chromite samples were done by taking a known weight of chromite sample in a platinum crucible and repeatedly heating it in a furnace and weighing after cooling in a dessicator to constant weight. The gain in weight was compared with the expected change in weight for complete oxidation of FeO in chromite to Fe_2O_3. It was found that the gain in weight obtained experimentally was 93% of the expected change. This essentially indicated that excess oxygen was somehow getting incorporated in the end product during material preparation. It was attributed to the diffusion of oxygen through the wall of the quartz tube at high temperature during sintering. Such phenomenon has been reported by Norton and Seybolt[62].

Finally a method introduced by Francomb[63] which was slightly different from the above one was tried. In this method, first a solid solution of Fe_2O_3 and Cr_2O_3 was made by taking weighed amounts of the two oxides according to the desired composition of the chromite by mixing and heating in a platinum crucible at 1250°C for a day. The sesquioxide solid solution so produced was mixed thoroughly with excess iron powder pressed into cylindrical pellets of $\frac{3}{8}$ inch dia.

and vacuum sealed inside a quartz tube. The sealed quartz capsule was then vacuum sealed inside another quartz tube of larger diameter. This double sealing was expected to minimize diffusion of oxygen through quartz tube at high temperature. The double sealed capsules were heated at 1000°C for seven days. The excess metallic iron reduced the sesquioxide solid solution to chromite during heating and chromite of desired composition could be produced. X-ray diffraction pattern of the powdered chromite samples so obtained was taken after magnetic separation of excess iron and the 'd' values were calculated and excellent agreement was obtained for terminal chromite with existing data[61]. Table IV shows the composition of the spinel as well as excess Cr_2O_3 and Fe in pellets for gas equilibration experiments.

To ensure the absence of any excess oxygen in the product, and completion of the reduction reaction of Fe_2O_3 - Cr_2O_3 solid solution by excess metallic iron, chemical analysis of the chromite samples were carried out by two tests e.g. (i) gain in weight on complete oxidation,

(ii) estimation of excess metallic iron in chromite.

(i) Oxidation Test:

A known weight of the chromite sample was repeatedly heated at 850°C-900°C in a platinum crucible, cooled in a dessicator and weighed till constant weight. The gain in weight was compared with the expected

TABLE IV

Compositions of Pellets Used For Gas Equilibration Experiments

Composition No.	Excess Cr_2O_3, percent	Excess Iron, percent	Values of x in $FeFe_{2-x}Cr_xO_4$
1	14.3	14.3	2.0
2	nil	20.2	1.83
3	nil	23.0	1.69
4	nil	25.3	1.43

change on complete oxidation of FeO to Fe_2O_3. The comparison between the expected change and the observed change was excellent indicating that double sealing of quartz capsules could eliminate diffusion of oxygen across quartz at elevated temperature during sintering.

(ii) Estimation of Excess Metallic Iron:

As a known excess of metallic iron was added to the sesquioxide solid solution for its reduction to chromite spinel of desired composition, a part of it should react with the Fe_2O_3 of sesquioxide solid solution. So in case of reduction reaction remaining incomplete, percentage of excess metallic iron remaining unreacted would be higher than the expected value. For chromites of all composition, excess metallic iron was estimated according to the procedure followed by Katsura and Muan[37]. In a conical flask weighed amount of powdered mixture of chromite and excess iron was heated with 1:4 H_2SO_4 solution under a CO_2 atmosphere. The solution was boiled for ten minutes for complete dissolution of metallic iron. After cooling under a tap, the solution was filtered and the filtrate was titrated against $KMnO_4$ solution. $KMnO_4$ was standardized against oxalic acid solution. Percentage of excess metallic iron in the sample was calculated from the titration data. For each composition two estimations were done. Excellent agreement was obtained between the estimated values and the expected percentages of excess metallic

iron within the limits of experimental error for all the four compositions of chromite.

As the chromite pellet for gas equilibration experiments should contain metallic iron apart from chromite, the addition of excess metallic iron powder during sintering yielded pellets ready for use. In the case of terminal composition e.g., composition number 1, the pellet should contain excess Cr_2O_3 alongwith $FeO-Cr_2O_3$ and metallic iron. This excess Cr_2O_3 was added during the preparation of sesquioxide solid solution.

As mentioned in section I-3, the composition of iron chromite spinel can be represented as $FeFe_{2-x}Cr_xO_4$, where x is a variable parameter between 2 and 0 corresponding to the terminal phases $FeO.Cr_2O_3$ and $FeO.Fe_2O_3$ respectively. The variation of the parameter x in the four compositions made for thermodynamic study was between 2 to 1.43, because the subject matter of this investigation is $FeO.Cr_2O_3$-rich side of the solid solution.

III-3 PREPARATION OF SPHERICAL CHROMITE PELLETS FOR REDUCTION EXPERIMENTS:

Terminal chromite ($FeO.Cr_2O_3$) was prepared from stoichiometric mixture of Cr_2O_3, Fe_2O_3 and metallic iron powders, mixed thoroughly under acetone, pressed into cylindrical pellets and sealed inside a quartz tube under vacuum and that quartz capsule was again sealed under vacuum

inside another quartz tube of larger diameter. After heating the mixture at 1000°C for seven days, the chromite so prepared was crushed, ground to fine powder, pressed into pellets, double sealed under vacuum inside quartz tubes and resintered at 1000°C for seven days to ensure compositional homogeneity. X-ray diffraction pattern and oxidation test as described in the previous section indicated that the material was pure chromite. The chromite pellets were crushed and ground under acetone in an agate morter and pestle. The powder was moistened with distilled water and spherical pellets were prepared from the moistened powder by careful handrolling. The pellets were dried in a vacuum dessicator for about ten hours.

Trial experiments showed that sintering of chromite pellets to a high density near the theoretical value was possible at a temperature around 1650°C and a sintering time of 2-3 hours with an approximate heating and cooling rate of about 100°C/hr.

Fig. 7 shows the sketch of the gas train and the 24 inch long vertical graphite tube furnace used for sintering. Purified argon atmosphere was maintained over the chromite pellets during sintering. Cylinder argon was purified by passing the gas first through a tower filled with 'Indicarb' supplied by Fisher Scientific Co. which principally consists of sodium hydroxide for absorption of carbon dioxide from the gas. Subsequently, the gas entered a tower filled with phosphorous pentoxide and then a copper gauze furnace

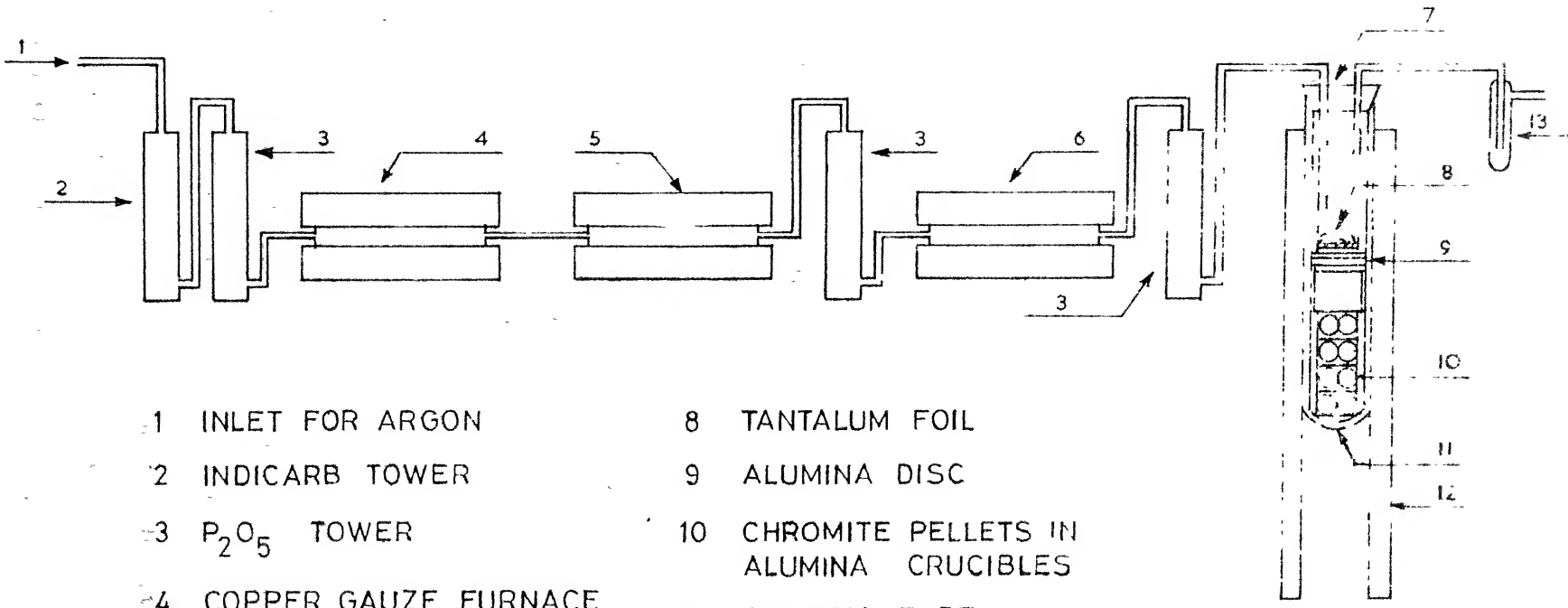

1 INLET FOR ARGON

2 INDICARB TOWER

3 P_2O_5 TOWER

4 COPPER GAUZE FURNACE

5 BTS CATALYST FURNACE

6 TITANIUM CHIP FURNACE

7 SILICONE RUBBER STOPPER

8 TANTALUM FOIL

9 ALUMINA DISC

10 CHROMITE PELLETS IN ALUMINA CRUCIBLES

11 ALUMINA TUBE

12 GRAPHITE TUBE OF FURNACE

13 BUBBLER

FIG. 7: SINTERING APPARATUS.

kept at 500°C for removal of moisture and the bulk of oxygen present in the gas. The remaining oxygen and moisture and any hydrogen present in the gas could be absorbed from the gas by successively passing it through BTS catalyst furnace, phosphorous pentoxide tower and titanium chip furnace at 600°C and finally again through a phosphorous pentoxide tower.

An one end closed alumina tube of $1\frac{1}{4}$ inch I.D. was kept vertically inside the graphite furnace and served as the sintering chamber. The green chromite spheres contained in four 28 m.m. dia. recrystallized alumina crucibles of 15 m.m. length were slowly lowered one after another inside the alumina tube. A 3 inch long empty alumina crucible was placed above the crucibles containing chromite pellet as a spacer. Then a few circular alumina discs were kept as radiation shields above which an alumina crucible containing tantalum foil was placed as an additional precaution to take care of any oxygen which might escape into the sintering chamber. The alumina tube was carefully positioned inside the graphite furnace so that the crucibles containing the chromite pellets were evenly distributed within the constant temperature zone of the furnace which was $2\frac{1}{2}$ inch long. The open end of the alumina tube was closed with a silicone rubber stopper with inlet and outlet tubes for argon in it. The inlet tube was connected with purified argon flow line and the outlet tube was connected to a bubbler. The joint between the silicone

rubber stopper and alumina tube was sealed with silicone sealant just as all glass to rubber joints. The copper gauze, BTS catalyst and titanium chip furnaces were switched on and heated to the operating temperatures of 500°C, 200°C and 600°C respectively. After flushing the system with purified argon for about 8 to 10 hours, the graphite furnace was switched on and gradually heated upto 1650°C and maintained at that value for about 3 hours. Then it was slowly cooled down to room temperature with a cooling rate of approximately 100°C/hr.

X-ray diffraction pattern of the surface of the dense pellets together with the oxidation test mentioned in the previous section was carried out to ensure the compositional consistency of the chromite at the end of sintering and the results of these tests were satisfactory.

The procedure for preparation of the porous pellets of terminal chromite was the same as that of the dense pellet, excepting that a lower temperature of 1300°C was employed for 3 hours during sintering.

III-4 DETERMINATION OF DENSITY OF CHROMITE SPHERES:

The densities of the pellets after sintering were determined from the measurement of their diameter by a micrometer and recording their weights. The density of the dense pellets was found to vary between 4.61 to 4.54 gms/cm^3

and that for the porous pellets between 2.52 to 2.91 gms/cm^3. Theoretical density value of $FeO.Cr_2O_3$ was found to be different in different compilations apart from a range of values reported by each compilation like 4.3 to 4.6 gms/cm^3[64] and 4.5-5.1 gms/cm^3[65]. But since the lattice parameter of $FeO.Cr_2O_3$ is precisely known[38] it was decided to calculate the theoretical density from X-ray data using the relationship[66] (III-1):

$$\rho_T = \frac{1.66020.n_2.M}{V} \qquad \ldots \quad (III\text{-}1)$$

where ρ_T is the theoretical density of $FeO.Cr_2O_3$ in gms/cm^3, V is the volume of a unit cell in A^3 (having an edge length of 8.344A in this case[38]), n_2 is the number of molecules in a unit cell which is 8 in this case and M is the molecular weight of $FeO.Cr_2O_3$ i.e., 223.85. ρ_T was found to be 5.1 gms/cm^3. Porosity, ϵ, of the pellets was calculated as:

$$\epsilon = 1 - \frac{\rho_a}{\rho_T} \qquad \ldots \quad (III\text{-}2)$$

Where ρ_a is the actual density. In the case of dense pellets, porosities varied between 0.096 to 0.109 and for porous pellets between 0.505 and 0.43.

CHAPTER IV

EXPERIMENTAL PROCEDURE

The procedures for the reduction experiments, gas equilibration of terminal chromite ($FeO.Cr_2O_3$) and gas equilibration of chromites of other composition were not the same. Hence they are discussed separately.

IV-1 GAS EQUILIBRATION FOR TERMINAL CHROMITE ($FeO.Cr_2O_3$):

Through a cylindrical pellet of $\frac{3}{8}$ inch dia., containing terminal chromite, Cr_2O_3 and metallic iron, a $\frac{1}{16}$ inch dia. hole was drilled. The quartz rod of the suspension system was slipped through that hole and the pellet was suspended at the centre of the reaction tube by the nichrome wire. The brass head was tightly fixed onto the reaction tube by tightening the screws and the Mettler balance was placed in such a way that the nichrome wire of the suspension system did not touch the wall of the 1 m.m. dia. central hole on the brass head through which the wire passed. The copper gauze and the BTS catalyst furnaces were switched on for heating. Next purified nitrogen was allowed to flow into the reaction chamber. After flushing the reaction chamber for about two hours, the power to the furnace was switched on. Heating was slow in order to avoid thermal cracking of the specimen and took 12-14 hours. Then the constant temperature bath was switched on and the temperature was set at around

37°C. Within half an hour the mixture of oxalic acid dihydrate and anhydrous oxalic acid in the U-tube assembly inside the constant temperature bath reached the desired temperature. After about 12 to 14 hours time, the temperature of the reaction tube as recorded by the chromel-alumel thermocouple reached near 850°C. Next, the hydrogen flow was started through the oxalic acid mixture and was let out into the atmosphere through the by-pass. The hydrogen flow was allowed to stabilize for about half an hour for a definite flow rate between 200-250 c.c./min. The weight of the pellet was recorded. Then the hydrogen-water vapour mixture was introduced into the reaction tube and the nitrogen flow was stopped immediately. The weight and the temperature of the pellet were recorded at definite intervals of time. If two consecutive readings showed an increase or decrease in weight, indicating oxidation or reduction of the pellet, the furnace temperature was raised or lowered, until the temperature corresponding to no loss or no gain in weight i.e., equilibrium temperature was obtained. The time interval between two consecutive readings in weight varied between five minutes to an hour depending upon the temperature of equilibration and the difference of the furnace temperature and the equilibrium temperature. At higher temperatures, the rates of oxidation or reduction were faster, hence, weight changes were quick. On the average, the approach to the equilibrium took about fifteen hours

time. After obtaining the equilibrium temperature, the constancy in weight was checked on the average for 10 to 12 hours to make sure that true equilibrium temperature was being recorded. Then the water bath temperature was raised and the next higher equilibrium temperature was determined in the same manner. The replacement of the acid mixture if required could be done either by switching over to nitrogen without switching off the furnace or by shutting down the furnace and starting with a fresh pellet and acid mixture. After obtaining the equilibrium temperature, the atmospheric pressure was recorded from a barometer everytime to obtain $pH_2O + pH_2$ values at equilibrium.

IV-2 GAS EQUILIBRATION OF CHROMITES OF COMPOSITION 2, 3, AND 4:

For compositions of chromite other than that of the terminal phase there was a possibility of change in composition of the spinel due to oxidation or reduction during equilibration. As a result a slightly different procedure was followed in order to ensure compositional constancy. This could be attained by oxidising and reducing the pellet during equilibration in such a manner so as to return to the original weight of the pellet when the equilibrium temperature was located.

In this modified method, hydrogen gas was let into the reaction tube instead of nitrogen at room temperature.

The chamber was flushed for about an hour with hydrogen and then the flowrate of hydrogen was set at 0.8 litres/min. and was allowed to stabilize for some time. The weight of the pellet was recorded as the initial weight. In a thermogravimetric apparatus, the weight of the sample, to some extent, depends slightly upon the velocity of gas flowing past the sample due to buoyancy and drag effect. Between the temperature limits of gas equilibration experiments i.e., 1123°K to 1323°K, the volume of hydrogen is 3.7 to 4.4 times that of the room temperature volume. Hence, on an average a flowrate of 0.8 litres/min., four times the normal volumetric flowrate of 0.2 litres/min., should be maintained when the reaction tube is at room temperature in order to obtain the corrected initial weight of the pellet. The difference in weight for a four fold increase in hydrogen flowrate was around 2 to 3 milligrams. After recording the corrected initial weight of the pellet, nitrogen flow replaced hydrogen flow and the furnace power was switched on. The hydrogen-water vapour mixture was generated following the procedure outlined in the previous section. After attainment of the temperature of around 850°C, the gas mixture was let into the reaction chamber replacing nitrogen. The temperature of the furnace was adjusted frequently such that the weight of the pellet during oxidation or reduction steps did not change significantly from the corrected initial weight of the same. With this extra condition imposed on

equilibration, the approach to equilibrium took about 20 to 25 hours time on an average. The constancy in weight after obtaining the equilibrium temperature at the corrected initial weight of the sample was checked for about 12 hours. After recording the equilibrium temperature, the atmospheric pressure was recorded from the barometer, the water bath temperature was raised and then the next higher equilibrium temperature was determined in the same manner. The equilibration of composition 3 and 4 required higher percentage of moisture in the gas mixture which was succeptible to condensation at room temperature. Heating of the outlet glass tubing from the moisture generator with the nichrome wire winding to a temperature of 55 to 60°C prevented condensation of moisture.

As mentioned earlier in section II-1, equation (II-2) was established for a temperature range of 0°C to 50°C first by Baxter and Lansing[58] and later by Bookey and Tombs[59]. Equation (II-2) is related to the free energy change accompanying chemical reaction (II-1). The equation (II-2) was extrapolated upto 70°C i.e., 20°C beyond the established range for all the data points of composition 4 and 3 and one high temperature data point of composition 2.

IV-3 THE REDUCTION EXPERIMENTS:

The furnace was slowly heated upto a temperature around 700°C-800°C. Then the reaction tube was flushed for

about an hour with purified nitrogen. The nitrogen flow rate was increased and maintained at 2 to 3 litres/min. just before introduction of specimen. A spherical chromite pellet kept in a nichrome basket at the end of a 36-gauge nichrome wire was very quickly introduced into the reaction tube by opening the brass head and slipping the other end of the nichrome wire through the central hole in the brass head. The brass head was closed immediately and the nichrome wire was connected with the upper part of the suspension system i.e., the inconel rod. The length of the nichrome wire was preadjusted to keep the chromite pellet $\frac{1}{4}$ inch away from the thermocouple tip. The nitrogen flow rate was then reduced roughly to 0.5 litres/min. and the furnace temperature was raised to 1050°C in about three hours time. The Mettler balance was positioned carefully so that the nichrome wire of the suspension system did not touch the wall of the central hole in the brass head. The weight of the pellet was recorded as that corresponding to zero time when the temperature was stable. Flow of purified hydrogen at the rate of 0.5 litres/min. was established through the by-pass and was then introduced into the reaction chamber, and the nitrogen flow was stopped. The weight of the pellet was recorded at an interval of one hour in the case of dense pellets and fifteen minutes for porous pellets. Experiments were stopped at different stages of reduction as desired by switching over to nitrogen. The specimen was brought

immediately to the cooler top part of the reaction tube and the furnace was switched off for cooling to room temperature with the nitrogen flow on.

IV-4 IDENTIFICATION OF PHASES PRESENT IN REDUCED PELLETS:

Identification of the different phases that were produced during reduction of an iron chromite pellet was done by a combination of various techniques like microstructural examination, electron probe microanalysis, X-ray diffraction and chemical analysis. The procedure for all these are discussed separately.

(i) Microstructural Examination:

Microstructural examination[67] of partially reduced oxide pellets is a well established tool for identification of phases that are likely to appear during the reduction of an oxide pellet. Past experience[68] on preparation of oxide samples for microstructural examination show that development of microstructure is difficult for porous pellets as compared to the dense ones. Due to lack of cohesive strength in a porous pellet the oxide particles tend to chip off during specimen preparation leaving behind voids. Hence surface preparation is not possible unless a bonding material is used to fill up the void space in the pellet. Edstrom[67] used an acetone solution of bakelite to fill up the pores in iron oxide

specimens by first expelling air from the pores by evacuation and subsequently allowing the acetone solution to fill up the evacuated pores. After removal of acetone by drying, the green bakelite was cured by heating at 150°C for half an hour.

In the present investigation two solutions e.g., bakelite in acetone and lucite in chloroform were tried for filling up the void space in porous partially reduced pellets. The specimen was kept in a glass chamber which was evacuated by a mechanical pump for about 10 hours after which one of the solutions mentioned above was allowed to go into the chamber immersing the pellet completely. The solution was then boiled for half an hour with the pellet inside it for better penetration. The solvent chloroform or acetone could be completely eliminated by slow boiling. Curing of green bakelite or lucite could be done while mounting the specimen in a mounting press at 150°C and 4200 P.S.I. for half an hour. Unfortunately, this process was found to be unsuccessful with both the solutions because of lack of penetration of the solutions inside the porous pellet probably due to small sizes of the pores.

Partially reduced dense pellets were mounted in lucite and ground very slowly on belt grinder and emery papers. Polishing was done by using 0.5 micron alumina abrasive on a cloth polishing wheel at low speed. Number of pit holes were produced during grinding and polishing of

dense pellets. Their occurance could be restricted only by very slow grinding and polishing. Since the distinction between the different phases in the partially reduced dense pellets was clear even in the unetched condition, no etchant was tried.

(ii) Electron Probe Microanalysis:

After development of microstructure of dense pellets, the necessity of electron probe microanalysis was felt for the identification of different phases alongwith their compositions. The analysis was conducted at the Department of Metallurgical Engineering of the Ohio State University, Ohio, U.S.A. An aluminium layer of thickness around 2000A° was vacuum deposited onto the oxide to provide a conducting film. Several difficulties were encountered in the analysis because of fine grain structure in the reduced area. The position of the electron beam was difficult to determine because of the deflection of the beam coupled with the difficulty in optical identification of the fine structure due to the hindrance of the deposited film of aluminium. Scanning from unreduced area through the reduced layer produced very scattered intensity data. In order to obtain quantitative results, step scan of 1 to 2 micron steps were made over small areas. In general the beam diameter was larger than two phases of the reduced layer which further lowered the accuracy of the quantitative estimation of the

composition of the different phases. The standards used for the analysis were pure iron, pure chromium, and $FeO.Cr_2O_3$.

(iii) X-Ray Diffraction:

From the outer surface of the product layer of partially reduced porous pellets,the material was carefully ground off using a diamond file and it was further ground to fine powder size in an agate morter and pestle. X-ray diffraction pattern of this powder was recorded in a Debye-Scherrer camera of 57 m.m. diameter using unfiltered chromium radiation. This pattern was compared separately with powder pattern of Fe and Cr_2O_3 obtained under identical conditions. Next metallic iron powder was mixed with chromium sesquioxide in the weight ratio of 55.85:152.02 and after thorough mixing under acetone, X-ray diffraction pattern of this mixture was recorded in the same camera under exactly identical conditions.

The unreduced core of a partially reduced porous pellet was separated carefully by grinding off the outer layer. The X-ray diffraction pattern of the core was recorded in the same way as before in the same camera.

(iv) Chemical Analysis of the Metallic Phase in Partially Reduced Pellets:

Chemical analysis of the reduced layer of dense as well as porous partially reduced pellets were carried

out for the precise identification of the metallic phase appearing after reduction. A partially reduced pellet may contain unreduced chromite, Cr_2O_3 and metallic iron or an alloy of iron and chromium. The analytical technique should be such that while dissolving out the metallic phase in the partially reduced pellet, the leaching solution should not react with the oxide phases. By a series of trial experiments it was established that sulphuric acid in concentration higher than 1:3 starts reacting with $FeO.Cr_2O_3$ apart from dissolving the metallic phase. Hence a ratio of 1:5 was chosen. The rest of the analytical procedure was similar to that used for estimation of chromium in steel[69].

0.1 gm sample was taken in a conical flask and 20 c.c. 1:5 H_2SO_4 solution was added into it and slowly heated. The volume of the acid was kept constant by adding water. After heating for one hour it was cooled and filtered and the residue was checked for the incomplete dissolution by heating again with 1:5 H_2SO_4 and checking for iron and chromium in the solution after heating. The filtrate was boiled with 25 c.c. 1:1 HNO_3 and saturated $KMnO_4$ solution was added to it until a pronounced pink colouration was obtained and maintained for 10 minutes. After boiling for 10 minutes, 5 c.c. of 10% manganous sulphate solution was added to it. Then it was again boiled for 5 minutes. The solution was filtered through a pulp pad

and the filtrate solution was diluted to 250 c.c. To 50 c.c. of this diluted solution 25 c.c. standard ferrous ammonium sulphate solution was added and the excess was back titrated against standardized $KMnO_4$ solution and chromium content was calculated from the titration data.

CHAPTER V

RESULTS

The results of gas equilibration and the reduction experiments are discussed below separately.

V-1 RESULTS OF GAS EQUILIBRATION EXPERIMENTS:

From the atmospheric pressure recorded from barometer, the pH_2O was subtracted to obtain pH_2. Table V shows the logarithm of pH_2O/pH_2 ratios at different temperatures in equilibrium with the four compositions of the spinel. Fig. 8 shows the plot of $\log pH_2O/pH_2$ as an inverse function of absolute temperature for the four compositions. In the case of composition number 4, determination of equilibrium beyond a temperature of 950°C was not pursued, since it required a temperature of the oxalic acid bath above 70°C when the accuracy of temperature control in the constant temperature bath was found to diminish. Apart from that, prevention of moisture condensation in the glass tubing connecting the oxalic acid bath with the reaction tube also became difficult beyond a temperature of 70°C.

It is clear from Fig. 8 that the variation of $\log pH_2O/pH_2$ with $\frac{1}{T}$ for all the compositions of $FeFe_{2-x}Cr_xO_4$ is linear, in conformity to the expected behaviour. A smooth increase in slope of $\log pH_2O/pH_2$ with composition of the

Table V

Equilibrium pH_2O/pH_2 Values at Various Temperatures For Spinels of Four Compositions.

Composition Number	Log pH_2O/pH_2	Temperature, °K
1	-2.128	1173.7
	-2.115	1187.2
	-2.050	1215.7
	-1.917	1284.2
	-1.819	1336.2
2	-1.945	1138.2
	-1.833	1173.2
	-1.681	1230.7
	-1.514	1298.5
3	-1.795	1123.2
	-1.726	1146.7
	-1.619	1179.2
	-1.446	1240.7
	-1.330	1282.2
	-1.166	1351.2
4	-1.321	1129.0
	-1.324	1133.2
	-1.226	1159.2
	-1.116	1190.0
	-1.076	1204.2

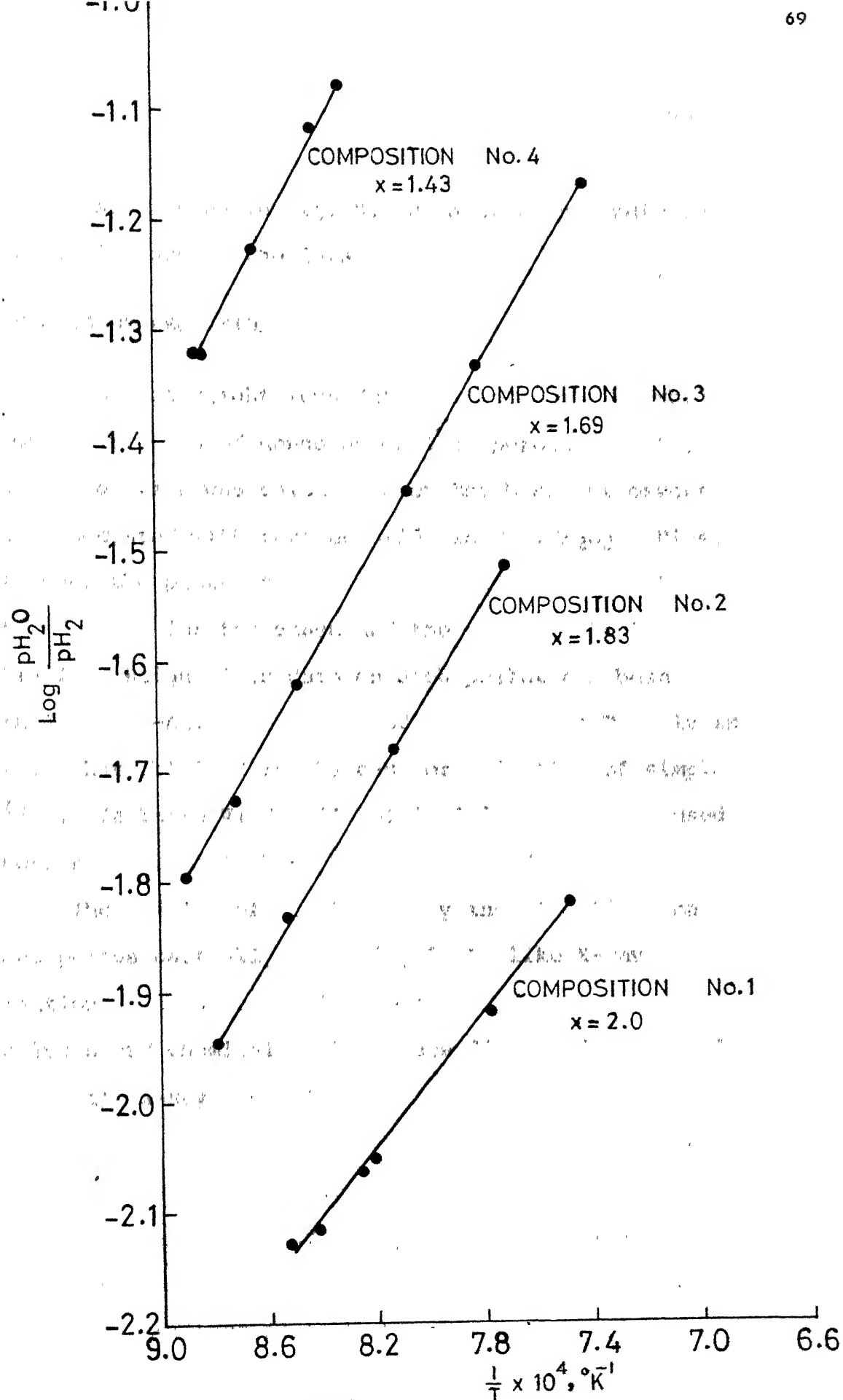

FIG. 8: LOG $\frac{pH_2O}{p_{H_2}}$ VS $\frac{1}{T}$ FOR THE FOUR COMPOSITIONS

spinel can also be seen in Fig. 8. Both of these indicate the self consistency of the data.

V-2 RESULTS OF REDUCTION EXPERIMENTS:

From the weight loss data collected during the reduction experiments of dense as well as porous pellets, percentage reduction was calculated on the basis of oxygen that was associated with ferrous oxide in $FeO.Cr_2O_3$. Figs. 9 and 10 show the plots of percentage reduction against time of reduction for the dense and the porous pellets respectively. Weight loss data on each pellet has been given in Appendix-A1. The nature of variation in Fig. 10 is similar to that obtained in the case of reduction of simple oxides[47]. In Table VI details of individual pellets used in reduction experiments have been summarized.

The results of supplementary investigations on dense and porous partially reduced pellets like X-ray investigation, microstructural examination, electronprobe microanalysis and chemical analysis are discussed separately.

(i) X-Ray Investigation:

X-ray diffraction pattern of the reduced layer in partially reduced porous pellets confirmed the presence of metallic iron and Cr_2O_3 in the product layer. The diffraction pattern of the core of partially reduced porous pellets confirmed it as $FeO.Cr_2O_3$.

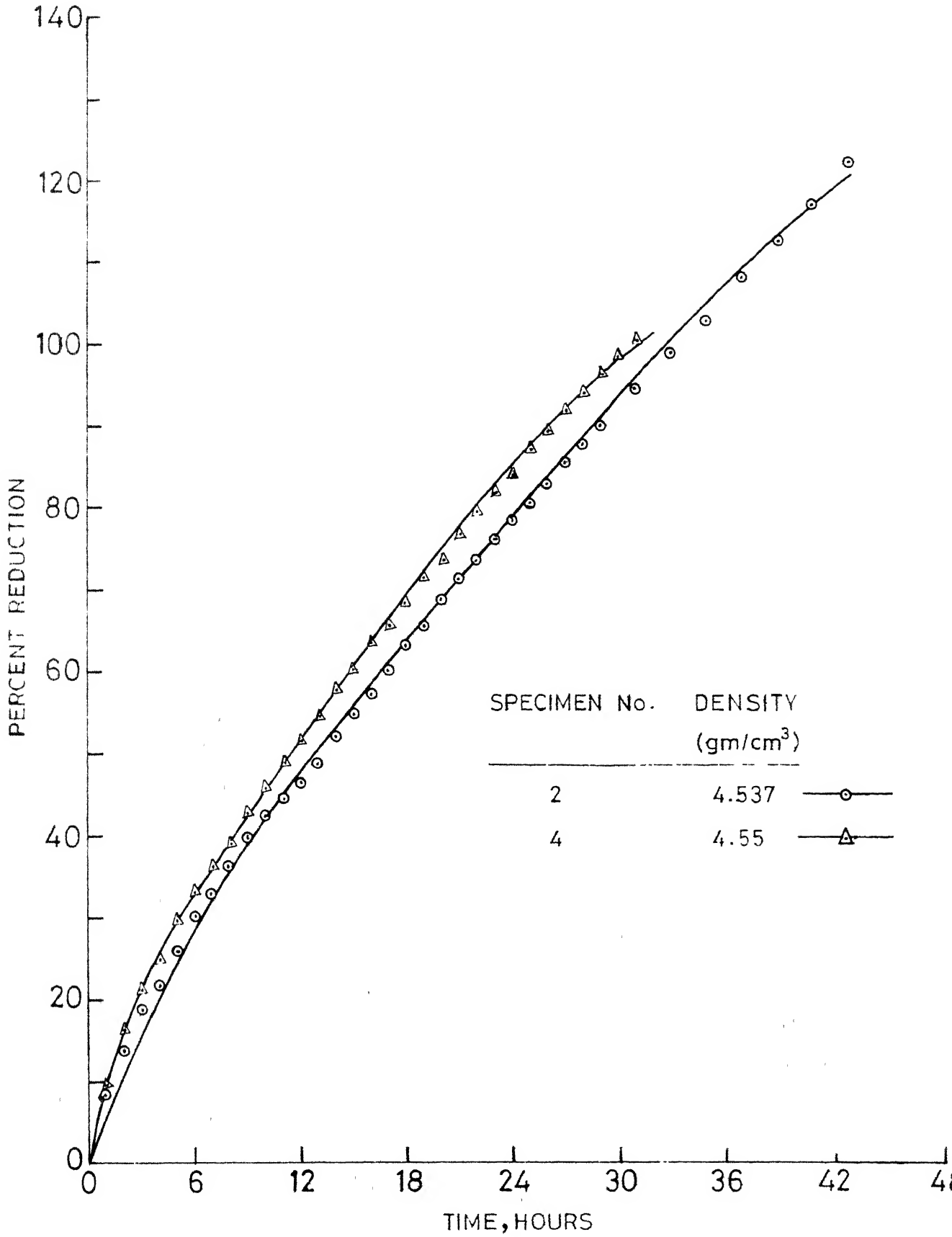

FIG.9: PERCENTAGE REDUCTION VS TIME FOR DENSE PELLET

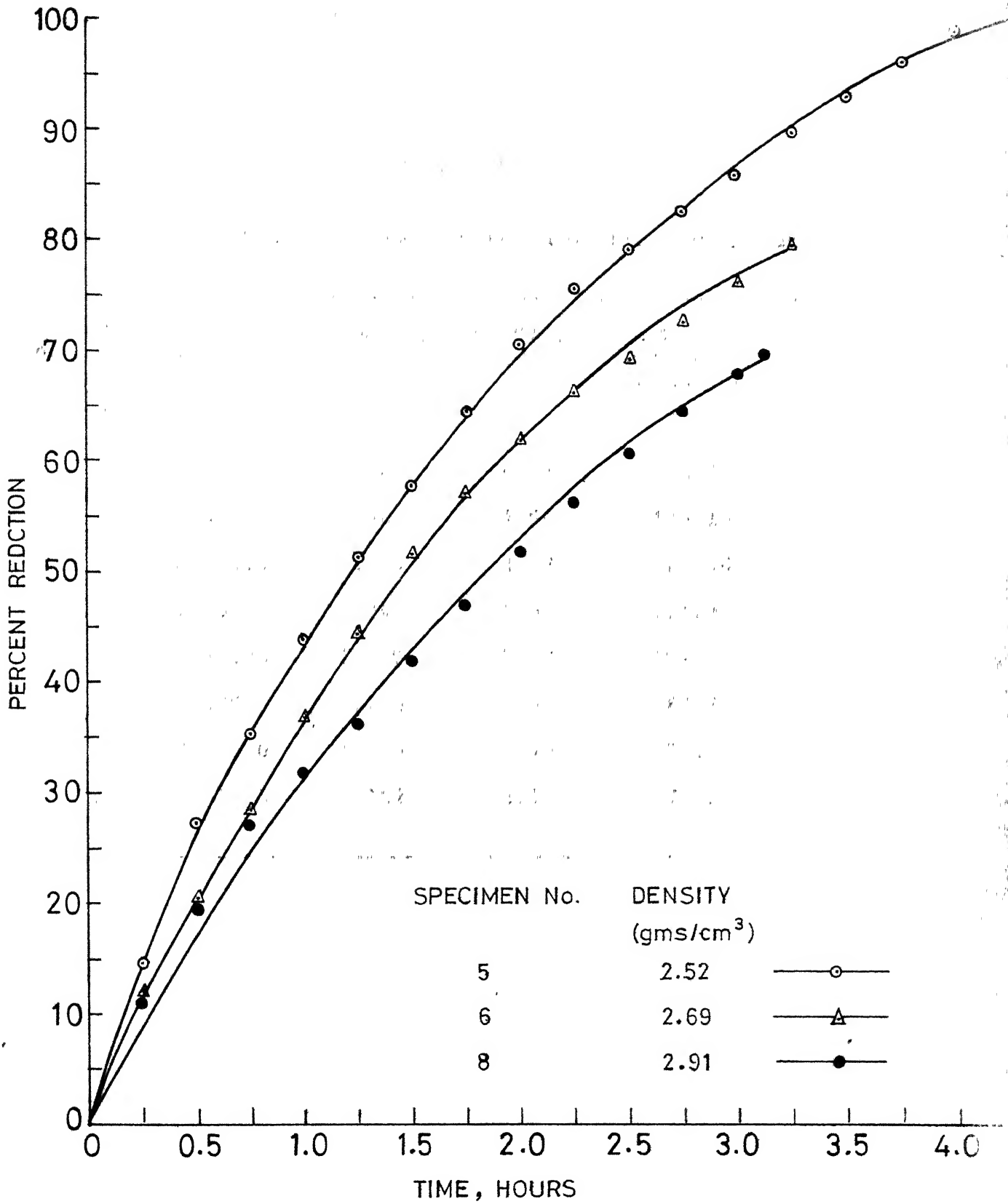

FIG. 10: PERCENTAGE REDUCTION VS TIME FOR POROUS PELLETS.

Table VI

Details of the Specimens Used in the Reduction Experiments

Specimen number	Initial weight, gm	Diameter, cm	Density, gm/cm^3	Terminal percentage reduction
1	2.62055	1.028	4.61	73.07
2	2.53022	1.021	4.54	123.15
3	2.20025	0.974	4.57	20.98
4	2.43073	1.007	4.55	101.3
5	2.70200	1.270	2.52	101.0
6	2.67015	1.238	2.69	80.2
7	2.71400	1.236	2.75	70.1
8	2.51485	1.182	2.91	70.0

(ii) Microstructural Examination:

After preparing the partially reduced pellets by grinding and polishing for microstructural examination the pellets were examined first under a low magnification (X 16). Figs. 11(a) and 11(b) show the photographs of dense (No. 1) and porous (No. 6) partially reduced pellets, subjected to 73% and 80% reduction respectively. Distinct colour difference between the unreduced brown core and green reduced product layer was observed in the case of porous pellets. In dense pellets, no colour difference was observed, although the interface between reduced layer and the unreduced core was distinct. It was observed that the interface between the product layer and the unreduced core in porous pellets was diffused over a zone instead of being sharp (Fig. 11(b)). The thickness of the diffused zone varied from pellet to pellet. The thickness of the product layer was measured by a travelling microscope with a magnification of X16 and a least count of .001 cm. The average thickness of the product layers was computed from about 20 measurements. From these average values, the volumes reacted were calculated and these were compared with the actual percentage reduction values obtained from the weight loss data. The comparison revealed disagreement in the case of dense pellets where the actual percentages of reduction obtained from weight loss data were always higher than the apparent values computed from the microscopic estimation.

Fig. 11(a): Photograph of partially reduced dense pellet (specimen number 1 subjected to 73 percent reduction); magnified approximately 5 times across the diameter.

Fig. 11(b): Photograph of partially reduced porous pellet (specimen number 6 subjected to 80 percent reduction); magnified approximately 4 times across the diameter.

Moreover, the difference between the actual and the apparent percentages of reduction in dense pellets increased with increase in the degree of reduction. This difference indicates that Cr_2O_3 was also getting reduced by hydrogen alongwith FeO. In the case of porous pellets the actual percentage of reduction compared well even upto 100% reduction with the apparent one computed from reduced layer thickness measurements. This essentially indicated that reduction of Cr_2O_3 was not taking place in the latter case.

It has been pointed out already in the previous chapter that preparation of partially reduced porous pellets for microstructural examination was found to be difficult because of poor strength. In partially reduced dense pellets at higher magnifications, three distinct zones could be detected in the reduced layer with an unreduced core at the centre of the pellet. Three phases were found under the microscope with their relative proportions varying in the different zones in the reduced layer. The microstructures of the different zones in the reduced layer of dense pellets have been shown in Figs. 12 through 15, and are discussed below.

(a) The Unreduced Core:

The microstructure of this region reveals grains of unreacted $FeO.Cr_2O_3$, alongwith uniformly distributed dark pits which were either discontinuous porosity in the

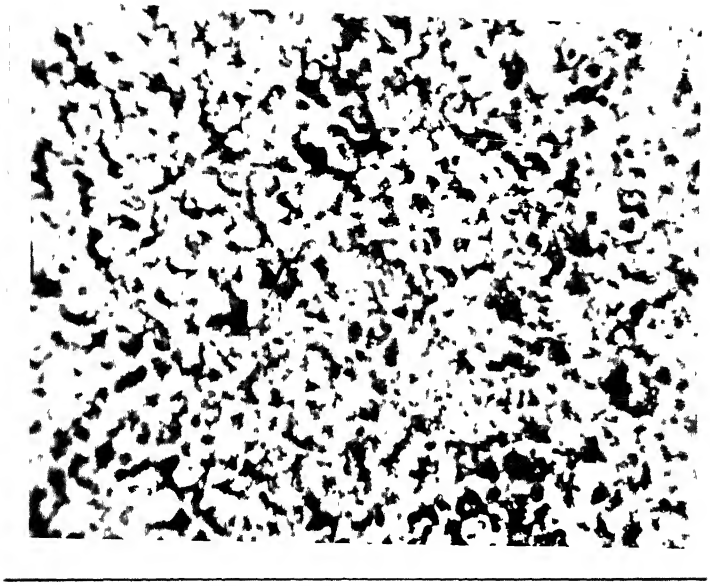

Fig. 12(a): Photomicrograph of the first zone of reduction (in specimen number 2 subjected to 123 percent reduction) at (X600) magnification showing the Fe-Cr alloy phase.

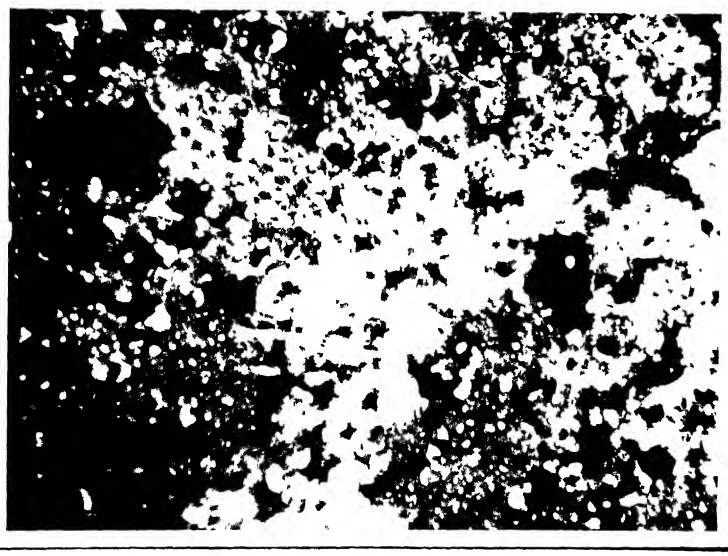

Fig. 12(b): Photomicrograph of the second zone of reduction (in specimen number 4 subjected to 101 percent reduction) at (X600) magnification showing the bright Fe-Cr alloy globules with dark Cr_2O_3.

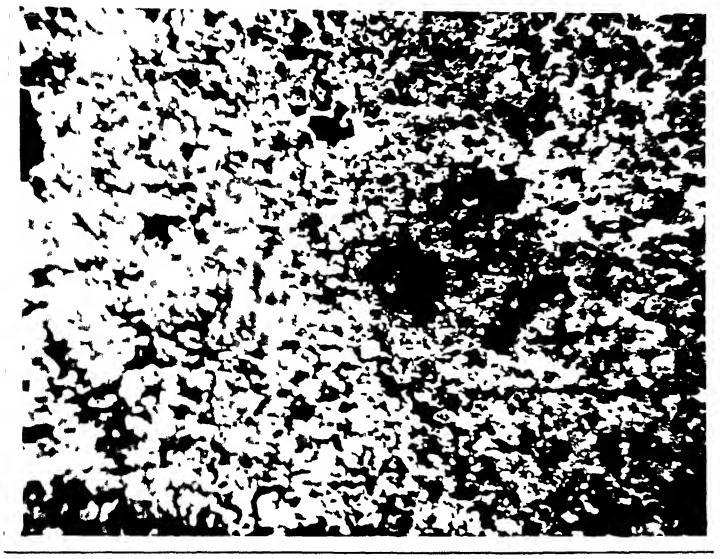

Fig. 13(a): Photomicrograph of the interface between the first and second zone of reduction (in specimen number 2 subjected to 123 percent reduction) at (X300) magnification.

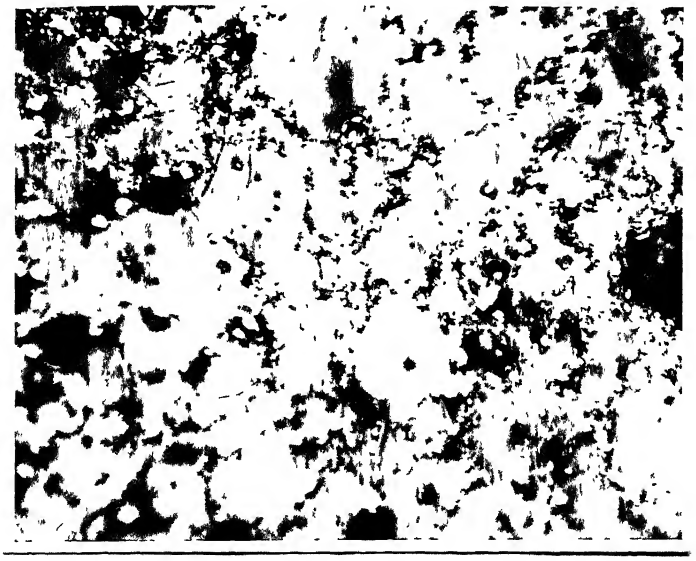

Fig. 13(b): Photomicrograph of the third zone of reduction (in specimen number 1 subjected to 73 percent reduction) at (X600) magnification showing the metallic iron globules and Cr_2O_3 along the grain boundaries.

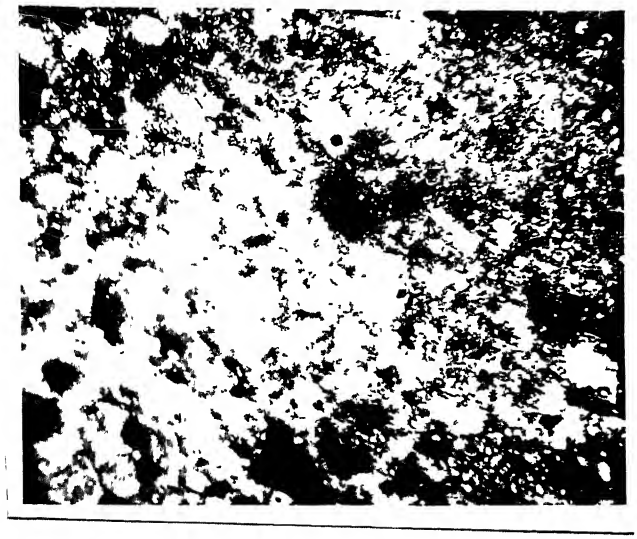

Fig. 14(a): Photomicrograph of the interface between the second and the third zone (in specimen number 1 subjected to 73 percent reduction) at (X300) magnification.

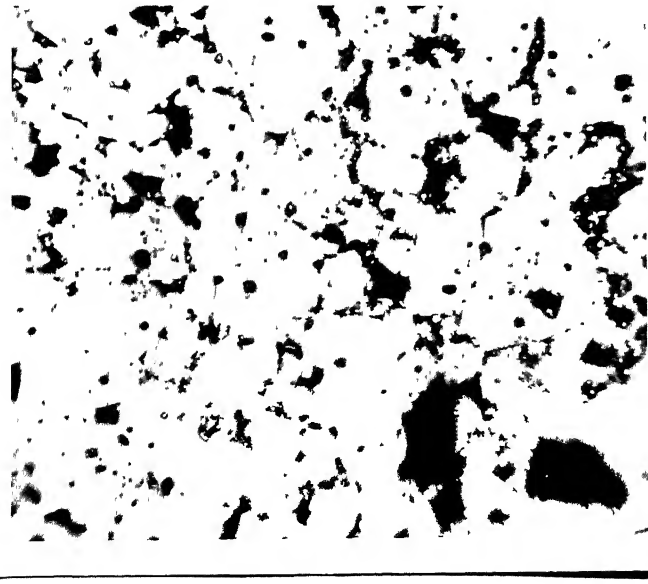

Fig. 14(b): Photomicrograph of the interface between the third zone and the unreduced core (in specimen number 1 subjected to 73 percent reduction) at (X600) magnification.

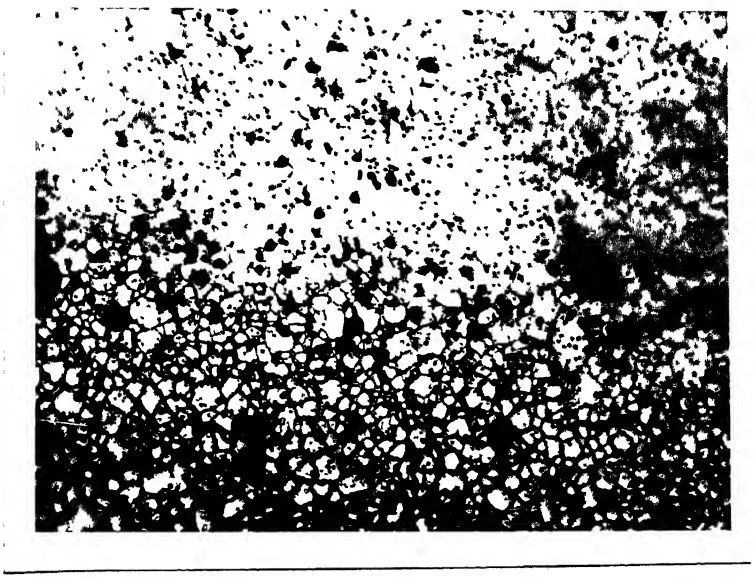

Fig. 15: Photomicrograph of the interface between the third zone and the unreduced core (in specimen number 3 subjected to 21 percent reduction) at (X100) magnification.

pellet or were produced due to removal of chromite during grinding and polishing.

(b) The First Zone:

This zone could be detected only at the outermost part in the reduced layer in specimens with higher percentage of reduction. It was characterized by a bright iron-chromium alloy phase. Fig. 12(a) shows the photomicrograph of this zone at X600 magnification in specimen no. 2 which was reduced upto 123% reduction. The dark region in the photomicrograph indicates the void space in the alloy. The visual porosity of this zone was found to decrease with increasing percentage of reduction of the pellet.

(c) The Second Zone:

The matrix of the second zone presumably consisted of Cr_2O_3 alongwith some unreduced $FeO.Cr_2O_3$. The bright alloy phase was distributed throughout the matrix as small globules. This zone constituted the outermost layer in pellets with lower percentage of reduction where the first zone was absent. Fig. 12(b) shows the photomicrograph of this zone at (X600) magnification in specimen number 4 subjected to 101% reduction. The globules of the alloy phase were interconnected with each other only near the interface between the first and second zone as shown in the photomicrograph in Fig. 13(a). Dark pits which were either discontinuous porosity or were produced due to the removal of Cr_2O_3 particles during grinding and

polishing of pellet were also present. The presence of unreacted $FeO.Cr_2O_3$ in this zone could not be detected clearly under microscope because the light reflecting property of the alloy phase was not very much different from that of chromite.

(d) The Third Zone:

Microstructure (Fig. 13(b)) revealed unreacted $FeO.Cr_2O_3$ grains as the predominant phase in this zone alongwith Cr_2O_3 and small globules of alloy phase appearing only at the grain boundaries. The size of the alloy globules were found to be smaller than those appearing in the second zone. The interface between this and the second zone is shown at (X300) magnification in Fig. 14(a). The frequency of appearance of pits in this zone was similar to that in the unreduced core appearing next to it at the centre of the pellets. Fig. 14(b) shows the interface between this zone and the unreduced core at a magnification of (X600) in specimen number 1. The distinct boundary between the reduced layer and unreduced core is clear from Fig. 15 taken at a magnification of (X100) in specimen number 4. The thickness of the Cr_2O_3 phase appearing along the grain boundaries of $FeO.Cr_2O_3$ phase increased gradually towards the interface between the second and the third zone. Although Cr_2O_3 phase at the grain boundaries was continuous, it was not present along all the boundaries.

(iii) Electron Probe Microanalysis:

The difficulties associated with electron probe microanalysis have been mentioned in the previous chapter. Fig. 16 shows the results obtained by step scanning (1-2 micron steps) on specimen number 1 subjected to 73% reduction from the interior unreduced core towards the outer edge of the specimen. An increase in chromium content from 46.5% (for pure $FeO.Cr_2O_3$) to 54%, with a simultaneous decrease in iron content from 25% (for pure $FeO.Cr_2O_3$) to 16% was observed. Fig. 17 presents the analysis of the third zone of reduced layer as the dark Cr_2O_3 phase at the grain boundaries was crossed in steps of 2 microns. A decrease in chromium and iron content was observed contrary to expectation. Fig. 18 shows the results of two scans of 2 micron steps in the second zone of the reduced layer. The scatter in the data was due to fine structural distribution of the different phases. However, the bright iron-chromium alloy phase could be identified from the two scans in Fig. 18.

(iv) Chemical Analysis:

The composition of the metallic phase appearing in partially reduced dense and porous pellets confirmed that Cr_2O_3 was simultaneously getting reduced alongwith FeO in iron chromite in the case of dense pellets, but not in the case of porous pellets. Table VII shows

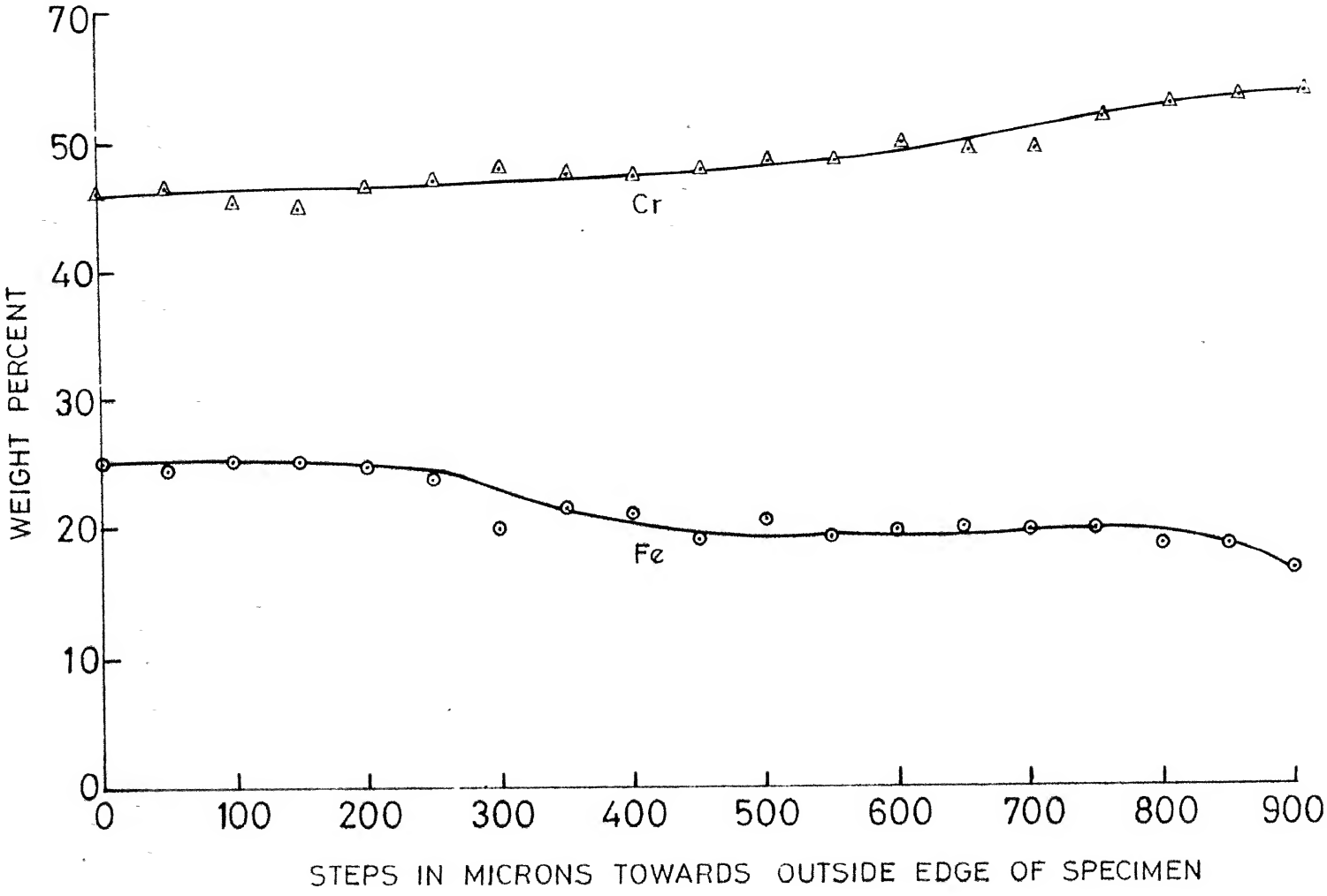

FIG. 16: ELECTRON-PROBE SPOT ANALYSIS OF LIGHT PHASE (MATRIX) FROM UNREDUCED AREA THROUGH REDUCED AREA.

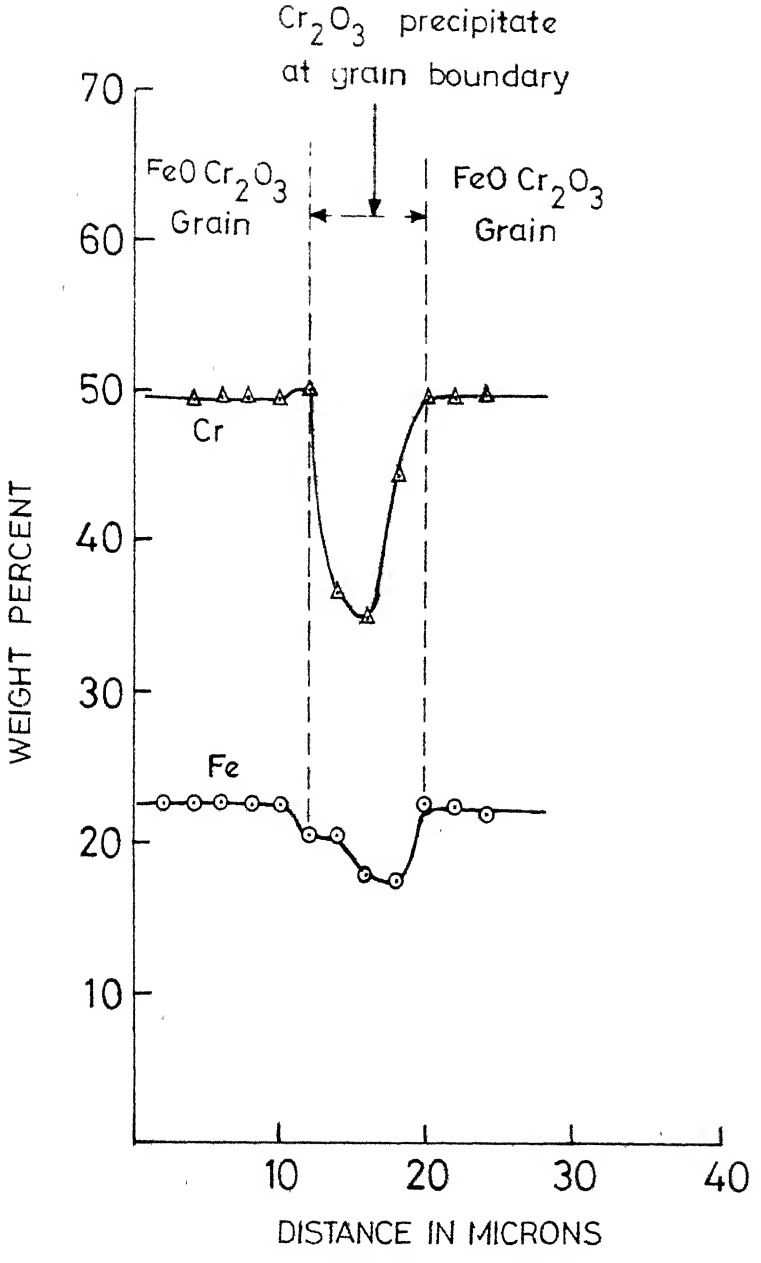

FIG. 17: ELCTRON-PROBE SCAN ACROSS THE GRAIN BOUNDARY IN THIRD ZONE OF REDUCED LAYER

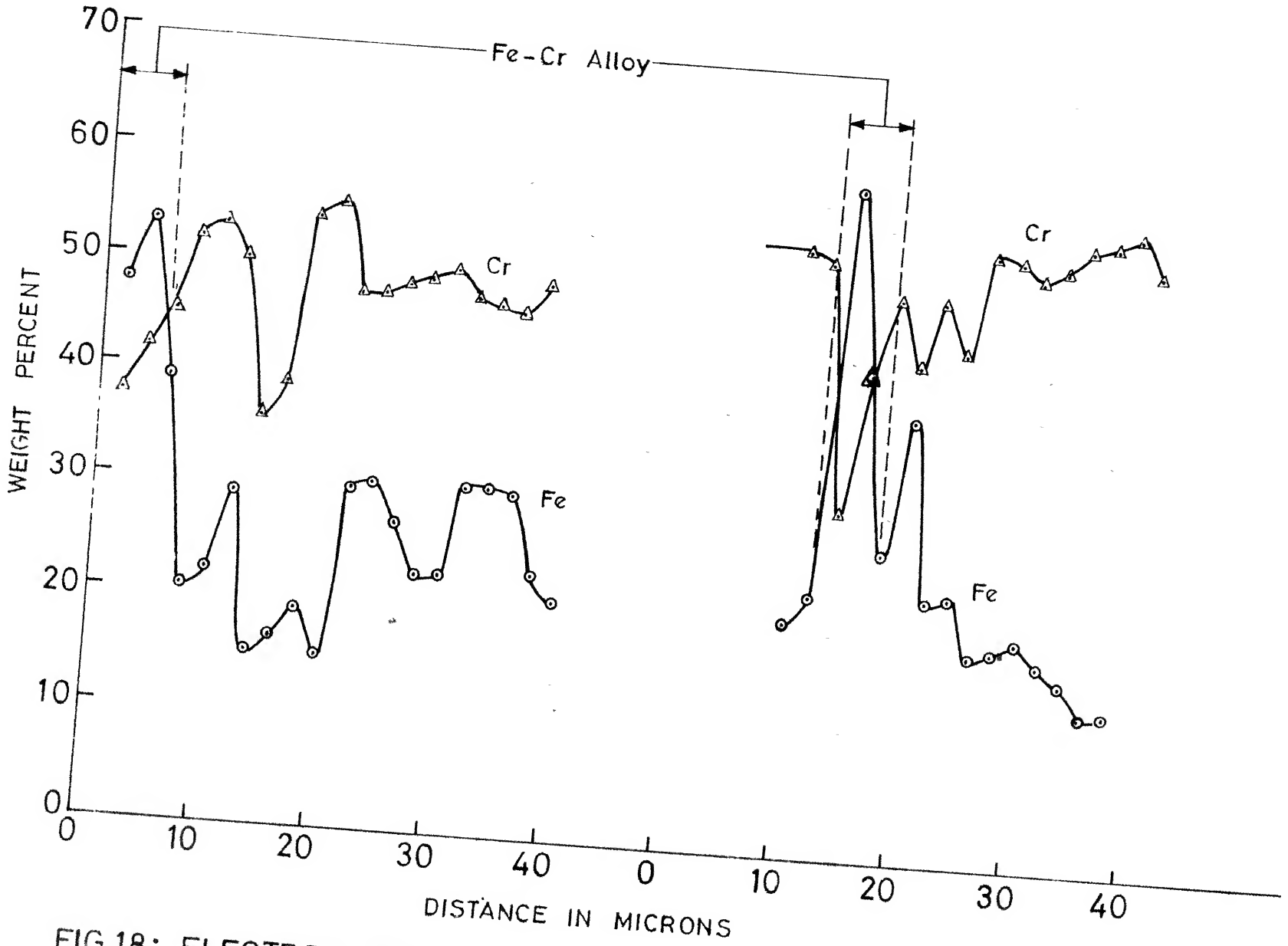

FIG.18: ELECTRON-PROBE SCAN OVER AREAS IN SECOND ZONE OF REDUCED LAYER.

the results of chemical analysis of the metallic phase in porous and dense pellets.

CHAPTER VI

DISCUSSION - GAS EQUILIBRATION

For comparison of thermodynamic data obtained in this investigation with the existing ones, the free energy values on terminal chromite reported by previous investigators[37,41-43,45] were converted into $\log pH_2O/pH_2$ and plotted against 1/T alongwith the data obtained in the present investigation as shown in Fig. 19. In experiments of Boericke and Bangert[41] adequate precaution against thermal diffusion in the gas phase was not taken and that might account for the high pH_2O/pH_2 values reported by them. The investigations by Abendroth[43], and Morozov and Novokharskii[42] are the two most extensive investigations on terminal chromite and good agreement between the data obtained in this investigation with those of these two studies and also with the one by Katsura and Muan[37] is evident from Fig. 19. Tretyakov and Schmalzried[45] used solid electrolyte cell and considering its merit, it is difficult to explain the high values of pH_2O/pH_2 obtained by them.

Oxygen potential, pO_2, for all the four compositions of $FeFe_{2-x}Cr_xO_4$ was calculated according to equation (I-6) and have been presented in Table VIII as a linear function of temperature alongwith the error in kilocalories in each

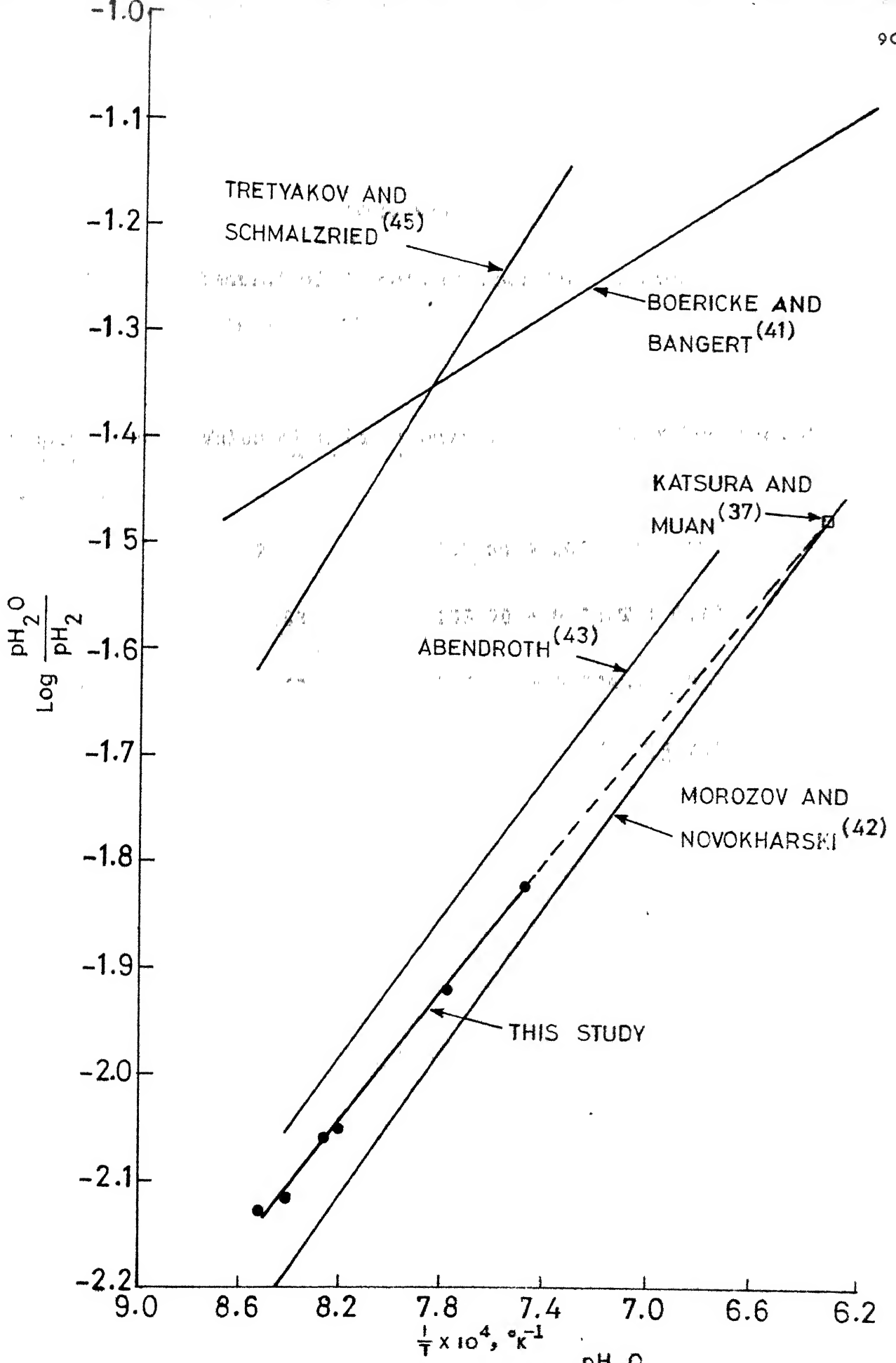

FIG. 19: COMPARISON OF EQUILIBRIUM $\frac{pH_2O}{pH_2}$ OVER TERMINAL

Table VIII

Oxygen Potential of Spinels of Four Compositions

As A Function of Temperature

Composition Number	Value of x in $FeFe_{2-x}Cr_xO_4$	Oxygen potential, Kilocalories
1	2.0	$-145.60 + .03xT \pm 0.16$
2	1.83	$-153.70 + 0.04xT \pm 0.13$
3	1.69	$-156.20 + 0.044xT \pm 0.1$
4	1.43	$-142.36 + 0.036xT \pm 1.0$

composition. Fig. 20 shows a graphical representation of the same against temperature.

It has been pointed out already that $FeFe_{2-x}Cr_xO_4$ is a solution between $FeO.Cr_2O_3$ and magnetite. From the equilibrium oxygen partial pressure data that have been collected on $FeFe_{2-x}Cr_xO_4$ of different compositions in equilibrium with metallic iron, we may proceed to determine the activity-composition relationship for the solid solution $FeO.Cr_2O_3$ - $FeO.Fe_2O_3$, with the help of the reaction (VI-1):

$$\tfrac{1}{2}Fe_3O_4 \text{ (in spinel solid solution)} = \tfrac{3}{2}Fe \text{ (in metal)} + O_2 \text{ (gas)} \quad \ldots\ldots \text{(VI-1)}$$

The activity of half a molecule of magnetite ($a_{Fe_{1.5}O_2}$) in the spinel solid solution relative to pure magnetite as standard state may be expressed as:

$$a_{Fe_{1.5}O_2} = \frac{pO_2}{pO_2^\circ} \quad \ldots\ldots \text{(VI-2)}$$

Where pO_2 and pO_2° are the partial pressures of oxygen in equilibrium with metallic iron and $FeFe_{2-x}Cr_xO_4$ and metallic iron and pure magnetite respectively. The values of pO_2 for the different compositions of spinel solution are known already and pO_2° was calculated from the standard free energy of formation of magnetite from the compilation of Elliot et al[2]. Table IX shows the activities

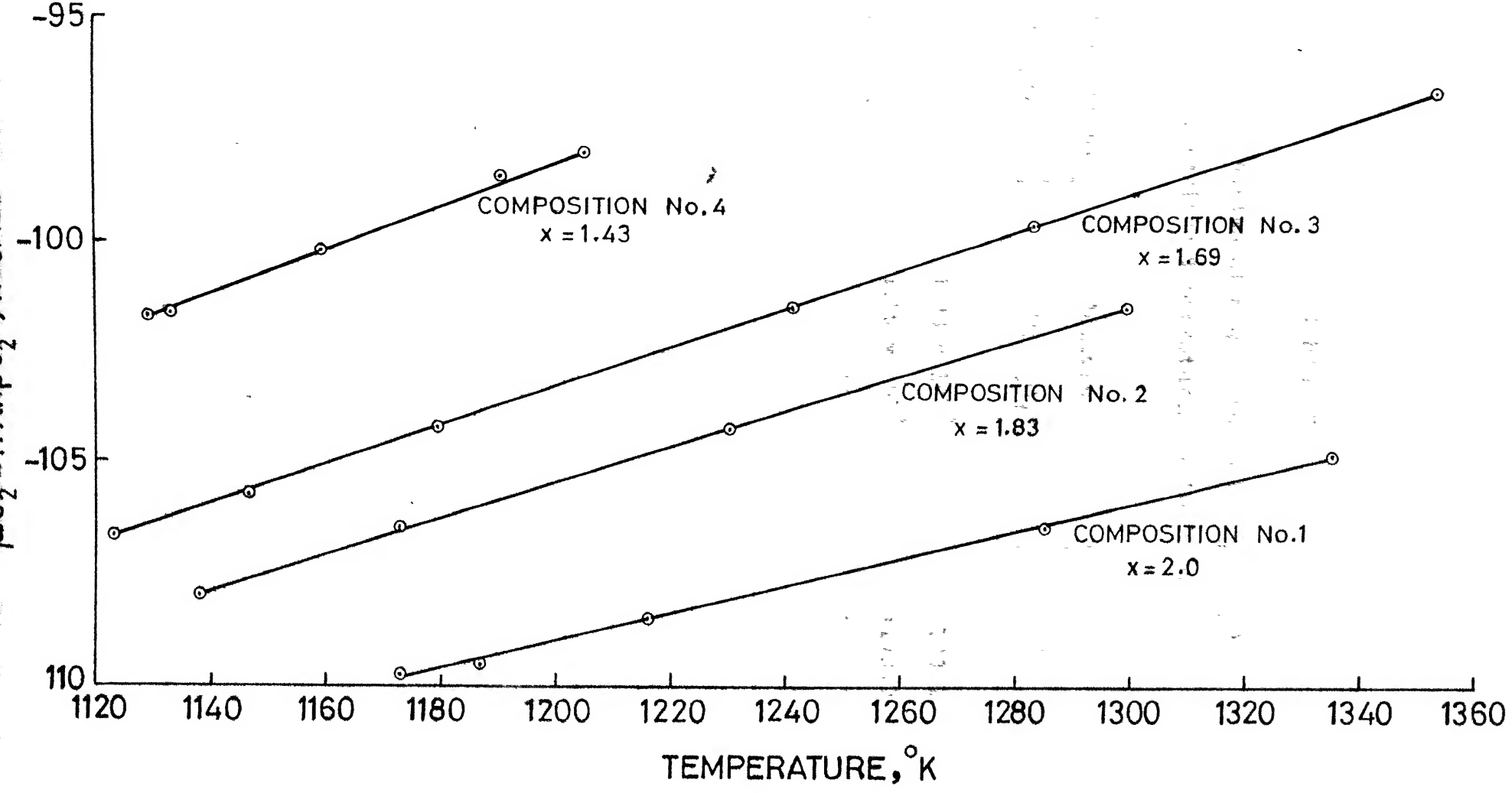

FIG. 20: OXYGEN POTENTIAL OF SPINEL AND IRON MIXTURES OF FOUR COMPOSITIONS.

Table IX

Activities of Magnetite in $FeFe_{2-x}Cr_xO_4$ At Various Temperatures of Equilibration

Composition, $N_{Fe_{1.5}O_2}$	Activity, $a_{Fe_{1.5}O_2}$	Temperature, °K
0.0855	3.33×10^{-4}	1138.2
	4.50×10^{-4}	1173.2
	6.00×10^{-4}	1230.7
	9.82×10^{-4}	1298.5
0.1544	7.20×10^{-4}	1123.2
	8.82×10^{-4}	1146.7
	1.23×10^{-3}	1179.2
	1.70×10^{-3}	1240.7
	2.44×10^{-3}	1282.2
	4.06×10^{-3}	1351.2
0.2837	6.22×10^{-3}	1129.0
	6.00×10^{-3}	1133.2
	8.60×10^{-3}	1159.2
	1.20×10^{-2}	1190.0
	1.08×10^{-2}	1204.2

of magnetite in $FeFe_{2-x}Cr_xO_4$ at the different temperatures of equilibration for the different compositions. Values of activity coefficient, $\gamma_{Fe_{1.5}O_2}$, were calculated from the activities at 1200°K and log $\gamma_{Fe_{1.5}O_2}$ when plotted against $(1 - N_{Fe_{1.5}O_2})^2$, where $N_{Fe_{1.5}O_2}$ is the mole fraction of magnetite in solution, a fairly reasonable straight line was obtained as shown in Fig. 21, indicating that the solution may be approximately regarded as a regular solution. Based on the regular behaviour, the straight line in Fig. 21 was extrapolated and activities of magnetite beyond the experimental range were calculated and shown in Fig. 22. Although it is understood[70] that the properties of a solution exhibited in the terminal composition region need not remain valid throughout the composition range, but in the absence of any investigation covering the whole range, the extrapolated values might become useful.

A strong negative departure of $a_{Fe_{1.5}O_2}$ from ideal behaviour is evident from Fig. 22 in the experimental range. Thermodynamic investigation on spinel solid solutions was initiated by Muan and his coworkers[71-73]. A strong negative departure from ideal behaviour was observed by Aukrust and Muan[72] in the activity of Co_3O_4 upto a mole fraction of 0.3 in Co_3O_4 - Fe_3O_4 solid solution in equilibrium with CoO-FeO solid solution. Aukrust and Muan[71] and later Schwerdtfeger and Muan[73] observed negative departure from Raoult's Law in Co_3O_4 - Mn_3O_4 and Fe_3O_4 - Mn_3O_4

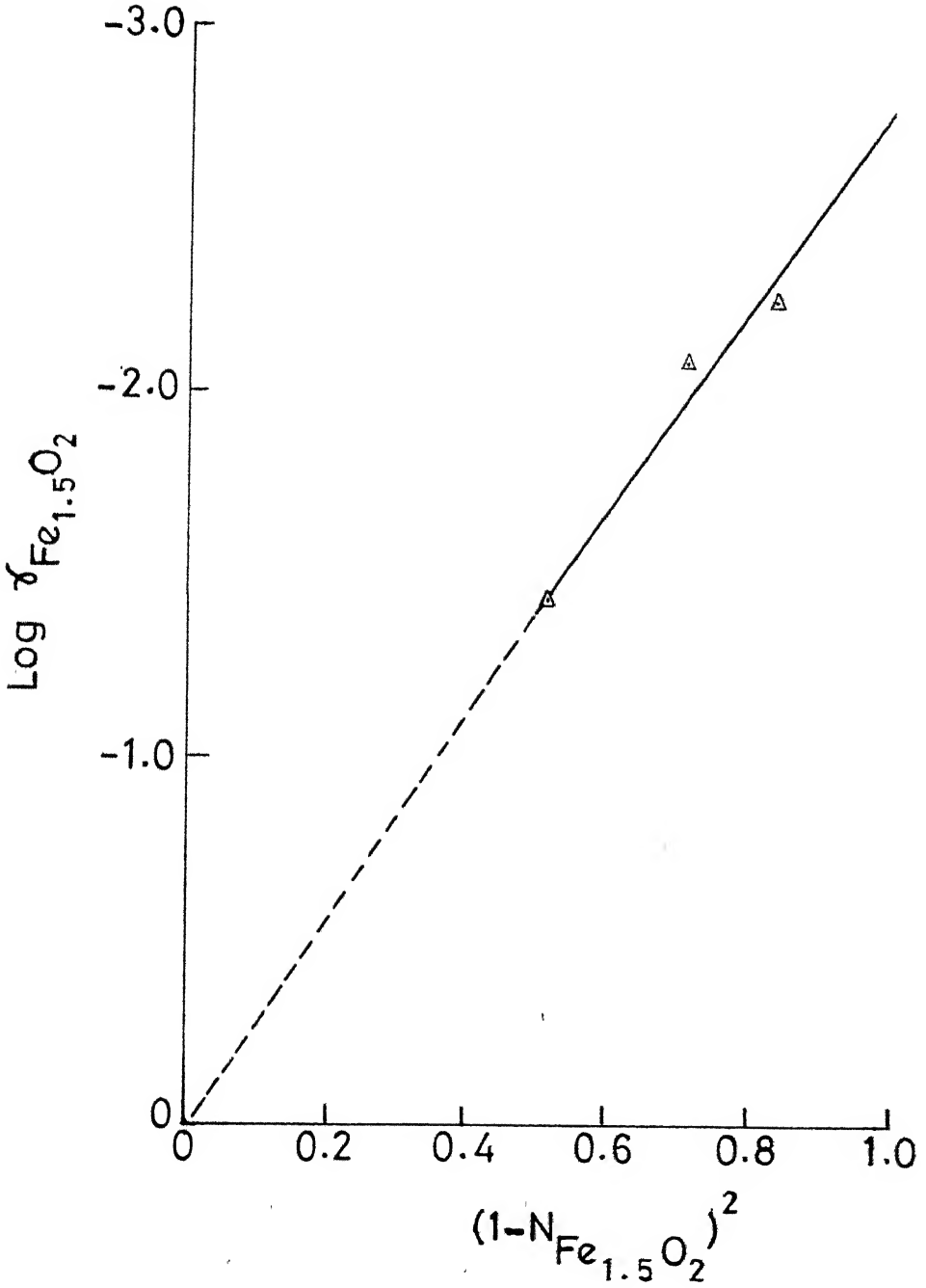

FIG. 21: PLOT OF LOG $\gamma_{Fe_{1.5}O_2}$ AGAINST $(1-N_{Fe_{1.5}O_2})^2$

solid solutions in equilibrium with CoO-MnO and FeO-MnO solid solutions respectively. Against this background, it appears that the activity-composition relationship observed in the present investigation is in conformity with those observed previously on similar solutions.

CHAPTER VII

DISCUSSION - KINETIC STUDIES

The results of the kinetic investigations on the porous and the dense pellets are discussed separately.

VII-1 POROUS PELLETS:

Gas-solid reactions may often suffer from appreciable buildup of product gas in the gas stream i.e., 'reagent starvation' in the experimental system. This leads to a situation in which the supply of the gaseous reductant to the specimen may become rate-controlling.

The virtual maximum rate[74] of transport across the stagnant gas film around the specimen was calculated for the porous pellet in order to ascertain the importance of the reagent starvation. The rate of reduction of pellet number 5 in the first 0.25 hours was used for the calculations as shown in details in Appendix - A2. Since specimen number 5 was the pellet with the highest porosity used in the reduction experiments, its initial rate of reduction was higher than those of other pellets. It was found that the virtual maximum rate of transport was 5.5 times the actual rate of transfer across the stagnant gas film for the first 0.25 hours of reduction. This indicates that the chances of reagent starvation during the reduction of all the porous pellets were remote.

It has been mentioned already that unlike the dense pellets, the simultaneous reduction of Cr_2O_3 in porous pellets alongwith FeO did not take place at all. This was verified by the following observations on porous pellets, viz.:

(i) Absence of any unreduced core in the specimen number 5 in which the loss in weight corresponded to 101 percent reduction of FeO.

(ii) Chemical analysis of the metallic phase produced due to reduction in specimen number 8 subjected to 70 percent reduction showed absence of chromium in it (Table VII).

(iii) Agreement between the actual percentages of reduction with those inferred from measurement of thickness of reduced layer on specimen 6 and 8.

It can be shown by thermodynamic calculations also that the experimental conditions ruled out the reduction of Cr_2O_3 to Cr. The concentration of H_2O in the bulk gas ($C^{(b)}_{H_2O}$) can be calculated according to the procedure outlined in Appendix - A2. The concentration of H_2O at the surface of the pellet ($C^{(s)}_{H_2O}$) may be obtained from equation (VII-1):

$$\frac{dn}{dt} = A \cdot K_m [C^{(s)}_{H_2O} - C^{(b)}_{H_2O}] \quad \ldots\ldots \text{(VII-1)}$$

where A = surface area of pellet, cm^2.

K_m = mass transfer coefficient, cm/sec.

$\frac{dn}{dt}$ = rate of production of H_2O due to pellet reduction, gm/sec.

For specimen number 5, where:

$A = 5.06\ cm^2$.

$K_m = 27.95$ cms/sec.

and in the last 0.25 hrs. of reduction

$C^{(b)}_{H_2O} = 1.68 \times 10^{-7}$ gms/cm^3.

and $\frac{dn}{dt} = 6.2 \times 10^{-6}$ gms/sec.

$C^{(s)}_{H_2O}$ was found to be 2.12×10^{-7} gms/cm^3. When converted to partial pressure, $\frac{pH_2O}{pH_2}$ at the surface turned out as 1.27×10^{-3}.

The standard free energy of formation of Cr_2O_3 according to equation (VII-2):

$$2Cr + \tfrac{3}{2}O_2 = Cr_2O_3 \quad \ldots\ (VII\text{-}2)$$

is given by

$$\Delta G^\circ = -266700 + 59.95T \pm 300\ Cal/mole^{(75)} \quad .. \ (VII\text{-}3)$$

The pH_2O/pH_2 in equilibrium with Cr_2O_3 and metallic chromium at 1050°C lies between the range 3.30 to 3.56×10^{-4} for the reported uncertainty in the free energy value. Comparing this value with that of $C^{(s)}_{H_2O} = 1.27 \times 10^{-3}$ obtained in the last stage of reduction of specimen number 5

it is clearly understood that from purely thermodynamic reason, the reduction of Cr_2O_3 could not have taken place. In the case of other porous pellets also the same analysis may be extended at any stage of reduction.

For the quantitative analysis of heterogeneous chemical reactions taking place inside a porous solid with gaseous reactant, sophisticated kinetic models are available in the field of heterogeneous catalysis[76,77]. But these models are not applicable to the present situation because the physical and chemical properties of the product layer after the reaction does not remain the same as the starting one. Also the reaction front or zone inside the solid keeps migrating towards the core throughout the course of reaction unlike the reaction in a catalyst pore.

Recently Szekely[78] and his coworker proposed a realistic kinetic model to treat gas-solid reaction taking place in a porous solid. But, for the application of this model to any reaction system a number of auxilliary informations are necessary. Hence, for the analysis of the present situation Szekely's model could not be used.

All other kinetic models assume chemical reaction taking place at a sharp receeding interface. The one proposed by Spitzer et al[79] is the most general of all. Although it was proposed for the reduction of dense hematite, there is no reason why it can not be applied in the case of porous pellet reduction with a single sharp

interface.

It has been mentioned in section V-2 already that in the porous pellet reduction the interface between the unreduced core and the product layer was diffused instead of being sharp. Even then it was considered worthwhile to analyze the kinetics of reduction with the help of the above model.

The various kinetic steps involved in this reduction may be identified as:

(i) Transport of hydrogen from the bulk gas phase to the outer surface of the pellet.

(ii) Diffusion of hydrogen through the porous product layer of Cr_2O_3 and Fe to the interface between the unreduced core and the reduced layer.

(iii) Chemical reaction of hydrogen with the solid oxide which includes some substeps.

(iv) Counter-diffusion of hydrogen and water vapour through the product layer of individual grains in the reaction zone.

(v) Diffusion of water vapour through the product layer back to the surface of the pellet.

(vi) Transfer of water vapour from the outer surface of the pellet to the bulk gas phase.

All the above steps are in series. The steps (iii) and (iv) cannot be identified separately because step (iv) is mathematically analogous to a first order chemical

reaction. Since a first order chemical reaction only has been considered in the model, steps (iii) and (iv) may be merged into one step in the formulation of the model of Spitzer et al. Mathematical expressions pertaining to each of these steps were represented in the form of Ohm's Law, having a potential gradient term, a conductance term and a flux term. The final generalized rate expression obtained on integration over each of the abovementioned steps was given as:

$$[1 - (1-F)^{1/3}] = 1 - \frac{X_i}{X_o} = \frac{\bar{K}_{ov}}{RTX_oC_o}\left(pH_2^{(b)} - \frac{pH_2O^{(b)}}{K_e}\right).t \qquad \ldots \text{(VII-4)}$$

where

$$\bar{K}_{ov} = \frac{1}{\underbrace{\frac{1}{3\bar{a}}\left[1 + \frac{X_i}{X_o} + \left(\frac{X_i}{X_o}\right)^2\right]}_{\text{gas film resistance}} + \underbrace{\frac{X_o}{6\bar{b}}\left[1 + \frac{X_i}{X_o} - 2\left(\frac{X_i}{X_o}\right)^2\right]}_{\text{transfer resistance in the product layer}} + \underbrace{\frac{1}{K_r}}_{\text{resistance of reaction step}}} \qquad \ldots \text{(VII-5)}$$

$$\bar{a} = \frac{K_e \cdot K_{m(H_2)} \cdot K_{m(H_2O)}}{K_e \cdot K_{m(H_2O)} + K_{m(H_2)}} \qquad \ldots \text{(VII-6)}$$

$$\bar{b} = \frac{K_e \cdot D_{H_2}^{(eff)} \cdot D_{H_2O}^{(eff)}}{D_{H_2}^{(eff)} + K_e \cdot D_{H_2O}^{(eff)}} \qquad \ldots \text{(VII-7)}$$

and K_e is the equilibrium constant for the reaction (VII-8):

$$H_2 + FeO.Cr_2O_3 = Cr_2O_3 + Fe + H_2O \qquad \ldots \text{(VII-8)}$$

where F = fractional reduction of the pellet.

X_i = distance of the reaction front from the core, cm.

X_o = radius of the pellet, cm.

R = universal gas constant, cm^3-atm./mole/°K.

T = absolute temperature, °K.

C_o = concentration of reducible oxygen, moles of atomic O/cm^3.

$p_{H_2}^{(b)}$, $p_{H_2O}^{(b)}$ = partial pressures of H_2 and H_2O in bulk gas, atm.

K_r = specific rate constant for surface reaction, cm/sec.

$D_{H_2}^{(eff)}$, $D_{H_2O}^{(eff)}$ = effective diffusivities of H_2 and H_2O through product layer, cm^2/sec.

$K_{m(H_2)}$, $K_{m(H_2O)}$ = mass transfer coefficients for H_2 and H_2O, cm/sec.

$\bar{K}_{ov}$, which is the integrated overall conductance, is composed of three parts. In the denominator of equation (VII-5), the first term corresponds to the gas film resistance, incorporating the steps (i) and (vi). The second term corresponds to the product layer resistance incorporating steps (ii) and (v) and the third term $(\frac{1}{K_r})$ represents the interfacial resistance term. To obtain the relative magnitudes of these three resistances, the reduction data for specimen number 5 was used for calculations acoording to the model of Spitzer et al[79] as per equations number (VII-4) through (VII-8).

Since the reducing gas was a binary mixture, the

coefficients $\bar{a}$ and $\bar{b}$ were simplified as follows:

$$K_{m(H_2)} = K_{m(H_2O)} = K_m \quad \ldots \text{(VII-9)}$$

$$D_{H_2}^{(eff)} = D_{H_2O}^{(eff)} = D_{H_2-H_2O}^{(eff)} \quad \ldots \text{(VII-10)}$$

and $\bar{a}$ and $\bar{b}$ were reduced to:

$$\bar{a} = \frac{K_e \cdot K_m}{K_e + 1} \quad \ldots \text{(VII-11)}$$

$$\bar{b} = \frac{K_e \cdot D_{H_2-H_2O}^{(eff)}}{K_e + 1} \quad \ldots \text{(VII-12)}$$

The effective binary diffusion coefficient in the gas mixture, $D_{H_2-H_2O}^{(eff)}$, in the porous product layer is related to the diffusion coefficient in the bulk gas phase, $D_{H_2-H_2O}^{(b)}$, as:

$$D_{H_2-H_2O}^{(eff)} = D_{H_2-H_2O}^{(b)} \cdot \frac{\epsilon}{\tau} \quad \ldots \text{(VII-13)}$$

Where ϵ is the porosity of the product layer and τ is the tortuosity factor depending upon the structure of the pore. Wheeler[76] suggested that a useful model of the pore structure could be developed by considering the pore as a collection of cylinders with frequent intersection with other pores. From geometric considerations, it was found that the value of τ could be approximately taken as 2.0. Porosity of the reduced layer was calculated as 0.6 from

the theoretical densities of the constituents (Cr_2O_3 and Fe). The binary diffusivity ($D^{(b)}_{H_2-H_2O}$) in the bulk gas phase was calculated from kinetic theory of gases[80] and was found to be 12.2 cm^2/sec. Using all these, the values of coefficients $\bar{a}$ and $\bar{b}$ were calculated as 0.3886 and 0.05087 respectively.

Fig. 23 shows the relative magnitudes of the three resistances in the reduction of specimen number 5. It is clear that the chemical reaction step is much slower compared to the other two steps in the entire reduction period. It was pointed out in chapter V that the interface between the unreduced core and the product layer in a porous pellet was not sharp, but diffused over a finite zone. This was observed in all the porous pellets and reaction zone thickness values were measured for specimens number 6 and 8 as 0.02 and 0.028 cms. respectively. In view of the slow rate of surface reaction (Fig. 23) this phenomenon is expected. In a gas-solid reaction, if the rate of interfacial reaction is sufficiently fast, all the reactant gas is expected to get consumed rapidly as soon as it reaches the reaction front. The interface in such a case should be sharp unlike the present one.

While investigating kinetics of reduction of iron oxides, Mckewan[81] proposed a simple reduction model based on the assumption that the interfacial chemical reaction is the rate controlling step. According to this model if

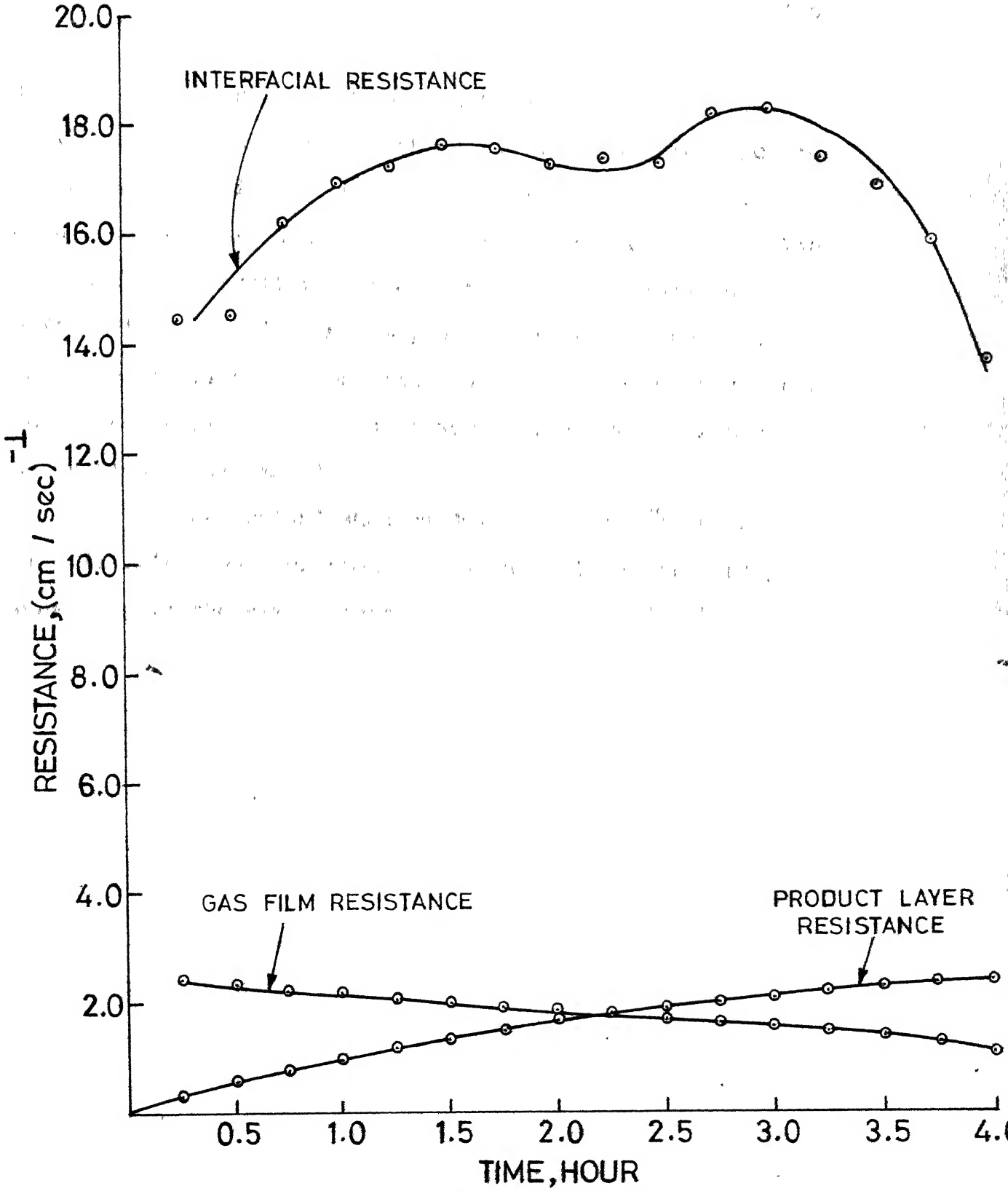

FIG. 23: VARIATION OF THE THREE RESISTANCES WITH TIME IN POROUS PELLET.

$[1 - (1-F)^{1/3}]$ is plotted against time, a linear behaviour would be observed. Fig. 24 shows the same plot for specimen number 5 and it is observed that the behaviour is linear with some scatter in the latter part of the reduction. The reason for the scatter in the last few data points is difficult to pinpoint, but may be attributed to the fact that the interface between the reactant and product was not sharp in the present case as assumed by Mckewan for the derivation of his model.

It was established by Spitzer et al[79] that $[1 - (1-F)^{1/3}]$ when plotted against normalized time t/t_c (where t_c is the time required for complete reduction) a straight line should be obtained if the reaction is 'completely' under interfacial control. Fig. 25 shows this plot for specimen number 5. However,a fairly pronounced departure from the ideal line for interfacial reaction control is to be noted. The reasons for this departure may be numerous. Firstly, the other two transport resistances though relatively small as compared to the interfacial resistance, but are not totally negligible. Hence their influence on the function $[1 - (1-F)^{1/3}]$ would definitely make the plot move downwards. Secondly, it has been mentioned already that the model of Spitzer et al[79] was derived on the assumption of a sharp interface between the reactant and the product, which as mentioned already is not valid in the present case. Thirdly, it has been shown

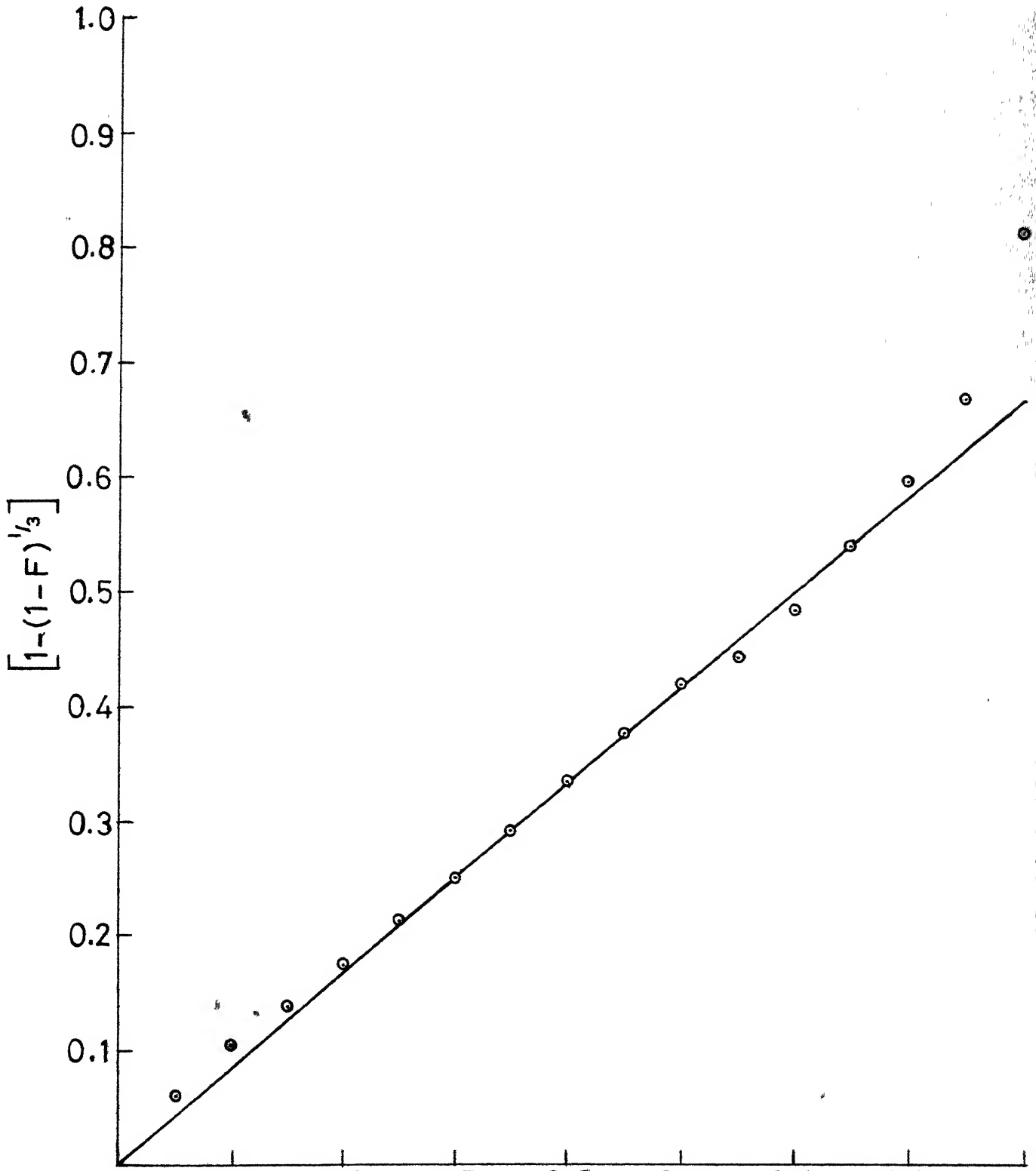

FIG. 24: $[1-(1-F)^{1/3}]$ VS. TIME FOR POROUS PELLET

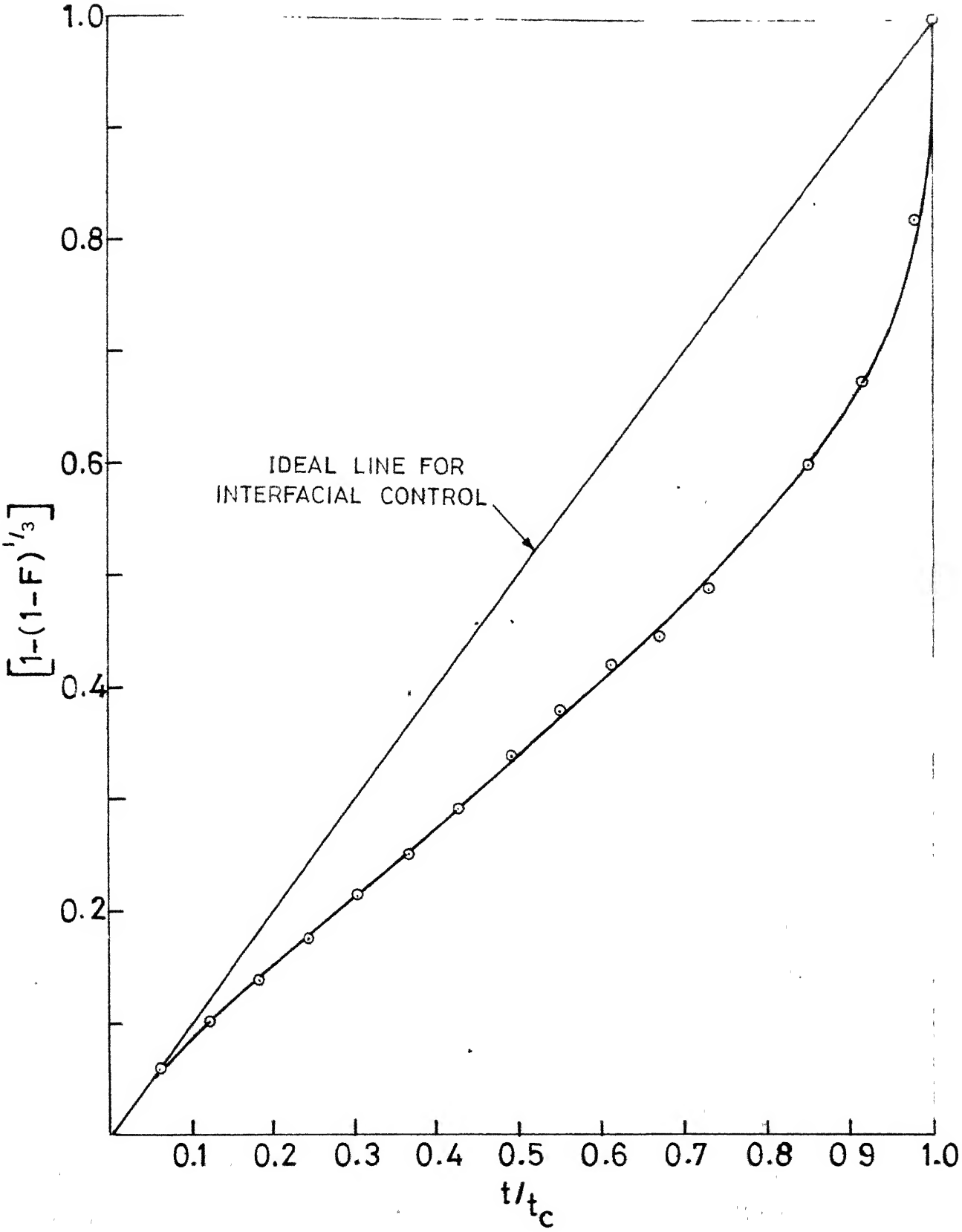

FIG.25: $[1-(1-F)^{1/3}]$ AGAINST NORMALIZED TIME FOR POROUS PELLET.

by Spitzer et al[79] that the plot of the type shown in Fig. 25 is extremely sensitive to any error in F during the latter part of the reduction.

Amongst the above three factors, it is clear that the first and the third taken together are insufficient to explain so much of departure from ideal interfacial control line in Fig. 25. Hence it appears that the second reason listed above i.e., the error in assumption of sharp interface might have caused such a marked departure.

It is clear from the above discussions on porous pellet that the chemical reaction between hydrogen and $FeO.Cr_2O_3$ at the reaction zone is the rate-controlling step in the over-all reduction process.

VII-2 DENSE PELLETS:

The reduction of Cr_2O_3 alongwith FeO in dense pellets have been established already by (i) chemical analysis of metallic phase (Table VII), (ii) mismatch between the actual percentage of reduction and the microscopically estimated percentage, and (iii) electronprobe microanalysis (Fig. 18).

In a partially reduced dense chromite pellet, the expected phases are $FeO.Cr_2O_3$, Cr_2O_3 and Fe-Cr alloy. However, the results of electronprobe microanalysis (Figs. 16-18) appear to cast doubt upon the identification of these phases. But this is traceable to the difficulties encountered

in the analysis (section IV-4), the most serious one being that the sizes of two phases (Cr_2O_3 and Fe-Cr alloy) were smaller than the beam diameter. In Fig. 16, a gradual increase of Cr content accompanied by a decrease in Fe is observed instead of a constant value for both. Since the crystallite size of $FeO.Cr_2O_3$ became smaller and smaller towards the outer edge of the pellet, the scan got more and more influenced by the Cr_2O_3 phase surrounding the grains changing Fe and Cr values. Fig. 17 shows an unnatural lowering of Cr and Fe as the Cr_2O_3 phase at the grain boundary was crossed in the third zone (Fig. 13(b)) of reduced layer. Ideally an increase in Cr corresponding to that of Cr_2O_3 and a zero value for Fe should have been obtained. Porosity in the Cr_2O_3 phase or fluorescence may be responsible for this anomalous behaviour. In Fig. 18, the existence of an Fe-Cr alloy phase is clear, although in no case the alloy compositions add up to 100 percent because of high degree of uncertainty in the analysis. The fluctuating intensity plot outside the alloy phase indicates a phase mixture.

The simultaneous reduction of Cr_2O_3 to Cr in dense pellets alongwith the reduction of ferrous oxide is a factor which complicates the reduction phenomenon. An important feature of Cr_2O_3 reduction in dense pellets is that once the reduction of Cr_2O_3 starts, the equilibrium pH_2O/pH_2 value for Cr_2O_3 reduction will be different from

that calculated assuming unit activity of Cr in equation (VII-2) because of alloying of reduced Cr with Fe and the consequent change in activity caused thereby. From thermodynamic calculations as shown in previous section, the beginning of Cr_2O_3 reduction in a dense pellet can be identified easily, e.g., between the 90th and 120th minute in the case of specimen number 3 (reduction data given in Appendix-A1).

From a comparison of percentage reduction vs. time plots in Figs. 9 and 10, it is clear that the rates of reduction of dense pellets are an order of magnitude lower as compared to those of the porous pellets. A comparison of Figs. 9 and 10 also reveal that the percentage reduction in the case of dense pellets beyond a certain stage of reduction does not decrease much with time as in the case of porous pellets.

Another important feature of dense pellet reduction is the existence of three zones in the reduced layer, viz., the outermost being the first zone consisting of an alloy of Fe and Cr (Fig. 12(a)), the second zone consisting of Cr_2O_3, $FeO.Cr_2O_3$ and an alloy of Fe-Cr (Fig. 12(b)) and the third zone appearing next to the unreduced core consisting of $FeO.Cr_2O_3$ grains with Cr_2O_3 and Fe globules along the grain boundaries (Fig. 13(b)). It is clear that there is a qualitative similarity between the dense and the porous pellet reduction, both being characterized by a

reaction zone instead of a sharp reaction interface. The thickness of the reaction zone in dense and porous pellets are comparable, e.g., 0.02 and 0.028 cms. in specimens 6 and 8 respectively (porous) as against 0.045 cms. in specimen number 4 (dense). It has been mentioned in the previous section that a reaction zone instead of a sharp interface indicates a slow rate of chemical reaction. The first zone of reduced layer was observed only in specimens with higher degree of reduction, e.g., in specimens 2 and 4 and not in number 1. The porosity of the first zone was found to decrease with time, probably due to sintering at 1050°C (in specimens 2 and 4). The thickness of the second zone was very small in specimen number 3, which was subjected to 21 percent reduction. This indicates that at the beginning of reduction at the outer surface of the pellet, the reduction pattern should be the one corresponding to that of the third zone. This type of "grain boundary penetration of reaction" is expected and was observed previously amongst others by Endom et al[82]. Grain boundaries being the region of highest imperfection in a crystalline solid, are expected to offer more favourable sites for heterogeneous chemical reactions. Hence, the reduction reaction should start there only and gradually proceed in a topochemical fashion towards the core of a grain. The second zone should start growing at the surface of the pellet only when the rate of generation of H_2O has decreased such that Cr_2O_3 reduction is thermodynamically

feasible.

Both the second and the third zones are porous because of the difference in theoretical densities of reactant and products. However, the porosity of the third zone is restricted along the grain boundaries only where reaction has taken place. Compared to this in the second zone, porosity is more uniformly distributed due to smaller size of unreduced core of $FeO.Cr_2O_3$.

A quantitative treatment of the dense pellet reduction is difficult because of a number of complicating factors, viz.,

(1) Simultaneous reduction of Cr_2O_3 in dense pellets.

(2) Two reactions, the reduction of Cr_2O_3 and $FeO.Cr_2O_3$ taking place simultaneously in the second zone over an appreciable depth.

(3) The driving force for Cr_2O_3 reduction (i.e., the difference between actual pH_2O/pH_2 with the equilibrium pH_2O/pH_2 for Cr_2O_3 reduction) changing with the activity of Cr in Fe-Cr alloy, which depends upon the composition of the alloy phase, another time dependent variable.

(4) The reaction in the third zone taking place only along the grain boundaries over an appreciable depth.

It is readily understood that, it is extremely difficult to describe factors (2), (3) and (4) mentioned above in the form of mathematical equations. However, it

is possible to grossly assess the importance of the three resistances involved in the dense pellet reduction. The transport resistance across the gas film around the pellet has been shown to be negligible for porous pellet reduction. Hence, it should definitely be negligible in this case also. Similarly the transport resistance through the reduced layer should also be negligible as compared to the observed rate. The base porosity of the unreduced pellet was 0.1 (section III-4). Due to reduction and consequent density change, further porosity develops in the reduction zone. The total porosity can be as high as 0.26 (for specimen number 4) if the reduction of FeO is complete. Such a porosity could be expected in the first and the second zone if there were no sintering in first zone. It can be shown that the rate of diffusion through these two layers with this porosity would be much higher compared to the observed rate of reduction. In the third zone, FeO reduction had just started and hence the porosity of that zone would be near the base porosity. At this low level of porosity all the pores may not be interconnected. Even then the diffusive flux is expected to be an order of magnitude higher than the observed rate of reduction. The appreciable thickness (of 0.03 cms. in specimen number 4) of the third zone is another evidence to rule out diffusion as the rate controlling step in this zone, in which case the thickness would have been much less. Hence, one is left with the chemical

reaction only as a step which should be slow enough to explain the low rate of reduction of a dense pellet.

After identification of the slow chemical reaction around the grains in the reaction zone as the rate-controlling step, it is necessary to obtain an explanation for the order of magnitude difference in the rates of reduction of dense pellets as compared to those for porous pellets.

The rate of chemical reaction would be proportional to the gas-solid contact area. Since, as discussed above, the porosity of the reaction zone (third zone) would be low because of lower degree of reduction, the gas-solid contact area would be much less compared to that available in the reaction zone of a porous pellet. The existence of closed pores, which are likely to be encountered in third zone due to the low porosity, would further reduce the possible gas-solid contact area in that zone. Although it is not possible to present a quantitative estimate of the surface area available to gas attack in this zone due to the lack of precise informations, it appears to be the most probable reason for such a large difference in rates of reduction of dense pellets in comparison to those of porous pellets.

Hence, it may be concluded that the reduction of a dense pellet is more complicated in comparison to the

reduction of a porous pellet due to the simultaneous reduction of Cr_2O_3 alongwith FeO and the existence of two zones of reaction; and it is most probably controlled by the chemical reaction step.

CHAPTER VIII

SUMMARY AND CONCLUSIONS

Thermodynamic and kinetic investigations were carried out on chromite system for a fundamental appraisal of the selective reduction of iron oxides in chromite.

Solid solutions of $FeO.Cr_2O_3$ and $FeO.Fe_2O_3$, represented as $FeFe_{2-x}Cr_xO_4$, of different compositions including the terminal $FeO.Cr_2O_3$ were prepared synthetically from Fe_2O_3, Cr_2O_3 and Fe by heating in evacuated and sealed quartz tubes at 1000°C. In the thermodynamic investigations, equilibrium oxygen potentials over mixtures of metallic iron and $FeFe_{2-x}Cr_xO_4$, including the terminal phase $FeO.Cr_2O_3$ were determined within the temperature range of 850°C to 1050°C by gas equilibration using H_2-H_2O gas mixture in a thermogravimetric apparatus. In the kinetic investigations, rates of reduction of synthetically prepared porous and dense single spherical pellets of $FeO.Cr_2O_3$ were studied at 1050°C in a stream of hydrogen in a thermogravimetric apparatus. The reduction products were examined by X-ray diffraction, microstructural studies, electronprobe microanalysis and chemical analysis. Following conclusions may be drawn from the present investigation:

1. The oxygen potentials over the terminal

chromite ($FeO.Cr_2O_3$) determined in this investigation is in good agreement with the previous investigations on it.

2. The activity of $FeO.Fe_2O_3$ in the $FeO.Cr_2O_3$-$FeO.Fe_2O_3$ system exhibits a strong negative departure from the ideal behaviour in the composition range investigated.

3. In the reduction of porous pellets, Cr_2O_3 reduction was not observed even upto the complete reduction of FeO. Instead of a sharp reaction front a reaction zone was observed. The chemical reaction at the gas-solid interface was found to be the rate-controlling step.

4. The dense pellet reduction was complicated by the simultaneous reduction of Cr_2O_3 with FeO. The rates of dense pellet reduction were an order of magnitude lower than those of the porous pellet reduction. Two reaction zones of appreciable width were observed. The reduction proceeded from the boundary to the interior of grains. The chemical reaction at the gas-solid interface was probably the rate controlling step in dense pellet reduction.

5. From this investigation it is clear that in the thermal beneficiation of low grade chromite ores, porous ore pieces, either natural or prepared by agglomeration, would offer a great advantage over dense pieces, since the reduction of the former would be much faster and would not be accompanied by the undesirable simultaneous reduction of Cr_2O_3. Since chemical reaction at the gas-solid interface is the rate controlling step in this sytem at 1050°C, a

higher temperature of reduction is expected to speed up the rate considerably which is desirable in commercial practice.

CHAPTER IX

SUGGESTIONS FOR FUTURE WORK

From this investigation some insight into the selective reduction of iron oxides in $FeO.Cr_2O_3$ have been obtained. But for a more complete and thorough analysis of the process, continued work is necessary in the following lines:

(1) Determination of the activity-composition relationship in the $FeO.Cr_2O_3$-$FeO.Fe_2O_3$ system for the entire range of composition.

(2) Study of the kinetics of reduction of iron oxides in $FeFe_{2-x}Cr_xO_4$ solid solutions of various compositions on both porous and dense pellets.

(3) Study of the reduction kinetics over a temperature range above and below 1050°C firstly to testify one conclusion of this study that the interfacial chemical reaction is the rate-controlling step in this process and secondly to obtain quantitative informations about the change in rate as a function of temperature, which is an essential information for commercial scale operation.

(4) Investigation on the influence of H_2O on the rates and mechanism of chromite reduction by hydrogen.

LIST OF REFERENCES

1. J.F. Elliot, M. Gleisser and V. Ramkrishna: Thermochemistry for Steelmaking, Vol. I & II, Addison Wesley Publishing Co. Inc., 1960.

2. C.E. Wick and F.E. Block: Thermodynamic Properties of 65 Elements - Their Oxides, Halides,Carbides and Nitrides - Bulletin 605 U.S. Bureau of Mines, Washington D.C., 1963.

3. E.J.W. Verwey and E.L. Heilmann: J. Chemical Physics, 1947, Vol. 15, p. 174.

4. G.C. Ulmer: Refractory Materials, Vol. 5, Part 1, Edited by A.M. Alper, Academic Press, N.Y., 1970, p. 251.

5. H.A. Heiligman and H.M. Mikami: Industrial Rocks and Minerals, Am. Inst. of Min. Met. Pet. Engr., 3rd Edition, 1960, p. 243.

6. The Controller, Indian Bureau of Mines, Nagpur: Private Communication, August, 1969.

7. Indian Bureau of Mines: Indian Minerals Yearbook 1962, p. 227.

8. ibid : ibid, 1963, p. 282.

9. N.J. Wadia: Indian Min. Journal, Special Issue, 1957, Vol. 5, p. 38.

10. P.I.A. Narayanan and G.P. Mathur: J. Scientific and Industrial Research, 1952, Vol. 11A, p. 202.

11. P.I.A. Narayanan and S.K. Banerjee: ibid, 1952, Vol. 11A, p. 205.

12. P.I.A. Narayanan and M.C. Sen: ibid, 1952, Vol. 11A, p. 207.

13. M.C. Sen and P.I.A. Narayanan: ibid, 1952, Vol. 11A, p. 505.

14. S.K. Banerjee and P.I.A. Narayanan: ibid, 1953, Vol. 12A, p. 136.

15. M.C. Sen and P.I.A. Narayanan:ibid, 1953, Vol. 12A, p. 186.

16. S.K. Banerjee and P.I.A. Narayanan:Indian Mining Journal, Special Issue, 1957, Vol. 5, p. 78.

17. M.C. Sen and A.B. Chatterjee: ibid, Special Issue, 1957, Vol. 5, p. 85.

18. S. Samanta, R.N. Misra and P.P. Bhatnagar: N.M.L. Technical Journal, 1965, p. 13.

19. S. Samanta, R.N. Misra and P.P. Bhatnagar: N.M.L. Technical Journal, 1964, p. 12.

20. R.N. Misra and P.P. Bhatnagar: Trans. Indian Institute of Metals, 1962, Vol. 15, p. 270.

21. R.R. Llyod et al: U.S. Bureau of Mines Report of Investigation No. 3834 in 1946.

22. F.S. Boericke: U.S.Bureau of Mines Report of Investigation No. 3847 in 1946.

23. A. Hammarberg: South African Patent No. 739/36.

24. E. Cohen and W.K. Ng: Advances in Extractive Metallurgy, Proceedings of Symposium Organized by Institute of Mining and Metallurgy, London, April 1967, p. 127.

25. P.R. Jochens and D.D. Howat: J.South African Inst. of Min. Met., 1964, Vol. 65, p. 236.

26. A.D. Ryon, F.L. Daley and R.S. Lowrie: Chem. Engg. Progress, 1959, Vol. 55, p. 75.

27. M.W. Walter: German Patent 11,35,668, August 30, 1962, Chemical Abstract, 1962, Vol. 57, 14816i.

28. G.H. Beers: British Patent 6,82,020, November 5, 1952.

29. W.H. Dyson and L. Atchison: British Patent 176,729 and 179,201, October 28, 1920.

30. A.S. Athawale and V.A. Altekar: Trans. Indian Institute of Metals, 1969, Vol. 22, p. 29.

31. H.M. Chen and J. Chipman: Trans. Amer. Soc. Metals, 1947, Vol. 38, p. 70.

32. D.C. Hilty, W.K. Forgenj and R.L. Folkman: J. Metals, 1955, Vol. 7, p. 253.

33. W. Koch, J. Bruch and H. Rohde: Arch. Fur. das Eisenhuttenwesen, 1960, Vol. 31, p. 279.

34. R.G. Richard and J. White: Trans. British Ceramic Society, 1954, Vol. 53, p. 422.

35. D. Woodhouse and J. White: Trans. British Ceramic Society, 1957, Vol. 56, p. 569.

36. A. Muan and S. Somiya: J. Amer. Ceramic Society, 1960, Vol. 43, p. 204.

37. T. Katsura and A. Muan: Trans. Met. Soc. AIME, 1964, Vol. 230, p. 77.

38. H.J. Yearian, J.M. Kortright and R.H. Langenhein: J. Chemical Physics, 1954, Vol. 22, p. 1196.

39. P.V. Riboud and A. Muan: Trans. Met. Soc. AIME, 1964, Vol. 230, p. 88.

40. A. Hoffmann: Archiv. fur. das Eisenhuttenwesen, 1965, Vol. 36, p. 155.

41. E.S. Boericke and W.M. Bangert: U.S. Bureau of Mines, Report of Investigation No. 3813, 1946.

42. A.N. Morozov and I.A. Novokharski: Russian Met. Fuels (English Translation), 1962, No. 6, p. 3.

43. R.P. Abendroth: Trans. Met. Soc. AIME, 1966, Vol. 236, p. 559.

44. W. Kunmann, D.B. Rogers and A. Wold: J. Physics and Chemistry of Solids, 1963, Vol. 24, p. 1535.

45. J.D. Tretyakov and H. Schmalzried: Ber. Der. Bus. Phys. Chem., 1965, Vol. 69, p. 396.

46. P.J. Roychowdhury: Master's Thesis, Department of Metallurgy, Indian Institute of Technology, Kanpur, India, June, 1970.

47. W.M. Mckewan: Steelmaking: The Chipman Conference, J.F. Elliot Edited, The M.I.T. Press, Cambridge, Mass., 1965, p. 141.

48. F.S. Manning and W.O. Philbrook: Blast Furnace Theory and Practice, Vol. II, J.H. Straussburger Edited, Gordon Breach Science Publishers, N.Y., 1969, p. 839.

49. B.V. Shults and E.I. Khazanov: Trudy Vostochno-Sibir. Filiala, Akad. Nauk S.S.S.R., 1959, No. 24, p. 167, Chemical Abstract, 1961, Vol. 55, 6796c.

50. D.J. O'Brien and T. Marshall: New Zealand Journal of Science, 1968, Vol. 11, p. 159, Chemical Abstract, 1968, Vol. 68, 71392u.

51. S.I. Suchilmikov: Chemical Abstract, 1965, Vol. 63, 12708g.

52. Kamal Hussain et al: Indian Journal of Technology, 1967, Vol. 5, p. 97.

53. Kamal Hussain et al: ibid, 1967, Vol. 5, p. 369.

54. Kamal Hussain et al: Z. Erzbergban Metall., 1964, Vol. 17, p. 192, Chemical Abstract, 1964, Vol. 61, 3973b.

55. R.H. Walsh et al: Trans. Met. Soc. AIME, 1960, Vol. 218, p. 994.

56. S.S. Lisnyak and N.F. Eseev: Sb. Nauchn. - Techn. Tr. Nauchn - Issled. Inst. Met. Chelyab. Sovnarkhoza, 1961, No. 3, p. 12, Chemical Abstract, 1962, Vol. 56, 13873A.

57. S.S. Lisnyak, A.M. Belikov and A.N. Morozov: Sb. Nauchn - Techn. Tr. Nauchn - Issled. Inst. Met. Chelyab. Sovnarkhoza, 1961, No. 4, p. 3, Chemical Abstract, 1963, Vol. 58, 6487B.

58. G.P. Baxter and J.E. Lansing: J. American Chemical Society, 1920, Vol. 42, p. 419.

59. J.B. Bookey and N.C. Tombs: Journal of Iron and Steel Institute, 1952, Vol. 172, p. 86.

60. W.H. McAdams: Heat Transmission, McGraw-Hill Book Co. Inc., N.Y., 1954, p. 233.

61. G.P. Chatterjee and S.S. Sidhu: J. Applied Physics, 1947, Vol. 18, p. 519.

62. F.J. Norton and A.U. Seybolt: Trans. Met. Soc. AIME, 1964, Vol. 230, p. 595.

63. M.H. Francomb: J. Physics and Chemistry of Solids, 1957, Vol. 3, p. 37.

64. N.A. Lange: Handbook of Chemistry, McGraw-Hill Book Co. Inc., N.Y., 1960, p. 160.

65. R.C. Weast and S.M. Selby: Handbook of Chemistry and Physics, The Chemical Rubber Co., Ohio, 1967, p. B-280.

66. B.D. Cullity: Elements of X-ray Diffraction, Addison-Wesley Publishing Co. Inc., Reading, Massachussetts, U.S.A., 1959, p. 317.

67. J.O. Edstrom: Journal of Iron and Steel Institute, 1953, Vol. 175, p. 289.

68. W.C. Coons: Ceramic Microstructures, Their Analysis Significance and Production, Edited by R.M. Fulrath and J.A. Pask, John Wiley & Sons. Inc., N.Y., 1968, p. 187.

69. E.C. Piggott: Ferrous Analysis, Modern Practice and Theory, Chapman & Hall, London 1954, p. 154.

70. L.S. Darken: Trans. Met. Soc. AIME, 1967, Vol. 239, p. 80.

71. E. Aukrust and A. Muan: ibid, 1964, Vol. 230, p. 378.

72. ibid: ibid, 1964, Vol. 230, p. 1395.

73. K. Schwerdtfeger and A. Muan: ibid, 1967, Vol. 239, p. 1114.

74. C. Wagner: The Physical Chemistry of Iron and Steel making, Edited by J.F. Elliot, Technology Press of the Massachussetts Institute of Technology, 1956, p. 237.

75. Y. Jeannin, C. Mannerskantz and F.D. Richardson: Trans. Met. Soc. AIME, 1963, Vol. 227, p. 300.

76. A. Wheeler: Advances in Catalysis, Vol. III, Academic Press, N.Y., 1951, p. 250.

77. A. Wheeler: Catalysis, Edited by P.H. Emmett, Vol. 2, Reinhold Publishing Co., N.Y., 1955, p. 105.

78. J. Szekely and J.W. Evans: Metallurgical Transactions, 1971, Vol. 2, p. 1691.

79. R.H. Spitzer, F.S. Manning and W.O. Philbrook: Trans. Met. Soc. AIME, 1966, Vol. 236, p. 726.

80. R.B. Bird, W.E. Stewart and E.N. Lightfoot: Transport Phenomena, John Wiley & Sons Inc., N.Y., 1960, p. 511.

81. W.M. Mckewan: Trans. Met. Soc. AIME, 1958, Vol. 212, p. 791.

82. A. Endom, K. Hedden and G. Lehmann: Reactivity of solids, Edited by G.-M. Schwab, Fifth International Symposium, Munich, 1964, Elsevier Publishing Co., Amsterdam, p. 632.

APPENDIX - A1

BASIC REDUCTION DATA FOR THE PELLETS

Specimen No. 1		Specimen No. 2	
Time (hr.)	Percent Reduction	Time (hr.)	Percent Reduction
0.50	4.53	1.00	8.57
1.00	7.46	2.00	13.82
1.50	10.39	3.00	18.68
2.00	13.75	4.00	21.83
2.50	17.32	5.00	25.97
3.00	20.14	6.00	30.11
3.50	22.64	7.00	33.15
4.00	25.46	8.00	36.35
5.00	29.57	9.00	39.66
6.00	62.93	10.00	42.53
7.50	66.40	11.00	44.57
9.00	73.07	12.00	46.39
		13.00	49.04
		14.00	52.19
		15.00	54.95
		16.00	57.71
		17.00	60.47
		18.00	63.43
		19.00	66.03

(Contd.)...

Specimen No. 2 continued

20.00	68.99
21.00	71.69
22.00	74.06
23.00	76.66
24.00	78.76
25.00	81.24
26.00	83.50
27.00	86.04
28.00	88.36
29.00	90.62
31.00	95.04
33.00	99.46
35.00	103.88
37.00	108.96
39.00	113.60
41.00	118.07
43.00	123.15

Specimen No. 3

Time (hr.)	Percent Reduction
0.50	7.31
1.00	11.76
1.50	16.21
2.00	18.44
2.50	20.98

Specimen No. 4	
Time (hr.)	Percent Reduction
1.00	9.78
2.00	16.23
3.00	21.12
4.00	25.04
5.00	29.76
6.00	33.27
7.00	36.14
8.00	39.14
9.00	42.88
10.00	45.76
11.00	48.75
12.00	51.62
13.00	54.62
14.00	58.07
15.00	60.72
16.00	63.59
17.00	65.90
18.00	68.89
19.00	71.77
20.00	73.95
21.00	76.94
22.00	79.99

Specimen No. 4 continued	
23.00	82.30
24.00	84.60
25.00	87.71
26.00	89.95
27.00	92.54
28.00	94.67
29.00	96.74
30.00	99.22
31.00	101.29

Specimen No. 5		Specimen No. 6	
Time (hr.)	Percent Reduction	Time (hr.)	Percent Reduction
0.25	14.50	0.25	12.05
0.50	27.18	0.50	20.43
0.75	35.20	0.75	28.56
1.00	43.74	1.00	36.68
1.25	51.40	1.25	44.54
1.50	57.97	1.50	51.61
1.75	64.59	1.75	56.85
2.00	70.90	2.00	62.09
2.25	75.87	2.25	66.54
2.50	79.44	2.50	69.43
2.75	82.80	2.75	73.09
3.00	86.42	3.00	76.76
3.25	90.30	3.25	80.16
3.50	93.51		
3.75	96.51		
4.00	99.35		
4.25	101.23		

Specimen No. 7		Specimen No. 8	
Time (hr.)	Percent Reduction	Time (hr.)	Percent Reduction
0.25	11.50	0.25	11.13
0.50	21.65	0.50	19.75
0.75	29.90	0.75	27.26
1.00	36.60	1.00	31.71
1.25	42.27	1.25	36.44
1.50	48.20	1.50	42.00
1.75	53.87	1.75	47.00
2.00	59.28	2.00	51.90
2.25	64.33	2.25	56.46
2.50	69.08	2.50	60.91
2.57	70.11	2.75	64.81
		3.00	68.14
		3.125	70.09

APPENDIX - A2

CALCULATION OF VIRTUAL MAXIMUM RATE

Volumetric flow rate of H_2 = 500 cm^3/min

= 8.34 cm^3/sec

Volumetric flow rate of H_2 at 1323°K = 36.78 cm^3/sec

Dia. of reaction tube = 1.75 inch = 4.45 cm

Area of reaction tube = 15.4 cm^2

Area of reaction tube available for flow = 14.6 cm^2

Velocity of H_2 = 36.78/14.6 = 2.51 cm/sec at 1323°K

Density of H_2 at S.T.P. = 0.9×10^{-4} gms/cm^3

Density of H_2 at 1323°K = 1.85×10^{-5} gms/cm^3

Viscosity of H_2 at 1323°K (calculated from kinetic theory[80])

= 2.4×10^{-4} pois.

Diffusivity of H_2 - H_2O gas mixture[80] at 1323°K = 12.2 cm^2/sec

Equilibrium pH_2O/pH_2 for $FeO.Cr_2O_3$ at 1323°K (from the present investigation) = 0.0141

So pH_2O = 0.0139.

Density of H_2O at 1323°K = 1.66×10^{-4} gms/cm^3

Let the concentration of H_2O at the surface of the sphere = $C^{(s)}_{H_2O}$. Assuming equilibrium of the reduction reaction prevailing at the surface, $C^{(s)}_{H_2O} = 1.66 \times 10^{-4} \times 0.0139$

$= 2.3 \times 10^{-6}$ gms/c.c.

In the experimental system,

Re = Reynolds number = 0.197

Sc = Schmidt number = 1.05

From the Ranz Marshall correlation:

Nusselt number = Nu = $2.0 + 0.6\ (Re)^{0.5}\ (Sc)^{0.33}$

= 2.2730

and from definition,

$$Nu = \frac{K_m \cdot (2X_o)}{D^{(b)}_{H_2-H_2O}}$$

where, K_m = mass transfer coefficient

$D^{(b)}_{H_2-H_2O}$ = Diffusivity in H_2-H_2O gas mixture

and X_o = Pellet radius.

Hence, K_m = 27.95 cms/sec.

From the weight loss data (Appendix - A1) at 1323°K

Weight loss in first 0.25 hrs for specimen number 5

= 0.0280 gms

and Weight loss in 1 sec. = 3.1×10^{-5} gms of O_2/sec

= 3.48×10^{-5} gms of H_2O/sec.

So the rate of generation of H_2O = 0.20 cm^3/sec

Let the concentration of H_2O at a distance δ (boundary layer thickness) from the surface of the sphere = $C^{(b)}_{H_2O}$

Hence,

$$C^{(b)}_{H_2O} = \frac{\text{rate of generation of } H_2O \text{ (in gms/sec)}}{\text{rate of generation of } H_2O \text{ (in } cm^3\text{/sec)} + \text{rate of flow of } H_2 \text{ (in } cm^3\text{/sec)}}$$

$$= \frac{3.48 \times 10^{-5}}{0.02 + 36.78} = 0.94 \times 10^{-6} \text{ gms/c.c.}$$

The surface area of the sphere = 5.06 cm^2

Virtual Maximum Rate of Transport

$$= \text{Area.mass transfer coefficient}.[C_{H_2O}^{(s)} - C_{H_2O}^{(b)}]$$

$$= 5.06 \times 27.95\ [2.3 \times 10^{-6} - 0.94 \times 10^{-6}]$$

$$= 1.92 \times 10^{-4} \text{ gms/sec.}$$

So the ratio of virtual maximum rate of transport to the actual rate of transport $= \dfrac{1.92 \times 10^{-4}}{3.48 \times 10^{-5}} = 5.5$

BIOGRAPHICAL NOTE

The author was born in Simla, Himachal Pradesh, on the 1st September, 1943. After his high school education in Howrah Zilla School, Howrah, he joined Bengal Engineering College, Howrah, under Calcutta University. After obtaining Bachelor's Degree in Metallurgical Engineering in the year 1966, he joined post graduate programme in the Metallurgical Engineering Department of Indian Institute of Technology, Kanpur, and received his Master's Degree in 1968. His master's thesis was on "The Influence of Porosity on the Kinetics of Reduction of Hematite by Hydrogen". His area of specialization is Physical Chemistry of Extractive Metallurgy with special interest on the kinetics and thermodynamics of gas-solid reactions at high temperature with reference to oxide reduction.